JOURNAL OF CONDENSED MATTER NUCLEAR SCIENCE

Experiments and Methods in Cold Fusion

Proceedings of the 12th International Workshop on Anomalies in Hydrogen Loaded Metals, Asti, Italy, June 5–9, 2017

VOLUME 26, October 2018

JOURNAL OF CONDENSED MATTER NUCLEAR SCIENCE

Experiments and Methods in Cold Fusion

JOURNAL OF CONDENSED MATTER NUCLEAR SCIENCE

Volume 26, October 2018

 ISSN 2227-3123

Orders, claims, author inquiries and journal inquiries

Please contact the Editor in Chief, CMNSEditor@iscmns.org or webmaster@iscmns.org

J. Condensed Matter Nucl. Sci. 26 (2018) 1–98
 ISSN 2227-3123

JOURNAL OF CONDENSED MATTER NUCLEAR SCIENCE

Volume 26 2018

CONTENTS

Preface

The 12th International Workshop on Anomalies in Hydrogen Loaded Metals was held at the Hotel Langhe e Monferrato, Costigliole d'Asti in Italy, June 2017. This is a four-star hotel with 55 rooms which overflowed with some 72 participants and guests. The choice of province of Asti continued the tradition of the original Asti Workshops organized by Fiat in 1993 and 1995.

The workshop format recognizes that half the value of scientific meetings consists of course of the formal sessions, the oral and poster papers, and the discussions. There were enough oral papers to justify three full days of presentations and in addition, ISCMNS held its Annual General Meeting and an excursion was made for wine tasting. David Nagel hosted a stimulating panel discussion on theory. Fabrice David was voted the author of the best poster paper entitled, About Discrete Breathers and LENR and received the ISCMNS bronze medal. David French chaired a very interesting mini-workshop on patent issues. But an equally valuable part of these meetings is the informal networking that takes place over meals and coffee. To this end the organizers chose a self-contained conference center offering not just the lecture theatre, but also food and accommodation so that participants did not need to disperse. There was the welcome reception at the swimming pool with an open bar where there was animated discussion until after midnight! However, the hotel could not offer dinners in the other evenings so a coach was rented to take participants to nearby restaurants. This seemed fairly satisfactory. The banquet was held at the "Duca Bianco" in Calosso where her Serene Highness, the Countess of Castiglione, presented the Giuliano Preparata Medal to Tom Claytor for his tritium work.

I would like to thank Barbara and Andrea at the hotel for their patience and hard work in making the Workshop a success. I am grateful to Mathieu Valat, Anais Kedikian, and Jenny Vinko for organizational assistance and advice. Also of course I thank Jean Paul Biberian and Jayantha Kumar without whom these proceedings would never have been published.

The videos of the meeting can be found at:
https://www.youtube.com/playlist?list=PLSXH-_auE_Vrnm9z-8A3KCMCJhRwTNFlB&jct=YTrl7i5IomZvsB7V-nkn_h15IXZ6hQ

Sincerely,

Dr. William Collis
August 2018

J. Condensed Matter Nucl. Sci. 26 (2018) 1–14

Research Article

LENR – What We must Do to Complete Martin Fleischmann's Undertaking

Michael C.H. McKubre*,†

Energy Research Center, SRI International, Menlo Park, CA, USA

Abstract

It is clear to most who have studied the matter carefully that condensed matter nuclear science (CMNS) expresses a real and new phenomenon in physics. The efforts to communicate this reality outside a rather small group have not been very convincing. For something of such potential importance this dichotomy seems strange. How might we improve this situation? A working theory could certainly help, and better correlation between experimental variables, both input and output. A working demonstration that stood alone even as a toy could help facilitate communication directly with influential technical but non-specialist individuals and groups. Some thoughts on the possibilities and constraints are offered below.
 ISSN 2227-3123

Keywords: Demonstration prototype, Fleischmann, Heat effect, Pons

1. Introduction

I would like to preface these remarks with a statement of my position and degree of certainty after having studied LENR for more than 28 years and the deuterium–palladium system for nearly 38. Without a working example certainty is approached only asymptotically. A working theory would certainly help us convince others and advance the field but even well developed models and theories must be anticipated to change and very few laws are so right and rigid as to be immune to change. That being said our failure to communicate effectively outside our community that nuclear processes can and do take advantage of the condensed state is mostly – or initially – due to incomplete or insufficiently well explained experiment, not weak theory. This last statement contains no apology or implied criticism. Much good work has been done in both domains: experiment and theory. Some of the experimental progress is summarized in this paper. More and better experiments should and will be done – and will inform theory.

So how is "asymptotic certainty" based on a preponderance of evidence achieved? Or, better still, working example? I will divide my answer into two parts. My personal confidence derives from tens of thousands of hours spent with my own hands in the company of extremely able individuals in my own laboratory, working with systems as simple

*E-mail: mmckubre@gmail.com.
†Retired

 ISSN 2227-3123

as they can be made, to understand the bases of the effects hypothesized and observed by Fleischmann and Pons, and their extrapolated consequences. The results of this personal effort is reinforced by the works of numerous others – many in the audience – whose skills I have come to trust and whose results form a consistent, if not complete, pattern of understanding.

On the basis of this collective effort I am convinced that condensed matter nuclear science (CMNS) expresses a real and new phenomenon in physics. What we need to do is to communicate this knowledge effectively others. My order of assurance in the various experimental claims of CMNS effects that are deemed anomalous is as follows:

(1) Tritium (and helium-3).
(2) Excess heat at levels consistent with nuclear but not chemical processes.
(3) The production of helium-4 in chemical energy environments ($\sim$1 eV), at levels consistent with the measured excess heat (>10^3 eV).
(4) An additional range of condensed matter nuclear effects that are inconsistent with pairwise, isolated nuclear reaction, but nevertheless require nuclear cause.

2. Discussion

Those expecting me to answer the charge implied in the title of this talk will be disappointed – perhaps doubly so – although I suggest you stay to the end. I do not have a clear answer for myself, let alone for the community – the technical equivalent of a "killer app" if you will – that, once accomplished (hopefully promptly), will convince working scientists with relevant skills to add their effort to ours. Over the years the research group at SRI has made several major contributions to the field of research now identified as CMNS, particularly studying the Fleischmann–Pons Heat Effect (FPHE), and I take some advantage from this. These contributions include the following observations and innovations:

(1) Postulate and demonstrate the importance of D/Pd loading in achieving FPHE [1].
(2) Demonstrate and calibrate the utility and applicability of electrical resistance ratio methods to measure D/Pd loading in LENR experiments [2].
(3) Confirm the importance of D/Pd loading and demonstrate a critical threshold onset of the FPHE [3] (jointly with Kunimatsu et al. [4] at IMRA-Japan).
(4) Confirm the existence of an initiation time delay in the FPHE (following Fleischmann–Pons and Bockris).
(5) Confirm the Miles–Bush correlation of excess heat and helium production in the Fleischmann–Pons electrochemical system, Arata–Zhang double-structured cathode and Case gas loading experiments [5].
(6) Demonstrate the critical importance of deuterium interfacial flux in the Fleischmann–Pons heat effect [6] (hypothesized by Hagelstein).
(7) With ENEA (Frascati) demonstrate the importance of metallurgical structure in achieving high D/Pd loading and surface morphology in producing the Fleischmann–Pons heat effect.
(8) With Energetics (New Jersey, USA and Omer, Israel) and ENEA (Frascati) [7] demonstrate the critical beneficial effects of superwave modulated electrochemical stimulus in achieving high D/Pd loading, high deuterium interfacial flux and large power and energy gains in the FPHE (hypothesized by Dardik).

Of crucial and pertinent relevance to my inability to answer the charge in the paper title, if I had "the secret", and presuming for a moment that any one person could conceive or carry such a secret to term, I would very likely be constrained from sharing this knowledge publicly, or perhaps at all with any except the people who paid for my labour. I worked for nearly 40 years in the world of contract research in which individuals, corporations and governmental and neo-governmental institutions provided funds and contractual binding to implement a pre-agreed-on research plan or

direction laid out in a formal "Statement of Work". Also and importantly pre-agreed is the ownership of intellectual "property" or "rights" to disburse the knowledge so developed. I have performed and directed more than $50 million of contract research and hold hundreds of "secrets" explicitly or implicitly for former sponsors, or as "non-disclosure" agreements with corporations and individuals.

Possibly a worse problem than the formal and codified secrecy of information held to be "IP" is the discouragement of research pursuit, analysis and publication. My first and largest sponsor of "cold fusion" research at SRI was EPRI – the Electric Power Research Institute located in Palo Alto, California. I have a long-standing, fruitful and joyous research partnership with EPRI extending back to 1978 – initially of the topic of the palladium-hydrogen and palladium-deuterium systems for purposes other than "cold fusion" [2]. All these works were "semi-public" in the sense that reports were prepared and made publicly available (occasionally behind a pay wall) and open publication was permitted, if not encouraged. EPRI sponsored our experiments that resulted in the first five contributions to my enumerated chronological list above; all of these were published openly. So what is this "possibly worse problem"?

Initially our research focused heavily on one critical research objective – testing Fleischmann and Pons' dramatic claims to determine their merit and possible application and implications for the US utility power industry. So narrow was our focus that we were not able to analyze fully our results and chose to ignore innumerable potentially promising scientific and technologic avenues. On previous occasions I have estimated that only $\sim$10% of the work done by the 10–12 person Energy Research team under EPRI sponsorship at SRI was fully processed to the point that public statement or publication could be made of it. With reflection (and memory sag) I would now rate our early success of converting laboratory results into "known knowns" as $\sim$30% - the majority remaining as "relic knowledge" or intuition in the minds of the principal investigators.

The last potential knowledge problem that we face is "unsound certainty" associated with the unwillingness/inability to reject old knowledge and replace it with new. Josh Billings, an American humorists in the second half of the 19th century, said: "*It ain't what a man don't know that makes him a fool... It's all the things he does know... that just ain't so"*. In some ways we are too well trained by and too respectful of our teachers and their teachings. If the observations of any one of a half dozen or more novel phenomena discovered pursuing Fleischmann and Pons elucidation are sound – if nuclear effects take place in condensed matter by means, at rates or with products different from nuclear reactions in free space – then something we have been taught and believe about nuclear interaction is incorrect – something we "know", "*just ain't so"*, or something important is missing.

More than 28 years have elapsed since the public announcement by Martin Fleischmann and Stanley Pons on March 23, 1989 of anomalous thermal effects and possible nuclear fusion associated with the super-loading of deuterium into palladium by electrochemical means. Rightly this announcement prompted the redirection of a significant fraction of relevant scientific resource albeit in a relatively small set of nations worldwide: USA/Canada, Japan, Italy, Russia and other former states of the USSR, China, India, and latterly France and Scandinavia. Participation elsewhere was strangely muted. In the "working nations" very few efforts were coordinated with sufficient vision and critical mass of appropriate talent to make progress in what we recognize retrospectively as a very challenging scientific problem.

Initial experimental efforts were not resourced, staffed or focused sufficiently to make reportable progress against this "tough problem". For reasons some of which are now quite well understood, the majority of replication attempts in 1989 and 1990 failed and most experimenters left the field. Cold Fusion (CF) or Low Energy Nuclear Reaction (LENR) became a scientific orphan with no country, institution or technical discipline accepting parentage or responsibility for what might if proven correct, controllable and scalable be mankind's most promising alternative for a secure, sustainable and benign energy future. How can this paradox be rationalized and what must be done to resolve it?

One of two things must be done – probably and preferably both:

(1) Clear scientific evidence must be furnished that nuclear effects take place in condensed matter by mechanisms different from reactions in free space.

(2) Demonstration must be made of a practical use of the energy so created.

Why is this so hard? Why is the bar set so high? The answers lie in history, tone, tradition and cognitive dissonance, none of which issues are we interested in addressing here. Having observed and contemplated this matter for a very long time I assert that "1" without "2" will not work to communicate effectively to the world the reality/importance of "cold fusion". I offer in support the case of tritium that is most certainly produced anomalously in some CMNS experiments. The evidence of this is sufficiently strong, well-published and replicated already to call into question at least an important core of what we believe that we "know" about nuclear processes and nuclear fusion in condensed matter. It is ignored because of our unwillingness/inability as a species to abandon a comfortable paradigm for no perceivable immediate advantage.

It is likely that "2" without "1" will not work either to convince the world of "cold fusion" reality for a different set of reasons. Our efforts to explore and develop Fleischmann–Pons (and other, later) claims have been ridiculed and marginalized. So much so that none but the most courageous dare pursue Martin Fleischmann's undertaking to engineering scale-up and device-production absent certain scientific backup[a]. Our required "proof" need not rise to the level of a fully developed theory. But reactant(s), product(s) and physics-based mechanism will need to be clearly identified before serious investment will be made[b]. Considerable progress occurred with the identification by Melvin Miles in 1990 of ^{4}He as a product, presumably of deuterium reaction, in quantity effectively commensurate with excess heat observation. Although replicated in a number of laboratories around the world the claim of heat-helium nuclear correlation has not produced persuasive effect in the broader scientific community and is challenged even within the CMNS community. If this is to be our "scientific proof" then considerably more and better scientific studies will be needed in this direction, or another.

An important part of the very effective ostracism of CMNS results and research is prevention of publication in mainstream journals. Most recently this has occurred behind an editorial modesty screen of "*we do not think our readers would be interested in this topic*" – even with the failure of review to identify technical error in attempted publications. If we cannot publish then academic pathways are voided and young aspiring academics will have little incentive to join our undertaking. Partly as a consequence of this action – or inaction – we are suffering seriously from a critical "missing generation" in cold fusion research. Fortunately scientist born after ∼1980 are largely unaffected by the negativity generated in 1989/90 and remain open and often interested in CMNS. It is time for us to assist and encourage their scientific pursuits.

Cold Fusion began its modern public incarnation on March 23, 1989, six days before Martin Fleischmann's 62nd birthday. Stan Pons was 45 … I was 40. I would argue that Physical Scientists do their best work from their late 30's through their early 60's (Physicists earlier, Mathematician even more so). Stan and Martin were well in this groove – Martin on the "leading edge". I was a youngster in what I now recognize reflectively as my most effective and productive scientific years. After graduating my PhD trained by one of John Bockris' first PhD students (John Tomlinson), I had taken advantage of two years of postdoctoral study at the University of Southampton in England. By 1989 I had more than a decade of "on the job training" at "Stanford Research Institute" (SRI) one of the research powerhouses of Silicon Valley, and the first and (at that time) the largest "not for profit private" research institute in the world. I had a research group of 16 Electrochemists supported by SRI technicians and administrators – I was primed, educated and well-equipped to start a new undertaking.

Twenty-eight years on we are missing precisely that middle generation of trained but energetic scientists who are young enough to contend comfortably with novelty but mature enough to temper innovation with experience. If you

[a] Several offers and claims have been made to produce a "useful", "scaled-up" product but none as yet have succeeded.

[b] Ironically when these three factors are identified most will not be able to invest as the most powerful forces on the planet will have commanded production and controlled IP.

accept my premise then examine the age distribution at our conferences or in our publications; you will find that my core age group is un-represented or at best grossly under-represented. We are obviously heavily blessed with the group 65+ whose access to funding is not closely coupled to perceived reputation in the broader scientific community. We are having some success attracting the <35 groups who avoided the "cold fusion stigma" (except via Wikipedia and the publication embargo). The young and the old have courage to look in new places but scientists of the age and position I was in in 1989 presently are heavily discouraged from entering CMNS. In a world of contract research where reputation is everything anyone except the most courageous seeking to build a research team simply cannot afford to swim against the mainstream – just the denial of publications and patents ensures this. I claim we cannot succeed by diligence and hope alone without this core group of mid-career scientists, and many such groups working well together.

How do we engage the critical group of researchers, giving them confidence that there is a "there there", that it may be of supreme importance to science and mankind, that funding will flow, and that insults will not. I would like to spend the remainder of my time on one thing that I think we can do to effect a complete revolution in thinking in the broader scientific community and dispel instantly the curses visited on us and discussed above. Some have argued for the development and promulgation of a procedure for a "reference experiment" that reliably embodies the elements of "new cold fusion" that produces unambiguous and obvious evidence, and is easily performed by anyone (or any laboratory) with "normal skill in the art". I argued against the wisdom of this at ICCF-14 in 2008 on the grounds of public safety but also made the point [8]: *"If the claim is made that replication is crucial to the development of our field to determine the parameters for advancement, to prove reality to critics, or to uncover systematic error, then it is astonishing that attempts to replicate the FPE have been so few, and methodologically so limited . . . it must be completely understood that this lack of attention to detail . . . is precisely the reason that the question of replicability remains on the table".*

The attempts at real replication are few and unconvincing (here I exempt Lonchampt and Biberian [9], some of the efforts at SRI, and few others). Part of the reason for failure is insufficiency of funding and experience. Although large amounts of money were available in 1989/90, and a tremendous amount of talent entered the field (if only briefly), no good procedure had been published (that is still true) and each of us was left alone to decide what it might be that Fleischmann and Pons had actually done. By and large the folk who enthusiastically or otherwise answered Admiral Watkins call [10] to the first ERAB panel on April 24, 1989 to . . .

(1) Review the experiments and theory of the recent work on cold fusion.
(2) Identify research that should be undertaken to determine, if possible, what physical, chemical, or other processes may be involved.
(3) Finally, identify what R&D direction the DOE should pursue to fully understand these phenomena and develop the information that could lead to their practical application.

. . . were simply unable to complete their assignment. Even with good will, ability and intent (which was not universal) this charge was impossible. There was no theory and the application of hot fusion concepts were, as Julian Schwinger pointed out [11] irrelevant and misleading. There was very little work complete at the time of ERAB-1, of sufficient duration to overcome what was later discovered to be a long initiation time for the FPHE, performed by people with "normal" (or sufficient) "skill in the art" of electrochemistry. And the work that was done by at least some of the folk who had skill sets pertinent to the experiments proposed and reported by Fleischmann and Pons was being done in secrecy, or at least semi-secrecy, and was not available for the ERAB panel to review in any detail (my work at SRI included).

With my personal knowledge of Fleischmann and Pons, (then) >18 years of training in the Bockris/Fleischmann school of physical electrochemistry, and already >10 years experience with the electrochemistry of the Pd/D system, I and my group were better positioned than most but still we had to guess at a lot of the detail behind what Fleischmann

and Pons had done. With detailed ignorance but considerable exposure to Martin's thinking and manner of research we simply set out to test the hypothesis that: "*there is an unexpected and unexplained source of heat in the D/Pd System that may be observed when Deuterium is loaded electrochemically into the Palladium Lattice, to a sufficient degree.*" This hypothesis was tested positively with funding support from EPRI, and several other conditions were discovered that control the FPHE. More conditions remained and remain to be discovered and we are not in a position to completely specify a written procedure that if followed by one of "normal skill in the art" will lead in every case (or in most cases) to a convincing demonstration of condensed matter nuclear effects – of any kind!

Ironically it was John Huizenga himself, cold fusion bête noire and co-chair of the ERAB-1 panel, who most succinctly identified the greatest barrier to early progress, although he used his wisdom to make the wrong point. Citing his principal reasons for rejecting cold fusion Professor Huizenga stated that: "*It is seldom, if ever, true that it is advantageous in science to move into a new discipline without a thorough foundation in the basics of that field.*" This is useful advice that could be well applied today. But what Huizenga did not note and probably never internalized is that the discipline of the Fleischmann Pons Heat Effect *is Physical_Electrochemistry* and the most pertinent diagnostic tool to study heat effects is calorimetry. Both were new and alien disciplines for most in the nuclear physics community and well out of their fields of competence or even comprehension.

Instead, by couching the argument in the terms of high energy physics, the nuclear physics community moved the debate from our field of mastery into theirs. In doing so they claimed or asserted the intellectual and moral "high ground" and could speak (legitimately) knowledgeably and (mostly) correctly about "absence of neutrons", "insufficiency of tritons", "no gammas", "coulomb barrier penetration" and other paraphernalia of hot fusion. Obviously we were politically outmaneuvered. None of these effects then or now appeared or appear necessarily to be relevant to condensed matter and coherent nuclear reaction. The prince of this field, Julian Schwinger, was at least willing to consider the findings of Fleischmann and Pons to be plausible. The discovery by Mel Miles of a statistically huge correlation between heat and helium production further underscored Schwinger's dictum that "*the circumstances of cold fusion are not those of hot fusion*". However irrelevant, simplistic, outmoded and out-of-discipline the hot-fusion-based objections appear on this side of Alice's looking glass we should pay great attention to the fact that these arguments have not gone away because they have not been effectively rebuffed! What do we need to do? Who is the audience that we need to convince? What is the most effective strategy? What disciplines and skill sets are most appropriate to define CMNS?

I do not think that "merely replicating" will be sufficient. To persuade the people that we need to engage will take more than "science" or "numbers". This has been very well understood by some in the "cold fusion" community and several implied offers or predictions have been made of practical device production on timescales as short as "next year" (see footnote 2). Each visit I have made to the Venture Capital community in the US has resulted in the same response: "*Very interesting; please keep us informed; come back when you have a prototype"*. My retort has been the same in each case: "*If I had a prototype why would I need you*?" This glib response ignores the fact that VC's offer more than capital and can support an effective path to commercialization as the success in Silicon Valley shows.

The Silicon Valley model, however, may not be well suited to develop something as technology-intense and critically important as an environmentally benign, universally-accessible, safe and effectively unlimited, large-scale primary energy source. Having watched and participated in the Silicon Valley "green energy revolution" – and shared in its disappointing (albeit predictable) under-success I feel we need another path. To quote myself [12]: "*The results we are seeking will benefit all mankind. Likewise the team of talent and consensus needs also to be multi-national.*" What other models do we have to attempt and succeed in that which Machiavelli [13] warned us so clearly about? "*There is nothing more difficult to take in hand, more perilous to conduct, or more uncertain in its success, than to take the lead in the introduction of a new order of things.*"

Who with the requisite power and influence has this courage, and what do we need to do to attract (and sustain) their attention? I see two levels in this. First while I do not expect the venture community to be likely allies, the people

who have become rich through ventures might be. These are technically adroit individuals (or groups of individuals), although none would be considered as having "normal skill in the art" of the FPHE (electrochemical or gas/metal). All such individuals will seek expert opinion. Having served often in a "due diligence" capacity I can confirm that the riskiest thing is to say "yes" to a complex prospect that requires large funding (and time) for completion. The talisman that we create to facilitate communication about CMNS must work on two levels:

(1) It must be sufficiently simple and obvious that no hidden error can possibly exist to negate the result, or leave any doubt. This obviousness must be clear to the potential sponsor so that simplistic negation (or introduced complexity) such as those used in the past[c] carry no weight.
(2) The energy produced must be sufficiently net positive that useful work can be, and is being, made of it.

So now we know:

- *Who*: rich, modern, successful industrialists and their selected experts, and
- *What*: something simple that makes power and thus energy, preferably in electrical form that is easily measured and can be used to supply the conditions needed for control, self-sustainment and utility.

The last sounds like a tall order but it is important to note that our first level prototype does not need to be practical, elegant, cheap or civilian-safe. It needs to be "somewhat reliable" limited by the patience of the reviewers, and "somewhat durable" since it will need to overcome any concerns about stored energy. The technology chosen for the demonstration prototype may have no more to do with ultimate engineering practice than a shared underlying mechanism of power production. Its purpose is to demonstrate that the effect is real and of sufficient scale potential to contribute to a solution of man's oncoming energy deficit. Engineers will use the demonstration prototype (perhaps in second generation form) to explore the parameters of control and scale-up.

It should be noted also that the means of operation of our demonstration prototype does not need a theory or a known and detailed mechanism to be effective. Theoretical help would greatly aid the development of the prototype and help with scale-up, and it would be quite irresponsible to scale a known nuclear effect (and particularly to impose it on society) if the underlying physics is not at least "somewhat in hand". Nevertheless, most technological inventions have been engineered into existence with the science backfilled afterwards. We must anticipate that this will also be the case for "cold fusion" (in inverted commas as we would not know what it really is until we have theory).

If you accept the argument so far, what are good candidates for the demonstration prototype? Which technology? What size? Our object is to make this *as easy as possible for ourselves* (at this stage) – and everyone will have a personal choice based on individual experience and training. At this stage I would like simply to mark out the terrain and see if by discussion and sharing of experience and analysis we can arrive at high probability choices for our demonstration prototype. I restrict attention here to effects explored and discussed under the rubric of "cold fusion" or CMNS (explicitly excluding zero point energy and the "black light" sub-quantum concepts of Randy Mills).

I see two major choices and one hybrid. Each has demonstrated useful characteristics and exhibited potential to conceive our demonstration prototype. This list is restricted to those technologies with which the author has had direct experience. Other approaches are possible and input is welcomed. A short list of proto-technologies that might be used to make a demonstration prototype follows:

[c] Requirements of an equal branching ratio (neutrons and tritons as in hot fusion); violation of the first law of thermodynamics; non-conservation of baryon number; the "impossibility" of measuring ^{4}He in a D_2 background; and similarly science-sounding but misapplied criticisms. Again for the sake of fairness and completeness it must be noted that legitimate criticisms have been leveled, and questions asked, that have not been fully answered or even addressed.

(1) *Electrochemical PdD/LiOD at elevated temperature* using superwave (or some alternative) disequilibrium stimulus. The progenitors of this avenue are Fleischmann and Pons (electrochemical PdD/LiOD), Fleischmann/Lonchampt/Biberian (elevated temperature), Dardik/Energetics (superwave stimulus). The best example of success is ETI-64 [14] which manifested >30 W thermal output with <1 W average electrochemical input. It exhibited an integrated thermal energy output of 1.14 MJ for an integral electrical energy input of 40 kJ over a 14-h period. This cell boiled the coolant (H_2O at ∼1 atm.) during this excursion and then again with greater energy output subsequently.
(2) *Metal–hydrogen gas systems at elevated temperature*. The metal, typically in small dimension form, can be palladium, nickel, some alloy or coating of Pd on Ni, or some other metal having the capacity for high hydrogen permeability. The gas is an isotope of hydrogen: protium, deuterium or tritium – or a mixture. Some observers suggest that protium "works" with nickel, not palladium, and that deuterium is effective with palladium and not nickel. I think it is fair to say that the Ni–H gas system has experienced less experimentation than Pd–D and the findings are more controversial. Nevertheless the claims, if shown to be valid, are stunning: power generation of hundreds of kW, at temperatures above 500°C, sustained for meaningful periods without input power. Certainly this could form the basis of an ideal demonstration or even working prototype.
(3) *Metal–gas modulated plasma*. Somewhere between items 1 and 2 lies glow discharge. This incorporates the advantages of electrochemistry (high chemical potential, high fluxes) and gas systems (short initiation time, low thermal mass, high temperature, low inventory of impurities and lower corrosivity). Representing Energetics Technologies (Incorporated and operating in Israel as ETI but headquartered in New Jersey) Arik El-Boher presented at ICCF10 [15] what was then and remains today one of the most exciting discoveries in Pd–D heat studies. Energetics struck a super-wave modulated glow discharge between thoriated tungsten and a thin palladium coating (on stainless steel) in sub-atmospheric D_2. The experiment produced boiling water with a power gain of 3.88 and an energy gain of 6.72 (because of conspicuous "heat after death") over a period of 10 h. Because the temperature of the plasma was quite high (although unmeasured) one can easily conceive of a demonstration prototype but this experiment has not been replicated to my knowledge despite the best efforts of El-Boher, Energetics and SKINR.

Of final consideration is the size of demonstration prototype. What size is easiest to accomplish with the selected proto-technology and on what scale do we need to operate to engage effectively our selected audience? This latter choice is personal – but critical – and would benefit from wide-ranging discussion. Hypothetically, knowing nothing about cold fusion, LENR or CMNS, having attended none of our conferences or read (or understood) any papers on this topic, what would it take to persuade you that a machine that you are looking at (measurements permitted) is converting nuclear energy to thermal or electrical? The power – in fact the point – of this claim is that the energy density of nuclear reaction is $\sim 10^7$ times that of chemical or mechanical energy storage. Obviously one would need to observe and interrogate the demonstration object and its power production (with full access) for periods sufficiently long to rule out all conceivable potential chemical or mechanical energy storage processes.

It is important to reflect that effects with these characteristics have been shown or claimed before – although not in a demonstration setting – which have so far failed to convince our target audience or the science community at large. Why has what we have done not compelled the acceptance of the FPHE? There are several reasons:

(1) *We have observed no (or few and incommensurate) energetic nuclear products*. In all situations except ours this would be a good thing (provided that the heat was real). A nuclear process without dangerous nuclear products prompt or long-lived, especially from plentiful, cheap and harmless reactants, may have the potential to secure a benign and sustainable energy source for the next millennia. But proving a nuclear effect without energetic nuclear products is challenging precisely because of our distaste for and fear of nuclear processes.
(2) *Calorimetry is not well respected or understood*. Heat is the principal product predicted and observed by

Fleischmann and Pons, and by all serious replicators of their claim (the FPHE). Most such experimenters relied on calorimetry in their cold fusion studies. Calorimetry is an ancient tool, little taught, used or comprehended. The SRI team needed to teach themselves calorimetry in order to interrogate and expand the Fleischmann–Pons claims. Even today confusion and controversy exist inside the field about the "best" – or even acceptable – means of calorimetry. This tool is considered (by some) to be intrinsically inaccurate – this despite the fact that calorimetry forms the basis for modern chemical thermodynamics for which considerable precision and accuracy is required to sustain the entire chemical industry.

(3) *Heat is ephemeral*. When heat is not present there is little evidence of it having been there unless work has been done with the heat. Failing this we may have indications of prior melting or phase change that only experts can interpret. To "sell" the pre-existence of excess heat one must make convincing argument on the basis of "measurements" and "numbers" alone. While this is a normal case in science many of the people we must convince are not scientists and are not willing to trust the proof of an "impossible" (or at best highly novel) effect to an analysis of "mere numbers", or the testimony of one "expert" over another.

(4) *The effect is "small"; relative*. The set of proto-technologies suggested above were selected precisely for their potential for large (and scalable) effects. Especially for electrochemical technologies the input power requirement is large and of long duration. Loading is achieved and maintained by the imposition of a potential gradient in a low impedance system (the electrochemical cell). The current that flows is large and must be maintained for very long times (hundreds of hours for bulk Pd) to overcome initiation effects while maintaining loading. Except during initial loading essentially all of this current flows to parasitic processes, primarily D_2 and O_2 evolution. For aqueous electrochemical loading this cannot be avoided but means that any excess energy generated by putative nuclear processes must be superimposed on a large input power (*IV*) and even larger input energy (*IVt*) because of the integration of energy during the long initiation phase. The maximum excess power typically observed at SRI in $>$100 successful experiments was 3–30% of P_{in}. Although statistically certain this is still a small heat effect relative to input power and is not persuasive to anyone unfamiliar with the experiment and calorimeter details. It is also "not enough" as will be shown later in this paper.

(5) *The effect is "small"; absolute*. In his first book published in 2007 [16] Ed Storms cites 242 successful heat-producing experiments around the world (123 electrolytic). Of these 117 (64 electrolytic) show excess power of 1.25 W or less. His histogram (Fig. 40 in [16] and reproduced as Fig. 1) falls off roughly exponentially and rapidly with maximum produced excess power so that cells exhibiting a maximum excess power of 1.25–2.5 W are only 35 (18 electrolytic) and 2.5–3.75W are only 23 (12 electrolytic).

How much heat is needed to convince a non-expert? It could be argued that since the FPHE cannot directly be seen "the evidence must be palpable to be real". The threshold of tactile perception depends on several factors but one might reasonably expect to be able to distinguish by touch the thermal difference due to switching 10 W thermal into or out of a "small" system. By the time we get to a "modestly robust" level of excess power with range 10 ± 1.25 W the count of successful FPHE experiments worldwide from 1989 to 2006 reviewed by Storms is 16 (nine electrolytic). But there is some power in the tail and Storms' world count of experiments producing $>$10 W of excess power is 40 (with only 15 electrolytic). This is 17% of all successful heat-producing experiments reviewed by Storms. The $>$10 W level reflects only 12% of electrolytic successes but the rapid drop-off in excess power levels from electrolytic experiments is likely due to the expense (as well as hazard) of large Pd/D_2O electrochemical experiments.

Figure 1 plots a histogram of all successful excess heat production reported in the interval 1989–2006 as reviewed by Storms [16]. The analysis inset in the upper left demonstrates the roughly exponential character of these data. But, as noted above there is "power in the tail" and if we accept 10 W as a "sufficiently robust" level of excess heat production for our demonstration prototype then this should be plausibly achievable. Our demonstration object is, however, required to do more than "feel warm". We need it to generate sufficient electricity to self-sustain for which

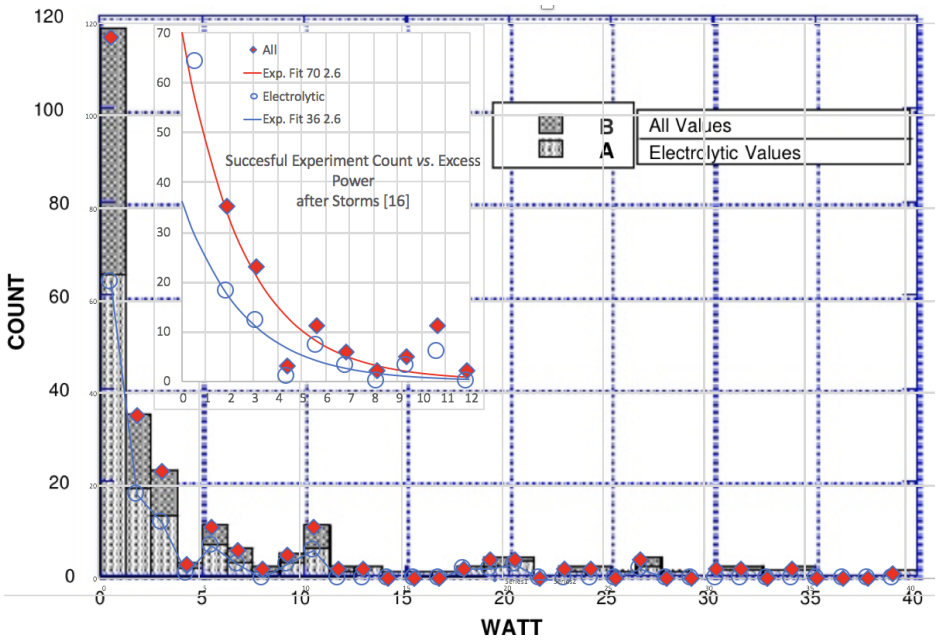

Figure 1. Histogram of successful excess heat production 1989–2006 from [16]. Filled diamonds are all experiments, open circles are electrochemical.

we require energy gain and significantly elevated operating temperature to offset the strictures specified by Sadi Carnot, and worse.

Figure 2 plots the Carnot limit as a solid blue line referenced to the right axis as a function of operating temperature with a heat rejection temperature of 20°C. Also plotted are a family of curves showing the electrical power (in W) "available for use" over the range of operating temperature, calculated for the stated hypothetical gains at a (nominal) input of 10 W. The gains selected are: 2, 3, 5 and 20. Note that Carnot is a limit that cannot be achieved and becomes increasingly difficult to approach as operating temperature reduces. What is clear is that for a gain (heat out/electrical in) of 2, at 10 W electrical power in, one could generate 1 W of power for demonstration above that needed for sustainment, *even in the limit, only above* ~ 460°C!

Obviously operating temperature is important and more is better. But gain is even more so. For a gain of 20 (the top curve) we achieve our "extra" 1 W of electrical power for demonstration (in the limit) at only 70°C. By 100°C (the minimum temperature of ETI-64) ~1.6 W of "extra" electrical power would be available for demonstration. Clearly gain is of the essence and the essence of gain is reducing the denominator. Superimposed in Fig. 2 are data points

Table 1. Characteristics of selected cells at SRI and ETI

P_{in} Electric (W)	Cell name	T° C	Net Electric (W)	Gain	Percentage of P_{in} (FM) (%)
2	P19	35	–1.7	2.9	–86
20	P15	65	–16.5	1.3	–83
1.25	L14-2	55	–1.01	1.8	–81
0.093	Pd-C	45	–0.07	3.0	–76
0.55	ETI-GD	**100**	0.24	6.7	44
1.1	ETI-64	**100**	5.3	27.5	490

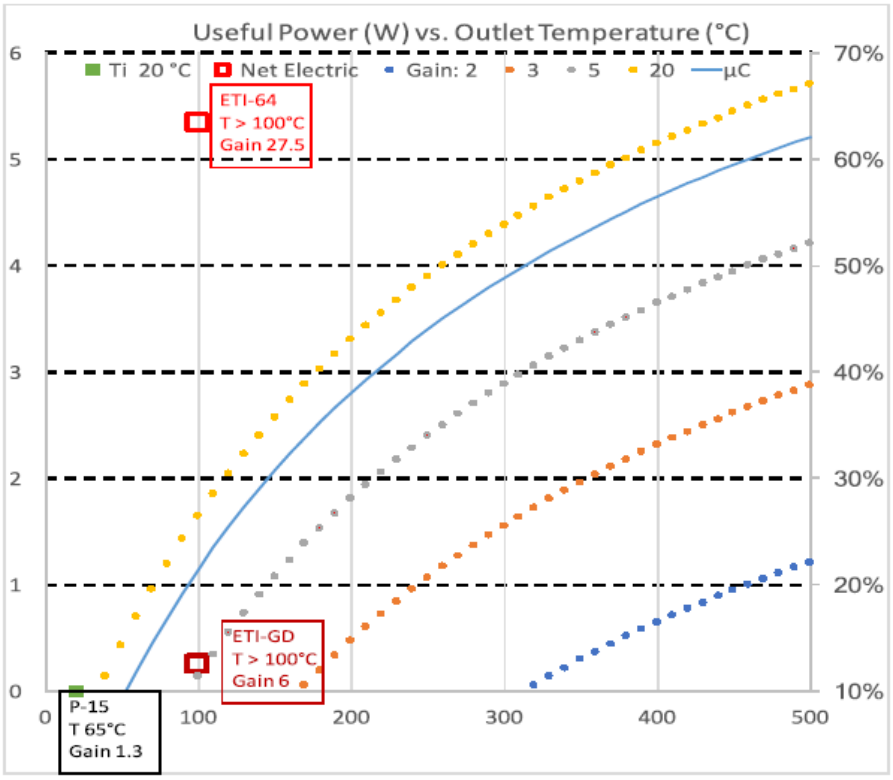

Figure 2. Carnot limitation (solid blue curve referenced to right axis) and hypothetical electrical output for ideal Carnot conversion at the temperatures and gains shown.

from performed experiments: four from SRI and the two cited above for ETI, with characteristics cited in Table 1. Note that the column "Net Electric" is the value calculated for demonstration from P_{in}, T, the measured power gain and Carnot. The percentage of P_{in} is Net Electric divided by P_{in} and can be read as a "Figure of Merit" (FM) for the different experiments. The temperature listed for the two ETI cells is reported as a minimum value and so therefore is the Net Electric Power that might potentially be available.

As clearly seen in Fig. 2 the SRI experiments "fail to register" and have negative FM. Even with perfect Carnot thermal-to-electric conversion the 4 SRI cells all would have produced less electrical output than input because their gains and operating temperatures were too low. This comparison is somewhat unfair in that these experiments were not designed or intended to achieve the conditions for self-sustainment or net electrical production (in fact the design criteria were largely antagonistic to this goal). Nevertheless the experiments cited are "the best" available and yet clearly do not meet the criteria stated as the object of this paper.

Not so for the two Energetics experiments mentioned and listed above, and plotted in Fig. 2. The glow discharge experiment [15] just passes the bar at the temperature limit of the calorimeter (boiling water) but it is certain that higher temperatures were available in the plasma and with different design the square could climb the red dotted curve into "useful" territory. No such extrapolation is needed for ETI-64. With a gain of 27.5 this experiment would have constituted a useful demonstration even at 100°C. This point is made more directly and dramatically in Fig. 3.

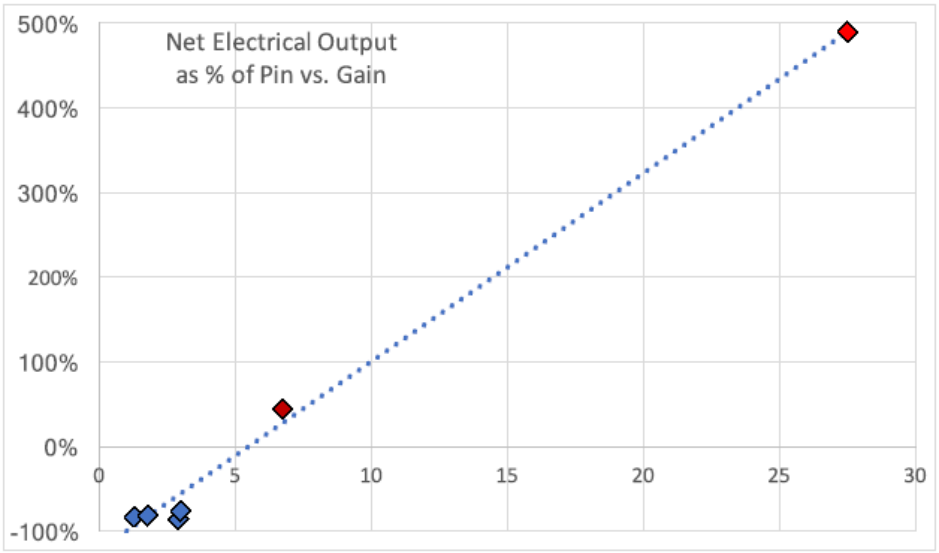

Figure 3. Net Electrical Output for ideal Carnot conversion as a percentage of P_{in} (FM) as a function of experiment thermal gain, for the experiments summarized in Table 1.

The SRI experiments (blue) all fall below zero with gains <3 and FM<0. ETI-GD comes in above the line and if repeatable might easily be "improvable" with increased operating temperature; I still regard this as one of if not the most important experiments ever performed in LENR. But based on the metric FM plotted in Fig. 3, and the goal elucidated in this paper, the star performer is ETI-64 that I have spoken of several times before – if not explicitly in the present context. If we are to approach the goal of self-sustainment with thermal output >10 W with some Watts electrical left over for convincing demonstration then we need to address the question of why ETI-64 "worked" and essentially all others did not.

3. Conclusions

(1) "Loading" (chemical potential) is important at least in creating the conditions in the lattice suitable for condensed matter nuclear processes.
(2) Flux is critical. This may be deuterium flux, electrons, or phonons (or other?). Static, equilibrium conditions do not result in the FPHE.
(3) Theory alone may not allow us to achieve our goal but will be needed for commercial acceptability and to win the help of other working scientists.
(4) To gain acceptance we must be able to demonstrate – more or less on demand – that novel nuclear effects take place in condensed matter and create net energy.
(5) Demonstration must be made of a practical use of this energy; for this we require a Demonstration Prototype
(6) To make effective demonstration, operating Temperature is important but *high gain is crucial to accomplish our goal.*
(7) Gain is more easily affected in the denominator than the numerator – our goal is to create the excess heat effect with low input electrical power stimulation.
(8) Multi-dynamic, multi-resonant processes appear to be involved or crucial in producing the FPHE. Irv Dardik

and Energetics have been demonstrated to be right in concept. To make progress we must better understand this teaching.

Acknowledgments

By "Figure of Merit" the "best" SRI experiments fail to meet my asserted demonstration criteria and were not intended to. These experiments nevertheless were crucial in establishing a basis for understanding and I would like to give special acknowledgement to the early core SRI/EPRI team who achieved this: Steve Crouch-Baker, Andy Riley, Romeu Rocha-Filho, Stuart Smedley, Fran Tanzella, Tom Passell, Joe Santucci, Sharon Wing and Susan Creamer. Particular credit needs also to be given to the Energetics team who worked so hard and succeeded so dramatically, sustained by the vision of Sidney Kimmel and Irv Dardik: Herman Branover, Arik El-Boher, Alison Godfrey, Ehud Greenspan, Shaul Lesin and Tanya Zilov. For special credit I would like to single out five individuals who have contributed immeasurably to my critical understanding: Trevor Dardik, Martin Fleischmann, Peter Hagelstein, Paolo Tripodi and Vittorio Violante. Thanks and credit is given also for valuable input to this paper from Peter Hagelstein, Abd ul-Rahman Lomax, David Nagel, Fran Tanzella and Vittorio Violante.

References

[1] M.C.H. McKubre, S. Crouch-Baker, R.C. Rocha-Filho, S.I. Smedley, F.L. Tanzella, T.O. Passell and J. Santucci, Isothermal flow calorimetric investigations of the D/Pd and H/Pd systems, *J. Electroanal. Chem.* **368** (1994) 55.

[2] D.D. Macdonald, M.C.H. McKubre, A.C. Scott and P. Wentrcek, Continuous in-situ method for the measurement of dissolved hydrogen, *I & EC Fundamentals* **20** (1981) 280.

[3] M.C.H. McKubre, S. Crouch-Baker, A.M. Riley, S.I. Smedley and F.L. Tanzella, Excess power observations in electrochemical studies of the D/Pd system, The influence of loading, in *3rd Int. Conf. on Cold Fusion, "Frontiers of Cold Fusion",* Nagoya, Japan, 1992, Universal Academy Press, Tokyo, Japan.

[4] K. Kunimatsu, N. Hasegawa, A. Kubota, N. Imai, M. Ishikawa, M. Akita and Y. Tsuchida, Deuterium loading ratio and excess heat generation during electrolysis of heavy water by a palladium cathode in a closed cell using a partially immersed fuel cell anode, in *3rd Int. Conf. on Cold Fusion, "Frontiers of Cold Fusion"*, Nagoya Japan, 1992, Universal Academy Press, Tokyo, Japan.

[5] M.C.H., McKubre, F.L. Tanzella, P. Tripodi and P.L. Hagelstein, The emergence of a coherent explanation for anomalies observed in D/Pd and H/Pd system: evidence for ^{4}He and ^{3}He production, in *8th Int. Conf. on Cold Fusion*, Lerici (La Spezia), Italy, 2000, Italian Physical Society, Bologna, Italy.

[6] M.C.H. McKubre, S. Crouch-Baker, A.K. Hauser, S.I. Smedley, F.L. Tanzella, M.S. Williams and S.S. Wing, Concerning reproducibility of excess power production, replication, in *5th Int. Conf. on Cold Fusion*, Monaco, 1995.

[7] M.C.H. McKubre, F.L. Tanzella, I. Dardik, A. El-Boher, T. Zilov, E. Greenspan, C. Sibilia and V. Violante, in *Low-Energy Nuclear Reactions Sourcebook*, J. Marwan (Ed.), ACS Symposium Series 998, Oxford University Press, Oxford, 2008, p. 219.

[8] M.C.H. McKubre, The importance of replication, in *14th Int. Conf. on Condensed Matter Nucl. Sci.*, Washington, DC, 2008.

[9] G. Lonchampt, L. Bonnetain and P. Hictor, Reproduction of Fleischmann and Pons experiments, in *sixth Int. Conf. on Cold Fusion*, Okamoto, M., Toya, Japan, 1996, p. 113.

[10] https://newenergytimes.com/v2/government/DOE1989/19890720-ERAB-Interim-Report.pdf, Appendix A.

[11] J. Schwinger, Nuclear energy in an atomic lattice, in *The First Annual Conf. on Cold Fusion*, 1990, University of Utah Research Park, Salt Lake City, Utah, National Cold Fusion Institute, *Prog. Theoret. Phys.* **85** (1991) 711.

[12] M.C.H. McKubre, CMNS research – past, present and future, *J. Condensed Matter Nucl. Sci.* **24** (2017) 1–10.

[13] N. Machiavelli, *De Principatibus / Il Principe*, 1532.

[14] I. Dardik, T. Zilov, H. Branover, E. El-Boher, A. Greenspan, B. Khachatorov, V. Krakov, S. Lesin and M. Tsirlin, Excess heat in electrolysis experiments at energetics technologies, in *11th Int. Conf. on Condensed Matter Nucl. Sci.,* Marseille, France, 2004.

[15] I. Dardik, H. Branover, A. El-Boher, D. Gazit, E. Golbreich, E. Greenspan, A. Kapusta, B. Khachatorov, V. Krakov, S. Lesin, B. Michailovitch, G. Shani and T. Zilov, Intensification of low energy nuclear reactions using superwave excitation, in *10th Int. Conf. on Cold Fusion*, Cambridge, MA, 2003.
[16] E. Storms, *The Science of Low Energy Nuclear Reaction*, World Scientific, Singapore, 2007.

Addendum

Not discussed at Asti and added in review is the possibility that new or more complete data on heat–helium correlation might provide a suitable basis to complete the initial phase of CMNS research and answer the question: *"is it real?"*, to allow us to proceed to phase 2: *"what is it good for?"*. Having pursued this experimental question intensively for several years my caution and condition is as follows. Helium (specifically ^{4}He but also ^{3}He and preferable both) will become much more easily measurable and convincing when the FPHE is triggerable more or less on demand. The issues of leaks and pre-occurrence of these isotopes can be effectively allayed if measurements can be made from samples taken from the gas phase immediately before and after a triggered heat event.

J. Condensed Matter Nucl. Sci. 26 (2018) 15–31

Research Article

Expectations of LENR Theories

David J. Nagel*

The George Washington University and NUCAT Energy LLC, 725 23rd Street NW, Washington DC 20052, USA

Abstract

The mechanisms that cause Lattice Enabled (or Low Energy) Nuclear Reactions (LENR) are still not understood, even though much is known empirically about LENR. We provide list of 24 observations from almost three decades of LENR experiments. These observations require theoretical explanations. This paper deals with two aspects of the many theories about the mechanisms. The first is the *theories themselves*, i.e., their characteristics and results. The few dozen available theories on LENR mechanisms are diverse and complex. Only a lengthy paper could properly summarize their essence, including all assumptions and implications. Such a thorough review of extant LENR theories would be challenging to write. Here, we merely indicate reviews and other sources of information on LENR theories. The second focus of this paper is the *status of development* of LENR theories, specifically, the completeness of their elaboration. It is possible to detail what is expected of LENR theorists by experimentalists, teachers, students, developers and other interested personnel. We provide and discuss ten questions for LENR theoreticians about the description (characteristics) and status (development) of their ideas. The nearly three decades of theoretical work on LENR has resulted in remarkably few well-developed theories. None of them has yet been adequately tested and widely accepted. There remains a great opportunity for some theoretician to provide the basic understanding of LENR. That understanding would enable or speed the commercialization of this new, clean, promising and much needed energy source.
 ISSN 2227-3123

Keywords: Empirical observations, Heat–He correlation, LENR, Low energy nuclear reactions, Theory

1. Introduction

There are two large opportunities for fame and fortune available in the field of LENR, understanding and exploitation. When scientific understanding of LENR has been achieved, the mechanisms active to produce LENR and their characteristics, notably their rates, will be known. It is likely that the person or team, which eventually provides that understanding, will be feted for their accomplishment.

Experiments have shown that LENR can provide high power and energy gains, with much more thermal energy coming out of LENR cells than is put into them electrically. Further, operation of LENR does not produce dangerous prompt radiation, significant radioactive waste or greenhouse gases. Commercial LENR generators are expected to be relatively small, so they can be distributed and independent of the grid. Their use in homes would give consumers

*E-mail: nagel@gwu.edu.

 ISSN 2227-3123

control over their energy generation, similar to how they now control their energy usage. Such generators would not be subject to brown or black outs, or other grid-related problems. Because of their gains and other favorable characteristics, safe and reliable generators based on LENR should be very cost-effective and attractive to customers. Hence, commercial exploitation of the features of LENR ought to be very remunerative. That is why over 20 small companies in at least nine countries [1] are seeking to develop prototypes of LENR generators even before the mechanisms that produce power and energy are understood.

Because understanding of LENR will solve a current major scientific riddle, and because that understanding will promote earlier and better commercialization, we focus on theories for LENR in this paper. Section 2 summarizes many of the empirical observations, which have come from over a quarter of a century of experiments. It is possible that some of those observations are either wrong or irrelevant. However, most of those observations will withstand the test of time. The entire body of empirical knowledge constrains and tests the activities of theoreticians. Put another way, the items listed in the next section challenge theoretical developments aimed at understanding LENR.

Section 3 is a summary of earlier reviews of the actual content of LENR theories. Those studies are important milestones on the road to eventual understanding of LENR. Section 4 is the body of this paper. It provides and discusses the 10 questions for LENR theoreticians. Those questions seek to determine the characteristics and status of the diverse theories. Section 5 gives a summary of the primary points of this paper, and adds some comments on what is needed to speed the theoretical and quantitative understanding of LENR. Appendix A provides a possible scenario for correlations between heat and helium generation beyond conventional single-step fusion reactions.

2. Empirical Observations of LENR Characteristics

The history of science has instances where it has taken decades for ideas to be verified or observations to be explained. Wegner put forward the idea of plate tectonics in 1912 [2], but observational evidence for its correctness did not emerge for about forty years [3]. Einstein published the equations for stimulated emission in 1917 [4]. However, it was not until demonstration of the MASER by Townes in 1954 that those equations were shown experimentally to be correct [5]. In both of those cases of theory-before-observation, the core ideas were relatively simple, and the needed observational or laboratory techniques had to be developed. The reverse also happens. Onnes discovered superconductivity in 1911 [6], but it was not understood until 1957 [7]. That phenomenon was found in many materials in the decades between the initial discovery and the elucidation. However, the core problem was relatively simple, namely how could electrical resistance go to zero at suitably low temperatures? The situation with LENR seems to be more complex, with very many types of experiments and diverse findings. But, the major observations can be stated simply. That is done in the rest of this section.

The central finding from thousands of LENR experiments over almost 30 years is the following: it is possible to use chemical energies on the scale of electron volts to release nuclear energies in the range of mega electron volts. It has to be emphasized that the ability to release nuclear energies by using chemical energies enables high energy gains. That is, it is possible conceptually, and has been demonstrated experimentally, that much more thermal energy can be gotten from an LENR experiment than is put into it to cause the nuclear reactions. The gain is defined as the ratio of the output thermal energy to the input electrical energy. LENR gains were summarized in a recent paper [8]. There is strong experimental evidence for gains as high as 26. The largest reported LENR gain, which is neither verified nor reproduced, is 800 [9].

A schematic perspective of barriers to reactions, and both chemical and nuclear energy gains, is given in Fig. 1. In chemical reactions, the barrier energy is on the order of the reaction energy on a scale of electron volts. The barrier arises from the energy needed to take apart the existing reactant molecules to produce new arrangements in the products. In nuclear reactions, the barrier is a significant fraction of a mega electron volt, and the reaction energy is commonly greater than one mega electron volt. That barrier is due to the electrostatic repulsion of two positive nuclei,

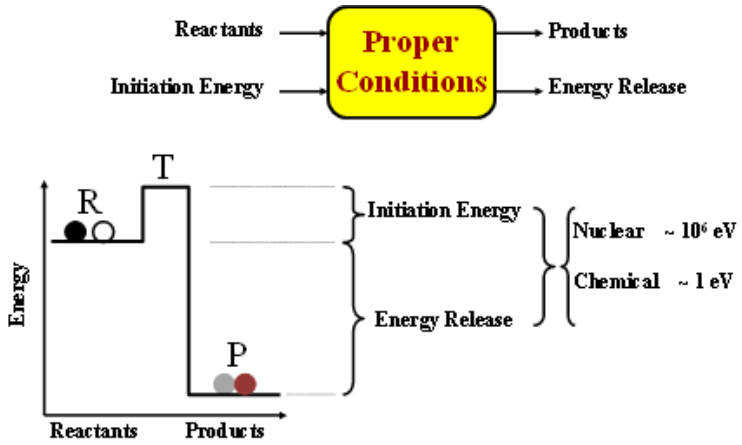

Figure 1. *Top*: Schematic of the flows of matter and energy into and out of a reaction, either chemical or nuclear. *Bottom*: Diagram showing the energy levels for the Reactants (R) in their initial and Transition (T) states, and the energy level of the resulting Products (P). As noted, the energy scale for nuclear reactions is roughly one million times larger than the energy scale for chemical reactions.

the so-called Coulomb barrier. The remarkable and still mysterious aspect of LENR is that chemical energies can turn nuclear reactants into nuclear products.

Even modest LENR gains, say, less than 10, would have great impact. Electricity generation is not efficient due to the multiple necessary steps. Currently, the chemical energy in fossil fuels is first converted to thermal energy, and then to mechanical energy, and then, finally, to electricity. Each step has inefficiencies due to various losses, such as conductive losses and friction, on top of the inescapable thermodynamic (Carnot) losses. Only about 40% of the energy in coal or gas can be converted to electricity [10]. And, a significant fraction of the electrical energy is lost in transmission from large generation facilities to users. The electricity transmission losses in the US average 7–8% [11]. There are over 7000 electrical generation plants in the US [12]. Hence, transmission inefficiencies waste the power generated by about 500 of them. The ability of LENR to (a) provide significant gains from (b) small distributed generators of heat and electricity would make electrical power more cost effective.

It is noted in passing that the largest current hot fusion experiment is seeking a gain of 10. The International Thermonuclear Experimental Reactor (ITER) is being built in the south of France for over $20B. The project is expected to take over 20 years. It will not necessarily result in the design for a large and costly practical power station. Yet another, similarly large experiment will be needed prior to commercialization of power from hot fusion. Ultimate hot fusion power stations will be large and expensive, with transmission losses. An investment in research and development for LENR at even 10% of the level of hot fusion funding could result in understanding and commercialization on a time scale as short of half of the time for the ITER construction and testing.

In addition to the central gain characteristic of LENR, there are many other empirical observations that must addressed by LENR theoreticians. Lists of empirical observations have been given by several authors. Storms 2007 book has a list of 12 observations [13]. The organizers of ICCF-14 provided 10 high-level statements about the results of many LENR experiments [14]. Recently, Hubler provided another list of experimental LENR observations that beg explanation [15]. There are other lists, but those three cover most of the salient points. The following list is an integration of the points made by those and other authors, with our wording.

(1) Nuclear reactions (MeV output) can be initiated by using chemical energies (eV input).

(2) There are many ways to produce LENR and to measure their results.
(3) Diverse solid materials have been shown to produce LENR (Pd, Ni, Ti, alloys, etc.)
(4) Both protons and deuterons can be involved in LENR under some circumstances.
(5) Many conditions can result in LENR, with lattices in liquids or gases.
(6) Initiation times for production of LENR vary widely in different experiments.
(7) Disequilibrium conditions, with high proton or deuteron fluxes, favor LENR.
(8) Some LENR occur in small and distinct regions on or near the surface of materials.
(9) A few measurements show that LENR can occur during sub-millisecond times
(10) High power and energy gains have been measured in diverse experiments.
(11) High power densities and energy densities, and energy per atom values, are possible.
(12) High temperatures are not needed to produce LENR, but rates increase with temperature.
(13) For electrochemical experiments, high ratios of deuterons to Pd atoms favor LENR.
(14) Excess power has also been measured with lower ratios of deuterons to Pd atoms.
(15) Cathode surface texture, roughness and impurities significantly influence LENR
(16) Application of laser light, magnetic fields and some other effects increases LENR.
(17) Different outputs from LENR experiments are measurable with diverse instruments
(18) Production of large heat, tritons and helium indicate that nuclear reactions occur.
(19) Heat »tritium »neutrons, so LENR are not due to conventional D–D fusion.
(20) Fe, Zn and Cu are the most common transmutation products (fission occurs?)
(21) Some evidences show that living organisms can cause nuclear transmutations.
(22) Heat production has sometimes been correlated with nuclear products, especially helium.
(23) Little prompt radiation or radioactive waste, and nearly zero green house gases come from LENR.
(24) LENR, when understood, reproducible and controllable, might provide the basis for new, clean, commercial, cost-effective, distributed energy generators.

It must be noted that some of these empirical observations are not consistent with each other. Items 13 and 14 on the loading of deuterons (D) into palladium (Pd) provide an example. Clear evidence has been presented that achieving a high ratio of D/Pd is necessary (but not sufficient) for production of LENR energy [16]. However, in contrast, Storms found that "…excess power is independent of the D/Pd ratio and applied electrolytic current, being only sensitive to temperature." [17] These statements, and the diversity of the entire list of empirical information, challenge those who seek to understand LENR. It is likely that full verification of these observations and their quantitative understanding will take many years to achieve.

An informed and diligent reviewer could take each of the two dozen observations listed above, and assemble a collection of publications to back up every observation. That is, these empirical "facts" are not the result of singular papers or other reports. This list, the result of over one-quarter of a century of careful experimentation, is a very stern challenge to LENR theoreticians.

Imagine a matrix that lists each of the above 24 empirical observations against each of the dozens of LENR theories. Many (most??) of the theories would be eliminated by one or more of the listed observations. Unfortunately, many LENR theories fail at the conceptual level, as will be discussed in Section 3.

3. Milestones in Evaluation of LENR Theories

There are dozens of theories about what causes LENR. Most are incompatible with other LENR concepts. Theories are ultimately in competition with each other. Understanding and assessing the *characteristics* and *status* of each theory is a major first step toward down selecting theories. Those goals motivate this paper.

There have been a few more or less thorough reviews of LENR theories since the 1989 Fleischmann–Pons announcement. Those reviews summarized papers on LENR theory and their content. We note the few such reviews in the rest of this section.

3.1. 1994 Paper by Fleischmann, Pons and Preparata [18]

The originators of the LENR field had a strong and abiding interest in explanations of what they and others measured. Because of that, they developed a close relationship with Preparata, a leading LENR theoretician. This paper resulted from their shared interests and collaboration. The paper includes a review of the energetics of the dissolution of hydrogen isotopes in palladium. It contains the list of seven observations that have to be explained by LENR theories, which were already noted in the last section. The authors provide a list of types of "Possible Models" and "Impossible Models" for each of those seven phenomena. The abstract for the paper follows:

- We review some of the key facts in the phenomenology of Pd hydrides usually referred to as "cold fusion". We conclude that all theoretical attempts that concentrate only on few-body interactions, both electromagnetic and nuclear, are probably insufficient to explain such phenomena. On the other hand we find good indications that theories describing collective, coherent interactions among elementary constituents leading to macroscopic quantum-mechanical effects belong to the class of possible theories of those phenomena

It is noted that, while this paper references many of the existing LENR theories in 1994, it is not a review of such theories. Rather, it provides constraints on LENR theories, given the noted observations.

3.2. 1994 Review paper by Chechin et al. [19]

This paper was an actual review of LENR (CF) theories by theoretical physicists. The abstract for the paper follows:

- We briefly summarize the reported anomalous effects in deuterated metals at ambient temperature, commonly known as "Cold Fusion" (CF), with an emphasis on important experiments as well as the theoretical basis for the opposition to interpreting them as cold fusion. Then we critically examine more than 25 theoretical models for CF, including unusual nuclear and exotic chemical hypotheses. We conclude that they do not explain the data.

The authors were outspoken in their criticism of extant LENR theories. They wrote the following in their Conclusion section:

- We conclude that in spite of considerable efforts, no theoretical formulation of CF has succeeded in quantitatively or even qualitatively describing the reported experimental results. Those models claiming to have solved this enigma appear far from having accomplished this goal. Perhaps part of the problem is that not all of the experiments are equally valid, and we do not always know which is which. We think that as the experiments become more reliable with better equipment, etc., it will be possible to establish the phenomena, narrow down the contending theories, and zero in on a proper theoretical framework; or to dismiss CF. There is still a great deal of uncertainty regarding the properties and nature of CF.

  Of course, the hallmark of good theory is consistency with experiment. However, at present because of the great uncertainty in the experimental results, we have been limited largely in investigating the consistency of the theories with the fundamental laws of nature and their internal self-consistency. A number of the theories do not even meet these basic criteria. Some of the models are based on such exotic assumptions that they are almost untestable, even though they may be self-consistent and not violate the known laws of physics. It is imperative that a theory be testable, if it is to be considered a physical theory.

It would be worthwhile to revisit each of the 25 theories considered in the review by Chechin et al. in order to (a) see which of them are no longer being actively developed, and (b) learn the status of each of those theories that have been advanced since 1994.

3.3. 2007 [20] and 2014 [21] books by Storms

Both of the books on LENR from Storms contain chapters on theoretical ideas. They are written from the perspective of a thoughtful experimentalist, rather than that of theoreticians. Chapter 8 of the 2007 book provides a list of four restrictions on LENR theories. It then discusses "Plausible Models and Expectations" for the production of heat, helium and transmutation products. That material references many of the ideas to explain LENR, but does not cover all of them. Storms then considered some potential approaches to fusion involving deuterons and other reactions with protons. He concludes that chapter by noting that "all theories have one or more major flaws".

Chapter 4 of Storms' 2014 book is a more systematic classification and review of LENR theories. Storms listed seven classes of LENR theories. They are (with the number of theories in each class in parentheses): Cluster Formation (5), Resonances (6), Neutron Reactions (4), Special Electron Structures (3), Transmutations (2), Tunneling (1) and Cracks and Special Structures (2). The 23 theories span most, but not all of the ideas that were and are competing for understanding of LENR. Overall, this chapter is the best summary of LENR theories in one source in recent years, and is very useful.

3.4. 2008 Matrix of theories presented at ICCF-14 [22]

The Proceedings of ICCF-21 contain a matrix of the 22 theoretical presentations given at that conference vs the characteristics of those theories. See Table 1. The features of the theories were noted in response to these questions:

(1) What is the form of the reaction(s) considered?
(2) Does the paper deal with the Coulomb barrier?
(3) Does the paper deal with energetic particles?
(4) What is the conceptual foundation of the theory?
(5) Has the concept been reduced to equations?
(6) Have numerical results been provided?
(7) Have the results been applied?

The matrix is copied on a following page. That format is meant to provide a facile way to compare different ideas about the mechanism(s) behind LENR. It would be useful to broaden this matrix to include theories not given at that conference and to add additional features, such as the calculation of LENR rates.

3.5. 2009 Review by Krivit and Marwan [23]

This paper includes a history of the study of LENR, and a survey of experiments and results. It also contains a review of thirteen LENR theories, and mentions a few others. The authors summarize their review of LENR theories by stating "There is no lack of effort to explain LENR. There are also very few comprehensive, qualitative evaluations of LENR theories." They also note that "Cyclical patterns have occurred in the views that have attempted to explain LENR." This is true for some theories that have been developed over several years.

3.6. 2013 Issue of Infinite Energy Magazine [24]

Issue number 112 of the magazine contained nine papers by the authors of various LENR theories [25]. They include, in the order of publication, Hagelstein, Dallacasa and Cook, Storms, Meulenberg and Sinha, Vysotskii and Vysotskyy,

Kozima, Meulenberg and, finally, Sinclair. Hence, these articles were not a "third party" review of such theories, as was the case for most of the compilations noted above in this section. However, the individual articles provide more depth for each of the theories than is usually available in reviews of various theories.

Biberian suggested this issue reviewing "Theoretical Models of Cold Fusion". In the introduction, he listed six criteria and questions about such theories and papers describing them:

(1) The papers are intended for experimentalists as further guidance on producing experiments.
(2) The papers should be short (maximum of 4000 words).
(3) The papers should make clear the initial assumptions of the theory.
(4) What experimental results are explained by the theory?
(5) What are the predictions of the theory?
(6) What should experimentalists do to produce successful experiments?

This listing of reviews of LENR theories is not exhaustive. There are some other examinations of multiple theories. However, these reviews give a fairly comprehensive listing and discussion of LENR theories as of the dates of their publications (see Table 1).

This paper is a related, but different, approach to the dozens of LENR theories. It is not a review or evaluation of LENR theories. Rather, it offers questions, the answers to which would enable people interested in LENR to understand the nature and situation for various theories. Presentation of those questions and comments on them constitute most of the rest of this paper.

4. Questions about LENR Theories

The topic of hypotheses and theories in science has a long and rich history. Our approach here is less philosophical and more practical. We simply ask developers of LENR theories about the *characteristics* and *status* of their ideas. A different view of LENR theory has been presented by Hagelstein, a sophisticated LENR theoretician [26]. Ten questions will be presented and discussed in Sections 4.1–4.10.

4.1. Q1. How is your theory connected to LENR?

Some concepts presented at LENR conferences have no stated or evident connection to LENR. It is reasonable to ask if a given idea seeks to explain everything about LENR, or just some aspect of what was measured. Some works on nuclear structures and on nuclear reactions, which are presented in LENR conferences, do not get as far as making a clear connection to LENR. That is not to say they are unscientific, or else, science not worth attention. However, it should be possible for a theoretician to state clearly which of the many empirical observations listed in Section 2 they seek to explain.

4.2. Q2. What is the key idea or concept of your theory?

All theoretical developments must start with some idea or concept about what is happening to make it possible to induce nuclear reactions with chemical energies. LENR theoreticians ought to be able to state unambiguously their core idea (or ideas) and *the associated assumptions*, which are adopted at the outset of a specific theoretical development. Without such clarity, it is impossible for the theoretician to develop their theory, or to explain it to interested people, especially experimentalists.

Table 1. Characteristics of theories presented at ICCF–14.

Authors	Which LENR?	Coulomb Barrier	Hi-energy Particles	Concept	Equations?	Numerical Results?	Use of Results?
Adamenko and Vysotskii	Transmutation	N/A	NA	Magnetic monopoles	Yes	Approx. bounds	No
Alexandrov	e+P $\rightarrow$ N+ν	Neutrons	No	Band theory, effective mass	Yes	Yes	Applied to semicond.
Bass and Swartz	D Fusion	No	No	Control theory	Computer Simulation	Yes	Future work
Breed	4D $\rightarrow \alpha+\ldots$	Yes	Yes	Band theory, effective mass, resonance	Yes	No	NA
S. Chubb	D+D $\rightarrow^4$He+heat	Yes	Yes	Nonlocal quantum effects, resonance	Yes	Yes	No
T. Chubb	Various	Yes	Yes	"Ion band states"	No	No	NA
Cook	Transmutation	No	NA	Lattice model of nuclei	Yes	Yes	Compared with expt.
Dufour et al.	Pd+D, D+D	Yes	Indirectly	New force	No	No	NA
Fou	D+D fusion	Yes	No	Neutron exchange, electrostatic fields	No	No	NA
Frisone	D plasma oscillations	Yes	NA	Gamow and Preparata Theory	Yes	Yes	No
Godes	e+P $\rightarrow$ N+ν	Neutrons	No	Various	No	No	NA
Hagelstein and Chaudhary	D+D $\rightarrow^4$He+24 MeV	Yes	Yes	Coupling two-level systems to phonons	Yes	Quali tative	NA
Hagelstein, Melich and Johnson	Various	Yse	Yes	Various	NA	NA	NA
Hagelstein et al.	Various	No	No	Existing theory	Yes	No	NA
Kim	D+D $\rightarrow^4$He+heat	Yes	Yes	Bose–Einstein condensate	Yes	Yes	Yes
Kozima	Not stated	No	No	Cellular automata, recursion equations	No	No	NA
Kozima and Date	Transmutation	Neutrons	No	"Neutron drops"	No	No	NA
Li et al.	P+D+e $\rightarrow$ ^{3}He+e+$\nu+\nu^-$	Neutrons	Indirectly	Resonance, tunneling	Yes	Yes	No
Sinha and Meulenberg	D fusion	Yes	No	Screening via local e^- pairs	Yes	Yes	No
Swartz	D fusion	No	No	Relations between operating parameters	Yes	Approx-imately	Yes
Swartz and Forsley	D Fusion	No	No	Relations involving operating parameters	Computer calculations	Qualitative	Yes
Takahashi	4D $\rightarrow^8$Be* $\rightarrow 2\alpha$	Yes	No	"Tetrahedrally symmetric clusters"	Yes	Yes	No

4.3. Q3. What is (are) the foundation(s) of your concept?

This question asks: what is the basis in physics, chemistry, biology, materials science, electromagnetics and other sciences of the mechanism(s) at the core of a theoretical idea? What advanced knowledge of which sciences is needed to proceed? Developing a theory, understanding a theory, and using a theory require expertise in particular disciplines. It is likely that physics will turn out to be the core discipline needed to fully understand LENR. However, the complexity of both LENR experiments and their results make it very likely that serious expertise in other disciplines will also needed. That is especially true of Chemistry and Materials Science.

4.4. Q4. Does your mechanism involve only one step or more than one step?

There is a general issue in the field of LENR that is very fundamental and unresolved. It is whether there is only one nuclear reaction or a sequence of two or more nuclear or other reactions. In fact, the situation is even more complex than that. Some LENR theories involve the formation of "compact objects", which have sizes and binding energies intermediate between those of atoms and nuclei. A recent review of such theories is available [27]. The formation of such objects would not involve nuclear reactions, and could be responsible for part, or even all of the heat seen in LENR experiments. However, compact objects might, after formation, go on to participate in nuclear reactions. There is a precedent for such behavior in muon-catalyzed fusion, an understood process [28]. So, LENR might occur by a two-step process, the first without any nuclear reaction and the second being a nuclear reaction.

Even more fundamental, there are three types of possible reactions relevant to LENR: chemical, exotic and nuclear. Chemical reactions include electrochemical and solid-state mechanisms, which are needed to create Nuclear Active Environments in Nuclear Active Regions. Exotic reactions include the formation of compact objects or other entities by neither ordinary chemical nor nuclear reactions. Nuclear reactions include any mechanism which produces changes in the nuclei that are involved in the reactions, whether fusion, fission, transmutations or other changes in a nucleus.

If production of a Nuclear Active Environment is always the initial step, then all LENR experiments involve two steps. That initial "reaction" is probably chemical in nature, and sets the stage for a nuclear reaction. Hence, there are two likely sequences needed for production of LENR: (a) Chemical, then Nuclear, or (b) Chemical, then Exotic and, finally, Nuclear. However, this does not exhaust possibilities. The number and sequence of multiple reactions can vary greatly. As noted above, some LENR theories do not involve nuclear reactions at all.

The number and type of reactions during LENR experiments is rarely discussed. This is a major deficiency in the theoretical side of the field. One paper by Widom and Larsen does have a discussion of possible sequential nuclear reactions, assuming the availability of lithium and of sufficient numbers of "ultra-low-momentum" neutrons [29]. The Appendix to this paper considers two sequential nuclear reactions leading to production of both heat and helium, and their correlation.

4.5. Q5. Are the equations that embody your concept written out?

If this is not done, the "theory" is nothing more than a concept, which is untestable, and has no value for either explaining past experiments or designing new experiments. The challenge is to have all the needed equations to embody the basic concept. Additional equations beyond those that are necessary can be counterproductive.

4.6. Q6. If the equations are written, have they been evaluated by reduction to numbers?

There is no way to know from equations alone if the idea(s) behind them is (are) correct, or if the equations are complete and correct. Science is all about numbers, and stopping at the equations stage is like preparing for and starting a race, only to quit part way through it. There are many choices and challenges in the computational part

of a theoretical program. Choices include the source of needed parameters, what algorithms to use, what computer language to employ, what machine to use for the calculations, and how to store and use the results. Each of these choices can influence the results of the calculations based on the starting set of equations. Post–calculation analyses are sometimes valuable, and they also require making several choices on what to do and how to do it.

4.7. Q7. How does your mechanism relate to experimental observations?

Comparison of the results of theoretical developments with experiment, and the design of experiments to test the results of theories, are critical to understanding of LENR. Hence, this and the remaining three questions have to do with the intersection of theories and experiments.

The list of empirical observations from LENR experiments in the second section is quite clear and challenging. However, some aspects are worth additional comments because they are both remarkable and important to applications

Power gains in excess of 25 have been observed in a few experiments [30]. Values of generated energy (in eV/atom of the metal catalyst) in excess of 2000 have been observed in LENR experiments [31]. Power densities exceeding those within nuclear fission fuel rods by about 50 times have been measured [32].

Materials are especially critical to production of LENR, including high loading, surface orientation and morphology, the presence of impurities and other unknown factors. When LENR are understood, the key materials parameters will be known, along with their range of acceptable values. Put another way, LENR theories ought to provide guidance on the composition and structure of materials that will lead to LENR. That is rarely the case.

It is known that application of external stimuli to LENR experiments can initiate (trigger) or increase (stimulate) such reactions, and their generation of energy and products. Figure 2 is a schematic relationship between LENR experiments, the various input stimuli that have been applied to them (left column) and the diverse attempted output measurements from them (right column) [33]. LENR theories ought to be able to explain the actions of applied stimuli, as well as the type and magnitude of measured quantities. There are very many challenges of this type.

For example, Radio Frequency (RF) has been applied to LENR experiments and increased excess power was observed. In other LENR experiments, RF emissions from LENR experiments were measured, both without and with the production of measurable excess power. A complete LENR theory ought to be able to rationalize the RF frequencies used to increase LENR reaction rates and the RF frequencies measured during LENR experiments, as well as the RF powers involved. A recent review of the overlap between LENR experiments and RF inputs or outputs is available [34].

4.8. Q8. What time histories and reaction rates are (quantitatively) predicted?

Reaction rates that come out of LENR theories are especially important and deserve separate attention for two reasons. First, empirical rates can be obtained from carefully designed and calibrated experiments, so they are testable. Second, reaction rates are the basis of applications. Whether or not LENR will turn out to be the foundation of practical commercial energy generators will depend on what reaction rates can be produced, controlled and sustained.

Many LENR experiments have shown the production of energy and reaction products to be uncontrolled and highly variable during a run. Understanding such variability, and achieving full control of power output, is another challenge to LENR theoreticians.

As discussed under Question 4, LENR might always, or at least often, involve at least two reaction steps. Hence, it must be asked, for theoretical mechanisms involving more than one step, which step is rate limiting? If there are two reactions, their rates can compare in only three ways, one or the other is dominant, or they are comparable.

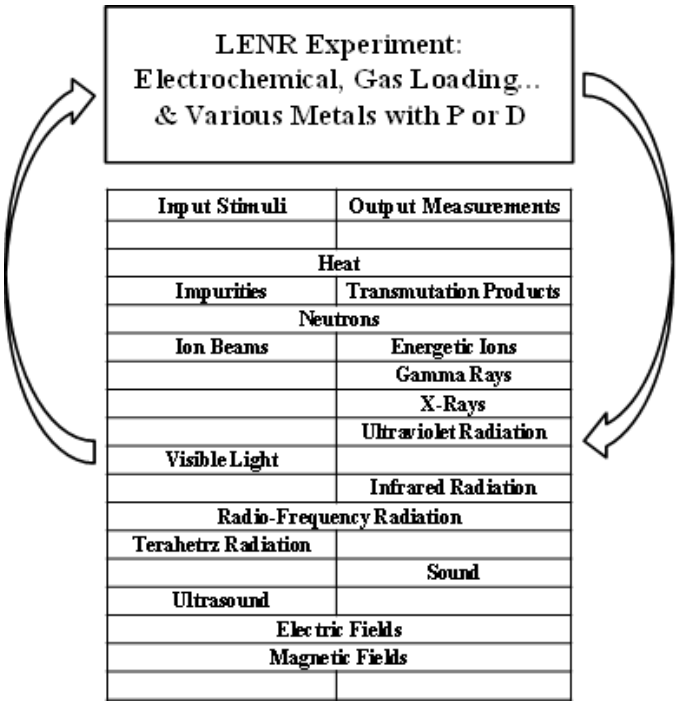

Input Stimuli	Output Measurements
Heat	
Impurities	Transmutation Products
Neutrons	
Ion Beams	Energetic Ions
	Gamma Rays
	X-Rays
	Ultraviolet Radiation
Visible Light	
	Infrared Radiation
Radio-Frequency Radiation	
Terahetrz Radiation	
	Sound
Ultrasound	
Electric Fields	
Magnetic Fields	

Figure 2. Stimuli that have applied to LENR experiments (*left column*) or measured from such experiments (*right column*). P stands for protons and D for deuterons. Blanks in the columns are possibilities that have not yet been applied or measured.

4.9. Q9. Can one theory explain all LENR observations?

LENR experiments have produced a remarkable great variety of observations. The question of whether only one or, rather, multiple theories are needed to explain the diversity of observations from LENR experiments. Again, a summary of those observations is in Section 2. This question is like the question on there being one or more steps when LENR occur, critical but rarely discussed. No paper on this issue is known to this author.

Theories and mechanisms are conceptually separable. That is, one could have multiple explanations for one mechanism. So, there is another question. Are all observations due to one mechanism, or are multiple mechanisms needed to understand all of the data? If the latter, what controls the pathway and outcome of any given experiment? Will a single theory be able to embrace multiple mechanisms?

4.10. Q10. The ultimate question: Is your theory testable?

It is widely accepted that failure to achieve the results predicted theoretically does not rule out a theory, because the experiments might have some type of unknown or unrecognized flaw. Agreement between quantitative theoretical predictions and the numerical results of measurements increases the probability that a theory is correct, but even this could be accidental and worthless.

The explicit comparison of the results of LENR theories with experiments is a rarity in the field. This author knows of only three parametric comparisons of measured and computed results from the past 28 years. They will be briefly noted here, and reviewed in detail in a forthcoming paper [35].

The first direct comparison of a LENR theoretical prediction with the results of an LENR experiment, known to this author, was published in a paper on ultra-low momentum neutrons by Widom and Larsen in 2006 [36]. They compared their theoretical neutron scattering lengths with the transmutation rates published by Miley and his collaborators [37], both as a function of atomic mass. The theoretical curve showed peaks where multiples of the neutron wavelength within nuclear matter fit the size of the mass-dependent nucleus. The experimental transmutation rates also showed peaks as a function of atomic mass. The positions of the computed and measured peaks are similar for all five peaks in both data sets. In a subsequent study, they were found to be statistically correlated [38].

Another direct confrontation of LENR laboratory data with theory comes from experiments performed by Letts, Cravens and Hagelstein [39]. Their cathode was irradiated with THz electromagnetic radiation from heterodyning two lasers, which could be varied in frequency (wavelength). Three main peaks in the production of LENR power were observed at specific frequencies. The authors associated the frequencies of two of the peaks with optical phonon frequencies in palladium hydride. An alternative explanation of the same data was offered later by Vysotskii and Vysotskyy in support of their Coherent Correlated States theory of LENR [40].

The two examples just reviewed basically involved comparison of LENR data with the results of quantum mechanical calculations. A third example, published in 2013, was qualitatively different. It involves measured excess powers from 40 experiments with the pair of lasers used to produce the THz frequency-dependent excess power noted in the last paragraph. Letts provided an equation involving several parameters relevant to those experiments [41]. He computed excess power as a function of frequency and compared the numerical results with the measured excess powers. The empirical and computational results were in remarkable agreement over a frequency range from below 5 up to 22 THz and excess power range from near zero up to 1.4 W.

5. Conclusion

Theory and related hypotheses really have only two primary functions: to explain the past or to predict the future. There is a large volume of good data from LENR experiments, which begs quantitative, or even qualitative, understanding. That is, there is ample opportunity for more theoretical explanations of what has already been observed. Reaction rates present a sterling opportunity for explaining measured results. The assumptions basic to any theoretical approach and physical constants are needed for computation of LENR reaction rates.

The three cases cited under Q10 involved theoretical explanations of earlier data. But, theory can also precede measurements. Design of experimental tests of theories and hypotheses is a time-honored and useful approach in the sciences. The chance to design LENR experiments and predict their outcome is also wide open. This author knows of only one program in which experiments have been designed to test a theory about LENR. It is reviewed next.

Hagelstein has been working for many years on reciprocal mechanisms for energy sharing between nuclear levels (MeV energies) and phonon states (meV energies) [42]. In one direction, he deals with the partition (fractionization) of high energy quanta in the MeV range (from nuclear reactions) into many low energy quanta in the meV range (due to phonons). In the other direction, his theoretical work considers the addition of many phonon (vibrational) energies to produce the much higher nuclear energies. If successful, the closely related mechanisms for down- and up-conversion will explain deuteron–deuteron nuclear reactions, which are able to avoid the Coulomb barrier and occur without emission of energetic radiation. In the recent past, Hagelstein and his team have been performing mechanical vibrational experiments and searching for the emission of X-ray energies associated with very low-lying nuclear states [43]. This is not a direct test of a theory on LENR, but rather a test of the mechanism that is central to an LENR theory.

Almost all extant LENR theories fall short of what is desirable, and actually necessary, in terms of their completeness. It could happen that, if all available LENR theories are carried to numerical completion and then compared with experiments, there would be no compelling agreement. That is, it is not certain that the theories now in play will prove to be adequate for understanding LENR. It is also possible that a new LENR theory will appear and provide the desired

understanding. Further, it is conceivable that the solutions of the challenge of understanding LENR will come from outside of the field, either from a new theory or even a theory that already exists. One possibility is given in the next paragraph.

The experimental work of Cardone and his large team has shown that it is possible to induce nuclear reactions by using ultrasound to excite liquid mercury at room temperature [44]. Three minutes of insonification turns the silvery liquid into a dark powder, which contains many new elements. That group interprets their results in terms of what is called Deformed Space Time (DST). A substantial body of theory on DST exists [45]. Is it possible that DST will (a) prove to be a correct explanation of the transmutation results in the ultrasound experiments and (b) explain what is seen in very different LENR experiments?

A discussion of how to down select LENR theories has been published [46]. Part of it reads:

- There is little evidence of convergence toward the few ideas that are most worthy of attention and funding. Of course, it is the nature of science that an individual researcher can work on whatever they want to pursue within funding constraints. However, having a limited number of LENR theories as a focus might speed the achievement of the desired ultimate understanding. If the mechanisms active in LENR were understood, the scientific development of the field could accelerate. And, importantly, the development of commercial products would proceed much faster and with greater assurance of success. There are problems associated with the evaluation, prioritization and down-selection of theories about LENR. One of them is the natural tendency of scientists, theoreticians included, to want others to pay favorable attention to their work. Another is the fact that some of the concepts are not clearly documented. Another challenge is due to the fact that many of the ideas are still evolving because of recent activities of their originators

It must be noted, even emphasized, that there has been much unpublished material and discussion about LENR theories on the internet. That is especially true for postings on the CMNS Google Group. For example, in April and May of 2016, there were 100 postings in a thread on LENR theories. It is difficult to reference such material for two reasons. First, that discussion is privileged to members of the group. And, even if it were not private, it is not accessible to others and, hence, cannot be referenced. The ideas in this paper were influenced by unpublished posting about LENR theory, but are solely the current views of the author.

This paper has focused on deficiencies in LENR theories. However, it is also true that many LENR experiments, and reports on what was done and found in a laboratory, are less than satisfactory. Experimental setups and materials are often not as good as they might be, in terms of modern equipment and software, and available materials science and engineering. Such shortfalls are usually due to insufficient funds. Analysis of data from LENR experiments is commonly not as thorough as is desirable. For example, few authors perform Fourier Transformations on time series data to obtain the distribution of frequencies (the spectrum) from the measurements. Such transformations are essentially trivial with modern software. Finally, many reports on LENR experiments are not adequately complete. This is especially bothersome if another scientist seeks to reproduce an earlier experiment. Overall, there are too many deficiencies in LENR experiments and papers. However, despite these problems, we have still learned a great deal about LENR in laboratories, as noted in Section 2.

The explanation(s) of the existence and many facets of LENR remains for some time in the future. It could be achieved soon, or only after many more years of struggling with the numerous experimental characteristics from diverse LENR experiments. Whatever and whenever the outcome, the discovery, experimental elucidation and theoretical understanding of LENR will constitute a significant chapter in the history of science.

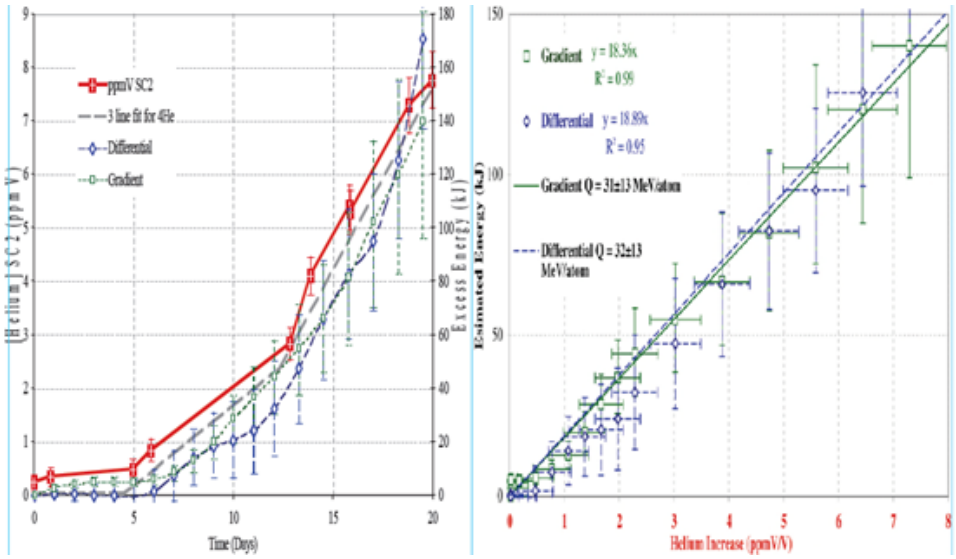

Figure 3. Helium production in an LENR experiment at SRI International. *Left*: Time history of the helium concentration in Parts per Million by Volume. *Right:* The excess energy in kJ vs the helium concentration. Fitting the data by different means gave approximately 31–32 MeV per helium atom produced.

Acknowledgements

Provision of information and comments by Peter Hagelstein, Dennis Letts, Michael McKubre, Andrew Meulenberg and Vladimir Vysotskii is much appreciated. A reviewer provided comments that improved this paper. William Collis is thanked for his organization of the 12th International Workshop on Anomalies in Hydrogen Loaded Metals, at which this paper was presented.

Appendix A. The Correlation of Heat Generation and Helium Production

The correlation of excess energy with the number of helium atoms, both produced in the same LENR experiment, was discovered by Miles [47]. Helium generation, and that correlation, were reviewed recently [48]. The best example of the linear relationship between heat and helium production was published by McKubre and his colleagues [49]. It is shown in Fig. 3. There are two notable characteristics of those data. The first is that the helium levels exceeded the 5.2 ppm level of helium in the atmosphere. Hence, the measured helium was not produced by a leak from the atmosphere into the experiment. The other significant characteristic of the results is the slope of the correlation curve, namely 31 or 32 ± 13 MeV/atom. Those values are close to the energy of the 23.8 MeV gamma ray, which is emitted in the rare (10^{-7}) branch of conventional D–D fusion.

There has been much discussion about that result. Some scientists rationalized the difference by noting that some of the helium might be trapped in the palladium materials of the experiments, and hence not measured. If that were the case, then the measured heat to helium ratios would be higher than the actual values.

There are also ideas that helium might be due to two (or more) nucleon or nuclear reactions in sequence [27]. The total energy E_T from two sequential nuclear reactions can be written simply. The equation for two reaction steps 1 and 2 is

$$E_{\mathrm{T}} = N_1\, E_1 + N_2\, E_2,$$

where N_1 and N_2 are the number of each type of reaction and E_1 and E_2 are the associated energies. Define F as the fraction of the first reactions that also produce a second reaction, so $N_2 = F\, N_1$. F can be taken as 1 for the purpose of this discussion. That is $N_1 = N_2$. Then, if each of the terminal second reactions produces a helium atom, $N_1 = N_2 =$ He, so the ratio of heat to helium is

$$E_{\mathrm{T}}/\mathrm{He} = E_1 + E_2.$$

That is, the slope of the correlation in the right part of Fig. 3 would be the sum of two reaction energies. In principle, the E_1 could be negative, that is, the first nucleon or nuclear reaction could be endothermic. But, then the first reaction would be unlikely. It is more probable that both of the energies E_1 and E_2 are exothermic, so they would add. In that case, the slope of a heat vs helium graph could be greater than expected from simple one-step hot fusion D–D reaction, as it is in Fig. 3.

Helium is a remarkably stable nuclear entity. If we assume that it forms during the second reaction, then 31.5–23.8 MeV = 7.7 MeV = E_1. This analysis is very simple. It is provided to illustrate the difficulty in interpreting the data in Fig. 3 as evidence of a single-step fusion process.

This present scientific uncertainty about the number and nature of the reactions involved in LENR certainly does not take away the strong evidence that both helium and heat are produced and are correlated, at least in experiments such as that reported by Miles, SRI International and others.

References

[1] G.W. Draper and F.H. Ling, LENRaries. A New Era of Renewable Energy, Anthropocene Institute, http://www.anthropoceneinstitute.com/wp-content/uploads/2017/02/LENRaries.pdf (2017).

[2] http://www.ucmp.berkeley.edu/geology/techist.html and Henry R.*Frankel, The Continental Drift Controversy: Volume 1, Wegener and the Early Debate,* Cambridge University Press, Cambridge, pp. 152, 584 (2012). ISBN 978-0-521-87504-2.

[3] http://www.ucmp.berkeley.edu/geology/tecmech.html and http://geography.unt.edu/~mcgregor/Earth_Science/plate.tectonics.revise.pdf.

[4] http://web.ihep.su/dbserv/compas/src/einstein17/eng.pdf and https://www.aps.org/publications/apsnews/200508/history.cfm.

[5] https://journals.aps.org/pr/abstract/10.1103/PhysRev.99.1264 and https://en.wikipedia.org/wiki/Charles_H._Townes.

[6] https://en.wikipedia.org/wiki/History_of_superconductivity.

[7] https://en.wikipedia.org/wiki/BCS_theory.

[8] D.J. Nagel, Energy gains from lattice enabled nuclear reactions, *Current Science* **108** (2015) 641–645.

[9] T. Mizuno and Y. Toriyabe, Anomalous energy generation during conventional electrolysis, in A. Takahashi, K.-O. Ota and Y. Iwamura (Eds.), *Proc. 12th Int. Conf. on Cold Fusion*, World Scientific, Singapore, 2006, pp. 65–74.

[10] http://www.mpoweruk.com/fossil_fuels.htm.

[11] http://www.mpoweruk.com/energy_efficiency.htm.

[12] https://www.eia.gov/tools/faqs/faq.php?id=65&t=2.

[13] E. Storms, *The Science of Low Energy Nuclear Reaction*, World Scientific, Singapore, 2007, p. 175.

[14] D.J. Nagel and M.E. Melich, Preface, page xi in D.J. Nagel and M.E. Melich (Eds.), *Proc. 14th Int. Conf. on Condensed Matter Radiation Sciences*, http://www.iscmns.org/iccf14/ProcICCF14a.pdf_ (2008).

[15] G. Hubler, Private Communication, 2015.

[16] M.C.H. McKubre, F.L. Tanzella, I. Dardik, A. El Boher, T. Zilov, E. Greenspan, C. Sibilia and V. Violante, Replication of condensed matter heat production, in *Low-Energy Nuclear Reactions Sourcebook*, J. Marwan and S.B. Krivit (Eds.), American Chemical Society, 2008, pp. 219–247.

[17] E. Storms, Anomalous energy produced by PdD, *J. Condensed Matter Nucl. Sci.* **20** (2016) 81–99.
[18] M. Fleischmann, S. Pons and G. Preparata, Possible theories of cold fusion, *Nuovo Cimento* **107** (1994) 143–157.
[19] V.A. Chechin, V.A. Tsarev, M. Rabinowitz and Y.E. Kim, Critical review of theoretical models for anomalous effects in deuterated metals, *Int. J. Theoret. Phys.* **33** (1994) 617–670. www.lenr-lanr.org/acrobat/ChechinVAcriticalre.pdf and arXiv:nucl-th/0303057v2.
[20] E. Storms, *The Science of Low Energy Nuclear Reaction*, World Scientific, Singapore, 2007.
[21] E. Storms, *The Explanation of Low Energy Nuclear Reaction*, Infinite Energy Press, Concord, NH, 2014.
[22] R.W. Johnson, Introduction to theory papers in D.J. Nagel and M.E. Melich (Eds.), *Proc. 14th Int. Conf. on Condensed Matter Radiation Sciences*, p. 476, http://www.iscmns.org/iccf14/ProcICCF14b.pdf_ (2008).
[23] S.B. Krivit and J. Marwan, A new look at low-energy nuclear reaction research, *J. Environmental Monitoring* **11** (2009) 1731–1746.
[24] C. Frazier, *Infinite Energy Magazine*, Issue 112, pp.12–48 ((November/December 2013).
[25] P. Hagelstein, V. Dallacasa, N. Cook, E. Storms, A. Meulenberg, P.K. Sinha, V.I. Vysotskii, M.V. Vysotskyy, H. Kozima and D. Sinclair, Theoretical models of cold fusion, *Infinite Energy Magazine*, Issue 112 (2013). http://www.infinite-energy.com/iemagazine/issue112/index.html.
[26] P.L. Hagelstein, on theory and science generally in connection with the F–P experiment, *Infinite Energy Magazine*, Issue 108, pp. 5–12 (March/April 2008).
[27] D.J. Nagel and R.A. Swanson, LENR excess heat may not be entirely from nuclear reactions, *J. Condensed Matter Nucl. Sci.* **15** (2015) 279–287.
[28] https://en.wikipedia.org/wiki/Muon-catalyzed_fusion.
[29] A. Widom and L. Larsen, Ultra low momentum neutron catalyzed nuclear reactions on metallic hydride surfaces, *Eur. Phy. J.* **46** (2006) 107–111. DOI:10.1140/epjc/s2006-02479-8.
[30] I. Dardik, T. Zilov, H. Branover, A. El-Boher, E. Greenspan, B. Khachaturov, V. Krakov, S. Lesin and M. Tsirlin, Excess heat in electrolysis experiments at energetics technologies, in condensed matter nuclear science, *Proc. 11th Int. Conf. on Cold Fusion,* J.-P. Biberian (Ed.), World Scientific, New Jersey, 2006, pp. 84–101.
[31] M.C.H. McKubre, Presentation at Short Course prior to the 10th Int. Conf. on Cold Fusion, Cambridge, MA, 24 August 2003.
[32] G. Preparata, Everything you always wanted to know about cold fusion calorimeter, in *Proc. 6th Int. Conf. on Cold Fusion,* M. Okamoto (Ed.), 1996, pp. 136–143.
[33] D.J. Nagel, Questions about lattice enabled nuclear reactions: experiments, theories and computations, *Infinite Energy Magazine*, Issue 119, p. 18 (January/February 2015).
[34] F. Scholkmann, D.J. Nagel and L. F. DeChiaro, Electromagnetic emission in the kHz to GHz range associated with heat production during electrochemical loading of deuterium into palladium: a summary and analysis of results obtained by different research groups, *J. Condensed Matter and Radiation Sci.* **19** (2016) 325–335.
[35] D.J. Nagel, LENR Theories vs LENR experiments, in preparation.
[36] A. Widom and L. Larsen, Nuclear abundances in metallic hydride electrodes of electrolytic chemical cells, https://arxiv.org/pdf/cond-mat/0602472.pdf (2006).
[37] G.H. Miley, Possible evidence of anomalous energy effects in H/D-loaded solids – low energy nuclear reactions (LENR), *J. New Energy* **2**(3–4) (1997) 6–13 and G.H. Miley and J.A. Patterson, Nuclear transmutations in thin-film nickel coatings undergoing electrolysis, *J. New Energy* **1** (3) 5–13 (1996) and G.H. Miley, On the reaction product and heat correlation for LENRs, in F. Scaramuzzi (Ed.), *Proc. of the 8th Int. Conf. on Cold Fusion*, Lerici, Italy, 2000, pp. 419–424.
[38] F. Scholkmann and D.J. Nagel, Statistical analysis of transmutation data from low-energy nuclear reaction experiments and comparison with a model-based prediction of Widom and Larsen, *J. Condensed Matter Nucl. Sci.* **13** (2014) 485–494.
[39] D. Letts, D. Cravens and P.L. Hagelstein, Dual laser stimulation and optical phonons in palladium deuteride in low-energy nuclear reactions sourcebook, Vol. 2, American Chemical Society, Washington DC, 2009, pp. 81–93. and P.L. Hagelstein, D.G. Letts and D. Cravens, Terahertz difference frequency response of PdD in two-laser experiments, *J. Condensed Matter Nuclear Sci.* **3** (2010) 59–76.
[40] V.I. Vysotskii and M.V. Vysotskyy, Coherent correlated states and low-energy nuclear reactions in non-stationary systems, *Euro. Phys. J.* A **49** (2013) 99 and DOI 10.1140/epja/i2013-13099-2.

[41] D. Letts, A method to calculate excess power, *Infinite Energy magazine*, Issue 112, pp. 63–66 (November/December 2013).
[42] P.L. Hagelstein, Current status of the theory and modeling effort bases on fractionation, *J. Condensed Matter Nucl. Sci.* **19** (2016) 98–109.
[43] F. Metzler, P.L. Hagelstein and S. Lu, Observation of non-exponential decay in X-ran and gamma emission lines from Co-57, *J. Condensed Matter Nucl. Sci.*, in press (2018).
[44] F. Cardone, G. Albertini, D. Bassani, G. Cherubini, E. Guerriero, R. Mignani, M. Monti, A. Petrucci, F. Ridol, A. Rosada, F. Rosetto, V. Salazz, E. Santoro and G. Spera, Deformed spacetime transformations in Mercury, *Int. J. Modern Phys*. B **31** (2017) 1750168, DOI: 10.1142/S0217979217501685.
[45] F. Cardone and R. Mignani, *Deformed Spacetime*, Springer, Dordrecht, The Netherlands, 2007.
[46] D.J. Nagel, Questions about lattice enabled nuclear reactions: experiments, theories and computations, *Infinite Energy Magazine*, Issue 119, p. 28 (January/February 2015).
[47] M.H. Miles, R.A. Hollins, B.F. Bush, J.J. Lagowski and R.E. Miles, Correlation of excess power and helium pproduction during D_2O and h_2o electrolysis using palladium cathodes, *J. Electroanal. Chem.* **346** (1993) 99.
[48] A. Lomax, Replicable cold fusion experiment: heat/helium ratio, *Current Science* **108** (2014) 574–577.
[49] M.C.H. McKubre, F. Tanzella, P. Tripodi and P. Hagelstein, The emergence of a coherent explanation for anomalies observed in D/Pd and H/Pd system: evidence for ^{4}He and ^{3}He production, in F. Scaramuzzi (Ed.), *Proc. 8th Int. Conf. on Cold Fusion*, Lerici Italy, Italian Physical Society, 2000.

J. Condensed Matter Nucl. Sci. 26 (2018) 32–44

Research Article

Isotopic and Elemental Composition of Substance in Nickel–Hydrogen Heat Generators

K.A. Alabin and S.N. Andreev

Prokhorov General Physics Institute, Russian Academy of Sciences, Moscow, Russia

A.G. Sobolev

Lebedev Physical Institute, Russian Academy of Sciences, Moscow, Russia

S.N. Zabavin, A.G. Parkhomov* and T.R. Timerbulatov

R & D Laboratory K.I.T., Moscow, Russia

Abstract

Results of isotopic and elemental composition analyses of fuel and matter near the active zone of nickel–hydrogen reactors before and after experiment with the integral excess energy up to 790 MJ are presented. No significant changes in the isotopic composition of nickel or lithium were observed. A significant increase in the concentration of impurities of a number of nuclides has been observed not only in fuel but also in structural elements adjacent to the active zones of the reactors.
 ISSN 2227-3123

Keywords: Elemental composition, Heat generation, Hydrogen, Isotopic composition, Nickel

1. Introduction

After publication of a report about Andrea Rossi's high-temperature heat generator test in Lugano [1,2], many attempts were made to create similar devices [3]. In some of them, heat generation significantly exceeding the energy consumption were shown. Excess heat release many times exceeds the potential of chemical reactions and is comparable to the energy release in nuclear reactions, although it is not accompanied by harmful radiation and radioactivity. But the nature of this surprising effect remains unclear. The study of elemental and isotopic changes in the operation of reactors is of paramount importance for clarifying the nature of this effect. This report provides information on the results of the analysis of changes in fuel and in structural materials that occurred in several nickel–hydrogen reactors created by our team.

*Corresponding author. E-mail: alexparh@mail.ru

 ISSN 2227-3123

2. Estimation of Possible Changes in the Isotopic Composition of Fuel

We can estimate the possible changes in the isotopic composition of the fuel assuming that the excess heat release occurs as a result of nuclear transmutations in accordance with the law of conservation of energy. For example, in nickel, containing hydrogen, the following nuclear reaction may occur:

$$^{58}\mathrm{Ni} + {}^{1}\mathrm{H} + 2\mathrm{e}^{-} \rightarrow {}^{59}\mathrm{Co} + 10.32\ \mathrm{MeV}. \quad (1)$$

Since 1 MJ is equal to 6.3×10^{18} MeV, about 6×10^{17} nickel nuclei (0.00006 g) are consumed as a result of this reaction to release 1 MJ of energy, and the same amount of cobalt is formed. Nickel–hydrogen reactors usually contain about 1 g of fuel. It is quite possible, using modern technology, to detect 0.00006 g of cobalt in 1 g nickel (0.006%).

It is more difficult to detect changes in the isotopic ratios. Conventional mass spectral analyzers allow one to capture changes in isotopic ratios of elements on the order of 1%. It is not possible to detect a change on the order of 0.01% that occurs when 1 MJ of energy is released into 1 g of fuel as a result of reaction (1). To reduce the content of the isotope ^{58}Ni by 1%, excess energy on the order of 100 MJ is necessary.

If the fuel contains lithium, then the following nuclear reaction is possible:

$$^{7}\mathrm{Li} + {}^{1}\mathrm{H} \rightarrow 2\ {}^{4}\mathrm{He} + 17.35\ \mathrm{MeV}. \quad (2)$$

As a result of this reaction, in a mixture of lithium isotopes (the natural mixture contains 92.6% of ^{7}Li and 7.4% of ^{6}Li) the content of ^{7}Li decreases and, accordingly, the content of ^{6}Li increases. Suppose that all excess energy release is associated with reaction (2). To release 1 MJ of energy, 4×10^{17} of ^{7}Li nuclei are required (4.2×10^{-6} g). A typical reactor with fuel mixture of lithium–aluminum hydride and nickel contains about 0.02 g of ^{7}Li. Therefore, when 1 MJ is released, only 0.02% ^{7}Li is removed. It is almost impossible to detect such a small change. With the release of 1000 MJ of energy, 20% of ^{7}Li is removed. This leads to an increase in the content of ^{6}Li from 7.4 to 10%. This change is quite possible to detect, although not easy because of the small mass of the material available for analysis.

Thus, the appearance of isotopes that are absent in the initial fuel can be detected with excess energy on the order of 1 MJ/g of fuel. To reliably detect changes in the ratios of isotopes in elements that originally are a part of the fuel, excess energy exceeding 100 MJ/g is required. So, naturally a thorough analysis of the fuel of the GS3 reactor made by Alan Goldwater did not reveal any noticeable isotope changes, since the excess energy production in it was about 50 MJ/g [3,4]. The excess energy production in Rossi's high-temperature heat-generator, according to [1], was 5800 MJ/g. This is quite sufficient for radical changes in the isotopic composition of both nickel and lithium. We will present the results of an analysis of isotope changes in fuel and in structural materials that occurred in several nickel-hydrogen reactors created in our laboratory.

3. Reactor AP2

A detailed description of the reactor design, the course of experiments and the methods for determining excess heat of reactor AP2 are given in [5] (Fig. 1). It was charged with a fuel mixture of 640 mg Ni + 60 mg $LiAlH_4$. It ran from March 16 until March 22, 2015, and produced about 150 MJ of excess heat.

Analyses of fuel before and after the experiment were made using several methods, in different laboratories. The analysis of the elemental composition using an electron scanning microscope was made at the Prokhorov General Physics Institute, Russian Academy of Sciences and All-Russian Research Institute of Experimental Physics (VNIIEF, Sarov). Two fractions significantly differ in the fuel mixture measured before experiment: gray crystals and white granules. Gray crystals mainly contain Al, O, and Cl. White granules consist of nickel with a small admixture of iron, aluminum and oxygen. In the fuel after the experiment, white molten and gray slag-like structures are visible. White

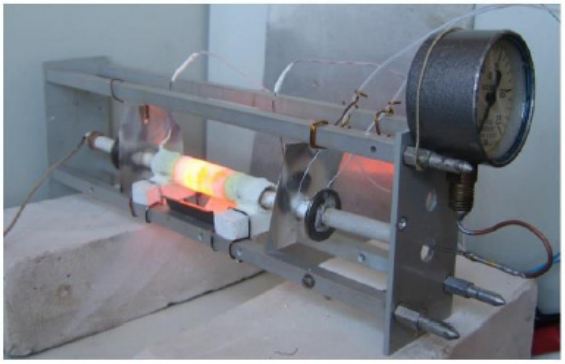

Figure 1. AP2 reactor.

structures contain mainly nickel with an admixture of Fe, Al, Cr, Mn, Si and O. Slag-like structures consist mainly of Al and O.

Analysis of the elemental composition of the fuel before and after an experiment using laser atomic emission spectrometer was made at the Kurnakov Institute of General and Inorganic Chemistry, Russian Academy of Sciences. It showed that the content of K and Cr increased tens of times after the experiment. The content of Si, Na, Mg, Ca, Ti and V increased manifold. The content of Al, Ni, Cl, Mn, Cu and Zn decreased. It should be noted that this method of analysis, as well as analysis using a scanning electron microscope, provides information on the atomic composition only on the surface of the test substance.

Analysis of the isotopic composition of the fuel before and after the experiment in the AP2 reactor was made using ICP-MS method, which gives information on the isotopic composition on average over the sample. Such analysis was made in the Vernadsky Institute of Geochemistry and Analytical Chemistry of Russian Academy of Sciences. The total content of aluminum and lithium after the experiment decreased, while the relative content of ^{6}Li increased slightly. However, this increase (by 0.5%) falls within the range of possible measurement error. There are no significant changes in the isotopic composition of nickel.

The analysis of AP2 reactor fuel by the ICP-MS method was also made at Uppsala University (Sweden). The results of these measurements are shown in Table 1.

According to these measurements, the relative content of ^{6}Li in the sample of spent fuel has more than doubled. Quite noticeable changes have occurred also in the ratio of nickel isotopes. These results differ from the results obtained in the Vernadsky Institute of Geochemistry and Analytical Chemistry RAS. This difference can be explained, perhaps, by the unevenness of the changes in the sample volume. It should be noted that reliable results for lithium are difficult to obtain because of a very low concentration of lithium in spent fuel ($< 0.01\%$).

Table 1. Analysis of AP2 reactor fuel by the ICP-MS method at Uppsala University (Sweden).

Percentage	^{6}Li	^{7}Li	^{58}Ni	^{60}Ni	^{61}Ni	^{62}Ni	^{64}Ni
Before	7.4	92.6	68.1	26.2	1.14	3.63	0.93
After	15.4	84.6	63.4	27.6	1.3	5.2	2.5
Nature	7.6	92.4	68.0	26.2	1.14	3.71	0.93

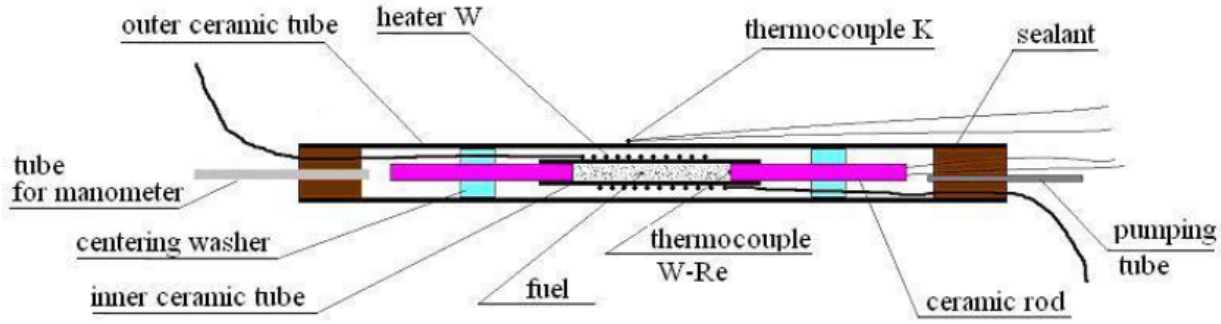

Figure 2. Schematic of the "Protok-6" reactor.

4. Reactor Protok-6

In experiments with devices that claim to obtain heat in amounts exceeding the energy consumed, it is very important to measure the heat released with the greatest possible accuracy. Taking this into account, a series of experiments was carried out in our laboratory using a calorimeter with flowing water, which makes it possible to measure the heat dissipation power with an error of less than 3%. A detailed description of one of reactors tested, "Protok-6", (including the design, the course of experiments, and the methods for determining excess heat) are given in [6] (see Fig. 2). The reactor was operated continuously with this calorimeter from April 11 to May 29, 2016, with the release of excess heat power from 20 to 65 W. The integrated excess energy in this reaction is about 100 MJ [6]. Unlike previous designs having an external heater, this reactor had a heater, made out of tungsten wire, located inside a sealed ceramic tube. The fuel (1.8 g of nickel powder mixed with 0.2 g of lithium aluminum hydride) was located in a ceramic tube wrapped in a tungsten heater. The tube with the heater was in a hermetically sealed ceramic pipe of a larger diameter.

After the experiment was over, the reactor was opened (Fig. 3). It was found that the inner surface of the outer tube near the heater was covered with lumpy gray glassy coating. The physical configuration of the inner tube and the heater winding was preserved. However, the changes inside were significant: a vitreous mass with inclusions of metal balls measuring about 0.1 mm was formed. Several balls had a diameter of up to 1 mm. At the ends of the fuel filling,

Figure 3. The "Protok-6" reactor after opening.

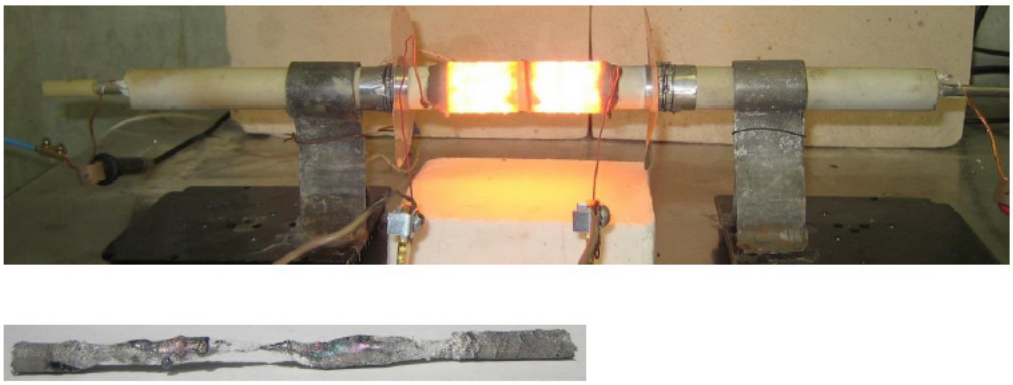

Figure 4. VV3 reactor and spent fuel extracted from it.

it took the form of a sintered mass containing small metal balls. Furthermore, powder from the inner tube poured out. Using a magnet, a fraction was extracted from this powder consisting of filaments with a transverse dimension of about 0.1 mm and length up to 5 mm.

Several samples were subjected to mass-spectroscopic analysis at the Vernadsky Institute of Geochemistry and Analytical Chemistry RAS using the ICP-MS method. The followings were investigated: the initial fuel mixture, a metal ball from the spent fuel, the fuel at the edge of the filling, the substance accumulated between the inner and outer tubes and the coating on the inner surface of the outer tube. Due to the large amount of information received, it is not possible to present it completely. Some of the results of the analysis are shown in Table 2. In addition to the data from samples recovered from the reactor after operation, information is given on the content of isotopes in the fuel, as well as in the ceramic and tungsten wire, before the experiment. This information is important, since the appearance of new elements can be associated not with transmutations, but with migration from structural materials, which is quite possible at high temperatures. Unfortunately, the ICP-MS method cannot determine the content of isotopes with masses of 1–5, 12–22 and 32, including isotopes of carbon, oxygen, nitrogen, fluorine and sulfur.

The obvious result is an increase in the content of many nuclides in comparison with their content in the initial fuel and structural materials. The exception is lithium (which decreased by a factor of about 100) and aluminum in fuel (decreased by a factor of more than 10). We note a particularly large increase in the presence of boron, iron, gallium, cerium, zirconium, strontium and bismuth. The most significant anomalies are found in the powder accumulated in the space between the inner and outer tubes. Especially, a great amount of ^{140}Ce appeared: 6.3% (in the initial fuel <0.0001%). A significant amount of tungsten found in the samples after being inside the reactor is probably due to the migration of this element from the incandescent tungsten coil.

The investigation of possible changes in the isotopic composition of lithium and nickel is of great interest. Unfortunately, the very low content of lithium in the samples after the experiment did not allow us to make reliable measurements. The results obtained for nickel are presented in Table 3. Since the data on ^{64}Ni is unreliable due to the uncontrolled additive of ^{64}Zn, when compiling the table, the value from the reference book [7] was used for the ^{64}Ni fraction. Since this fraction is small, such an assumption can change the fractions of the remaining isotopes only slightly.

It can be seen that the data for the various samples studied differ somewhat from the natural ratio [7], but differ insignificantly between different measurements. A noticeable increase in the ^{62}Ni fraction, due to a decrease in the fraction of the remaining isotopes, that was found in the experiment in Lugano [1,2] was not observed in any of the

Table 2. Relative content of isotopes (atomic %) in fuel and near the core of the "Protok-6" reactor before and after reactor operation. Isotopes with content $> 0.1\%$ are shown.

Before reactor operation						After reactor operation							
Initial fuel+B3:P36		Ceramics		W wire		Metal ball in spent fuel		Coating on inner inner surface of outer tube		Substance appeared between between inner and outer tubes			
^{7}Li	0.74	^{23}Na	7.03	^{23}Na	5.37	^{11}B	0.19	^{23}Na	1.56	^{11}B	0.44	^{75}As	0.43
^{23}Na	1.90	^{24}Mg	1.61	^{24}Mg	0.25	^{23}Na	5.07	^{24}Mg	1.16	^{23}Na	14.70	^{76}Ge, Se	0.16
^{24}Mg	0.12	^{25}Mg	0.23	^{27}Al	0.31	^{24}Mg	0.21	^{25}Mg	0.15	^{24}Mg	0.82	^{77}Se	0.17
^{27}Al	3.63	^{26}Mg	0.28	^{29}Si	1.88	^{27}Al	0.22	^{26}Mg	0.17	^{26}Mg	0.15	^{79}Br	0.97
^{29}Si	1.04	^{27}Al	65.05	^{31}P	0.18	^{29}Si	3.94	^{27}Al	0.23	^{27}Al	0.92	^{81}Br	1.03
^{39}K	1.60	^{29}Si	1.55	^{39}K	6.09	^{31}P	0.14	^{29}Si	0.77	^{29}Si	9.37	^{90}Zr	0.16
^{44}Ca	0.28	^{31}P	0.16	^{44}Ca	1.06	^{39}K	3.51	^{39}K	0.86	^{31}P	0.32	^{115}In, Sn	0.26
^{45}Sc	0.22	^{39}K	8.36	^{45}Sc	0.80	^{43}Ca	0.14	^{44}Ca	0.71	^{39}K	9.89	^{120}Sn, Te	0.12
^{51}V	0.68	^{44}Ca	0.94	^{54}Cr	0.40	^{44}Ca	1.08	^{45}Sc	0.24	^{43}Ca	0.35	^{127}I	0.15
^{53}Cr	0.22	^{45}Sc	0.61	^{56}Fe	10.46	^{45}Sc	0.91	^{51}V	0.10	^{44}Ca	2.15	^{138}Ba, La, Ce	0.36
^{55}Mn	0.17	^{48}Ti, Ca	0.16	^{182}W	18.50	^{51}V	1.56	^{52}Cr	0.57	^{45}Sc	1.95	^{140}Ce	6.54
^{56}Fe	0.99	^{54}Cr	0.41	^{183}W	9.52	^{52}Cr	0.14	^{53}Cr	0.10	^{48}Tl,Ca	0.13	^{142}Ce, Nd	0.85
^{58}Fe, Ni	55.91	^{56}Fe	10.00	^{184}W	21.48	^{53}Cr	0.51	^{54}Cr	1.17	^{51}V	6.08	^{182}W	3.50
^{60}Ni	23.58	^{58}Fe, Ni	0.15	^{186}W, Os	21.29	^{54}Cr	0.46	^{56}Fe	19.10	^{52}Cr	0.48	^{183}W	1.77
^{61}Ni	1.10	^{89}Y	0.25	^{200}Hg	0.20	^{55}Mn	0.14	^{57}Fe	0.45	^{53}Cr	2.07	^{184}W, Os	4.09
^{62}Ni	3.63	^{90}Zr	0.44	^{202}Hg	0.21	^{56}Fe	7.36	^{58}Fe, Ni	32.31	^{54}Cr	0.61	^{186}W, Os	3.82
^{64}Ni, Zn	1.24	^{92}Sr, Mo	0.16	^{198}Hg	0.21	^{57}Fe	0.18	^{59}Co	0.40	^{55}Mn	0.28	^{206}Pb	0.21
^{66}Zn	0.16	^{94}Sr, Mo	0.16			^{58}Fe, Ni	45.07	^{60}Ni	13.93	^{56}Fe	6.48	^{207}Pb	0.19
^{68}Zn	0.12	^{138}Ba, Ce	0.33			^{60}Ni	19.81	^{61}Ni	0.68	^{57}Fe	0.18	^{208}Pb	0.49
^{79}Br	0.13	^{206}Pb	0.13			^{61}Ni	0.86	^{62}Ni	2.10	^{58}Fe, Ni	8.25		
^{81}Br	0.12	^{208}Pb	0.29			^{62}Ni	2.97	^{64}Ni, Zn	5.06	^{60}Ni	3.30		
^{138}Ba, La, Ce	0.25					^{63}Cu	0.14	^{66}Zn	2.88	^{61}Ni	0.15		
^{206}Pb	0.32					^{64}Ni, Zn	1.62	^{67}Zn	0.47	^{62}Ni	0.54		
^{207}Pb	0.25					^{66}Zn	0.52	^{68}Zn	2.02	^{63}Cu	0.17		
^{208}Pb	0.69					^{68}Zn	0.40	^{88}Sr	0.11	^{64}Ni, Zn	1.48		
						^{75}As	0.15	^{115}In, Sn	0.13	^{66}Zn	0.81		
						^{79}Br	0.35	^{140}Ce	0.37	^{67}Zn	0.15		
						^{81}Br	0.36	^{182}W	2.81	^{68}Zn	0.63		
						^{138}Ba, La, Ce	0.14	^{183}W	1.54				
						^{184}W, Os	0.12	^{184}W, Os	3.52				
						^{208}Pb	0.17	^{186}W, Os	3.24				

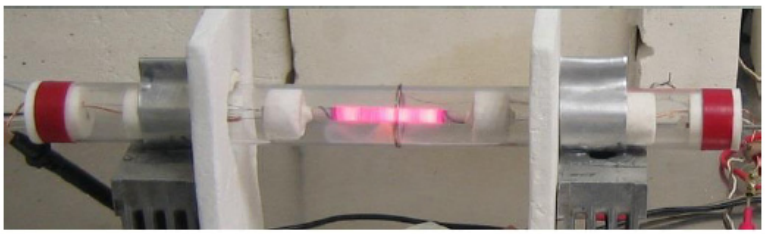

Figure 5. Reactor KV3 at the beginning of the experiment.

samples studied. It is possible that the effect is not visible due to the fact that the excess energy production in Lugano experiment was 60 times greater than in the described one.

5. Reactor VV3

The VV3 reactor (Fig. 4) differs from the "Protok 6" reactor with a different heater design and the absence of a calorimeter. A mixture of nickel powder with lithium aluminum hydride weighing 1.5 g was used as fuel. The fuel contained pieces of tungsten wire with a total mass of 0.77 g. The reactor ran from June 14 to July 24, 2016, producing excess power of up to 330 W. A total of 790 MJ of excess heat was generated. Determination of excess heat was carried out by comparing the temperature dependencies on the reactor surface from the consumed electric power obtained for reactors with fuel and without fuel having the same design.

After the experiment was finished, the spent fuel, which looked like a drop-shaped ingot, was extracted from it. It was analyzed at the Vernadsky Institute of Geochemistry and Analytical Chemistry RAS using the ICP-MS method, with separate analyses of the surface and deeper layers. Some of the results of the analysis are shown in Tables 4 and 5. In addition to the data for the samples recovered from the reactor after its operation, information is given on the content of isotopes in the initial fuel, including tungsten wires embedded in it.

It can be seen that the isotopic composition of fuel as a result experiment has changed noticeably. The content of boron, copper, cerium and silver increased significantly.

Just as in the above-described reactors, the data on the investigated samples, although slightly different from the natural ratio, differ insignificantly between each other.

6. KV3 Reactor

The main difference between the KV3 reactor (Figs. 5 and 6) and the previous reactors is that it was loaded with 1.8 g of nickel powder without an admixture of lithium aluminum hydride. Saturation with hydrogen was carried out by

Table 3. The ratio of nickel isotopes in fuel and near the core of the "Protok-6" reactor before and after the experiment.

Percentage	^{58}Ni	^{60}Ni	^{61}Ni	^{62}Ni	^{64}Ni
Initial fuel	65.78	27.74	1.29	4.28	0.91
Metal ball	65.00	28.57	1.24	4.29	0.91
Fuel at edge	65.58	27.88	1.27	4.36	0.91
Coating on ceramics	65.32	28.16	1.37	4.24	0.91
Power between tubes	66.74	26.71	1.23	4.41	0.91
Natural ratio	68.27	26.1	1.13	3.59	0.91

keeping it in hydrogen gas. In addition, unlike the above-described reactors, it had a quartz outer tube instead of a ceramic one. The heater was made from a tungsten–rhenium alloy, instead of pure tungsten. The KV3 reactor was operated from December 20, 2016 until January 31, 2017, with an excess power of 100–200 W. The integrated excess energy during the whole operating time of the KV3 reactor is about 400 MJ. Determination of excess heat was carried out by comparing the temperature dependencies on the reactor surface with electric power obtained for reactors with fuel and without fuel having the same design.

The ICP-MS analysis by the Vernadsky Institute of Geochemistry and Analytical Chemistry RAS was used to investigate: fuel and structural materials prior to operation of the reactor, as well as fuel in the central zone and near the edge, powder from the space between the inner and outer tubes, and structural materials after operating the reactor. Some of the results are shown in Table 6.

Just as in the Protok-6 and VV3 reactors, a lot of tungsten appeared in the space between the inner and outer tubes. In addition to tungsten, a lot of iron, sodium, potassium, nickel, silicon, calcium, scandium and a number of other elements accumulated there.

Comparing fuel before and after the experiment, one can see a decrease in the content of sodium, potassium and iron. Attention is drawn to the appearance of a significant amount of copper.

A lot of tungsten and rhenium appeared in the inner ceramic tube that holds the fuel, which was wrapped with a heater. Table 7 shows nuclides, the relative content of which in the ceramic tube has increased more than 10-fold.

It can be seen that in addition to tungsten and rhenium, the appearance of which can be explained by its migration from the heater coil, the boron content in the ceramic tube greatly increased, as well as nuclides with atomic masses of 43–53, 64–83, 107–130, and 198–208.

Table 8 shows the results of an analysis of the ratio of nickel isotopes in the fuel, as well as in the surrounding ceramic and in the substance accumulated between the inner and outer tubes, before and after the reactor was operated. When analyzing the isotopic composition, in order to avoid the errors associated with the registration of ^{64}Zn, the ^{64}Ni share was taken from the reference book [7].

It can be seen that the isotopic composition of nickel in the fuel before and after the experiment remained practically unchanged. Some differences are noticeable in the results obtained for the ceramic tube and the substance between the tubes. But these results cannot be considered accurate, since the concentration of nickel in the samples studied is not high enough for reliable analysis.

In addition to the Vernadsky Institute of Geochemistry and Analytical Chemistry RAS, the analysis of KV3 fuel before and after the experiment, as well as the substance from the space between the inner and outer tubes, was made by

Figure 6. Reactor KV3 opened after the experiment.

Table 4. Isotope content (atomic %) in the reactor fuel "VV3" before and after reactor operation. Isotopes with a content $> 0.1\%$ are shown.

Before		After					
Initial fuel		Surface		Surface		Deep layer	
23Na	2,61	10B	0,15	75As	0,17	10B	0,14
24Mg	0,15	11B	0,67	79Br	0,11	11B	0,66
27Al	2,93	24Mg	1,50	81Br	0,21	23Na	3,72
29Si	1,22	25Mg	0,12	88Sr	0,23	27Al	1,02
39K	2,52	26Mg	0,27	90Zr	0,20	28Si	0,25
44Ca	0,44	27Al	1,14	107Ag	1,13	51V	2,14
45Sc	0,34	28Si	0,54	109Ag	2,01	52Cr	0,30
51V	0,55	44Ca	0,16	127I	0,43	53Cr	0,73
53Cr	0,18	45Sc	0,18	140Ce	0,72	54Cr	0,21
55Mn	0,14	51V	2,41	182W	3,34	56Fe	2,55
56Fe	2,92	52Cr	0,31	183W	1,61	58Fe,Ni	44,47
58Fe,Ni	45,09	53Cr	0,81	184W,Os	3,39	60Ni	18,23
60Ni	19,01	56Fe	0,42	185Re	0,26	61Ni	0,87
61Ni	0,88	58Fe,Ni	46,08	186W,Os	2,91	62Ni	2,83
62Ni	2,93	60Ni	19,34	187Re,Os	0,60	64Ni,Zn	0,87
64Ni,Zn	1,00	61Ni	0,96	206Pb	0,18	75As	0,12
66Zn	0,13	62Ni	3,02	207Pb	0,13	79Br	0,19
68Zn	0,10	63Cu	0,39	208Pb	0,34	81Br	0,19
79Br	0,10	64Ni,Zn	1,31			90Zr	0,39
7Li	0,60	65Cu	0,16			92Sr,Mo	0,14
81Br	0,10	66Zn	0,37			94Sr,Mo	0,16
138Ba,La,Ce	0,20	68Zn	0,20			107Ag	1,37
182W	3,73					109Ag	1,39
183W	1,92					140Ce	0,78
184W	4,33					142Ce,Nd	0,10
186W,Os	4,29					182W	3,49
206Pb	0,26					183W	1,90
207Pb	0,20					184W,Os	4,17
208Pb	0,56					185Re	0,38
						186W,Os	3,72
						187Re,Os	0,60
						208Pb	0,17

the research company Coolescence LLC, Boulder, Colorado, USA. EDS analyses were performed using an electronic scanning microscope, as well as analyses using the ICP-MS method. These studies confirmed the insignificant changes in the isotopic composition of the fuel, the appearance in the fuel of about 1% of copper and the presence of many nuclides in the substance from the space between the tubes.

Table 5. The ratio of nickel isotopes in fuel VV3 before and after reactor operation.

Percentage	^{58}Ni	^{60}Ni	^{61}Ni	^{62}Ni	^{64}Ni
Initial fuel	65.93	27.98	1.19	3.98	0.91
Surface	65.79	27.61	1.37	4.31	0.91
Deep layer	66.36	27.20	1.29	4.23	.91
Natural ratio	68.27	26.10	1.13	3.59	0.91

7. Discussion

A significant change in the nuclide composition as a result of the operation of the investigated nickel-hydrogen reactors occurs not only in the fuel, but also in the ceramics surrounding the reactor core. In addition, a substance containing sodium, potassium, silicon, iron, boron, calcium, zinc and many other elements accumulated in the cavity between the inner and outer tubes. An especially large amount of tungsten appeared. It is reasonable to assume that the source of tungsten is the hot spiral of the heater. The most understandable mechanism of substance migration is evaporation in places with high temperature, and condensation in less heated places. As the measurements show, the temperature of the heater wire reaches 1700°C. But even at this temperature, the density of tungsten vapor ($< 10^{-10}$ Pa) is too low for such a mechanism to work with a noticeable intensity. Obviously, more complex physicochemical processes

Table 6. Isotope content (atomic %) in fuel and near the active zone of the KV3 reactor before and after reactor operation. Isotopes with a content $> 0.1\%$ are shown.

Before						After						Substance appeared between inner and outer tubes	
Initial fuel		Ceramic		Heater wire		Fuel central zone		Ceramic		Ceramic			
23Na	0,33	27Al	88,15	23Na	0,47	23Na	0,13	11B	0,13	64Ni,Zn	0,22	23Na	5,53
39K	0,38	23Na	1,98	29Si	0,27	31P	0,11	23Na	15,61	66Zn	0,11	24Mg	0,50
56Fe	0,45	24Mg	0,82	39K	0,40	39K	0,14	24Mg	1,06	76Ge,Se	0,20	27Al	0,32
58Fe, Ni	64,49	25Mg	0,12	44Ca	0,12	56Fe	0,23	25Mg	0,13	88Sr	0,21	29Si	1,42
60Ni	27,63	26Mg	0,14	56Fe	0,21	58Fe, Ni	65,39	26Mg	0,24	89Y	0,22	31P	0,16
61Ni	1,18	29Si	0,37	58Fe,Ni	0,12	60Ni	26,15	27Al	0,05	90Zr	0,42	39K	6,93
62Ni	3,88	39K	2,10	182W	20,24	61Ni	1,18	29Si	4,26	92Sr,Mo	0,22	44Ca	0,88
64Ni,Zn	1,21	44Ca	0,21	183W	11,02	62Ni	3,99	39K	15,26	94Sr,Mo	0,17	45Sc	0,82
		47Ti	0,88	184W,Os	24,39	63Cu	0,84	43Ca	0,26	109Ag	0,10	54Cr	0,26
		48Ti,Ca	0,18	185Re	6,97	64Ni,Zn	1,14	44Ca	3,15	127I	0,16	56Fe	7,04
		54Cr	0,14	186W,Os	22,23	65Cu	0,42	45Sc	2,04	138 Ba,Ce	0,39	58Fe, Ni	1,80
		56Fe	3,17	187Re,Os	11,85			48Ti,Ca	0,23	182W	4,32	60Ni	0,74
		58Fe, Ni	0,28	198Hg,Pt	0,12			51V	0,22	183W	2,35	62Ni	0,10
		60Ni	0,11	200Hg	0,14			54Cr	0,96	184W	5,01	63Cu	0,13
		89Y	0,13	202Hg	0,13			55Mn	0,10	185Re	5,95	64Ni,Zn	0,15
		138 Ba,Ce	0,17	208Pb	0,18			56Fe	21,14	186W,Os	4,77	182W	18,29
								57Fe	0,15	203Tl	0,15	183W	10,44
								58Fe, Ni	0,91	206Pb	0,15	184W	21,36
								60Ni	0,37	207Pb	0,15	186W,Os	20,90
								63Cu	0,14	208Pb	0,40	198Hg	0,17
												200Hg	0,20
												202Hg	0,18
												208Pb	0,15

take place with the participation of hydrogen and other reagents that may be present in the reactor. It is possible that a number of other elements appear as a result of migration from structural materials, since sodium, potassium, silicon, calcium, iron and a number of other elements are contained in appreciable quantities in the heater wire, thermocouples and in ceramics. However, there are some elements (cobalt, cerium, gallium, germanium, arsenic, selenium, cadmium and tellurium) that appeared in significant quantities, which are virtually absent from the initial fuel and structural materials. This indicates the possibility of their appearance as a result of nuclear transmutations. For example, cerium can be a product of the fission of tungsten:

$$^{182}\mathrm{W} \rightarrow {}^{140}\mathrm{Ce} + {}^{42}\mathrm{Ca} + 4\mathrm{e} + 76.04\ \mathrm{MeV}. \tag{3}$$

Attention is drawn to the appearance of a significant amount of copper in the fuel of the KV3 reactor (0.84% ^{63}Cu and 0.42% ^{65}Cu) with a total mass of about 20 mg. It can be assumed that this is due to the course of nuclear reactions given below:

Table 7. Relative content of nuclides (atomic %) in the ceramic tube before and after the operation of the KV reactor. Nuclides are shown whose content has increased more than 10 times.

	before	after	after / before		before	after	after / before
10B	0,0008	0,0318	41,8	114Cd,Sn	0,0005	0,0064	11,9
11B	0,0054	0,1277	23,4	116Cd,Sn	0,0022	0,0275	12,8
29Si	0,3709	4,2603	11,5	117Sn	0,0011	0,0129	12,0
43Ca	0,0158	0,2638	16,7	118Sn	0,0024	0,0422	17,9
44Ca	0,2123	3,1461	14,8	119Sn	0,0014	0,0165	11,7
45Sc	0,0507	2,0384	40,2	120Sn,Te	0,0034	0,0670	19,5
46Ti,Ca	0,0074	0,0836	11,3	119Sn	0,0014	0,0165	11,7
51V	0,0028	0,2151	78,0	122Te	0,0007	0,0101	15,0
53Cr	0,0057	0,0753	13,3	127 I	0,0062	0,1589	25,7
64Ni,Zn	0,0186	0,2224	12,0	128Te	0,0002	0,0046	22,8
66Zn	0,0099	0,1102	11,1	124Te	0,0008	0,0092	11,4
67 Zn	0,0014	0,0211	15,0	130Te	0,0006	0,0101	16,7
68Zn	0,0080	0,0808	10,1	182W	0,0076	4,3168	567,8
72Ge	0,0001	0,0037	27,2	183W	0,0035	2,3489	671,7
75As	0,0001	0,0138	102,2	184W	0,0076	5,0087	658,8
76Ge,Se	0,0115	0,1976	17,2	185Re	0,0006	5,9469	9827,0
77Se	0,0001	0,0055	82,2	186W,Os	0,0089	4,7748	537,6
78Se,Kr	0,0028	0,0542	19,7	198Hg	0,0001	0,0321	238,5
79Br	0,0028	0,0560	20,3	199Hg	0,0007	0,0248	33,5
81Br	0,0040	0,0790	19,6	200Hg	0,0004	0,0560	138,9
83Kr	0,0001	0,0009	13,7	202Hg	0,0005	0,0606	128,8
107Ag	0,0067	0,0863	13,0	203Tl	0,0015	0,1498	101,2
109Ag	0,0071	0,1020	14,3	204Pb,Hg	0,0010	0,0101	10,0
113Cd,In	0,0001	0,0009	13,7				

Table 8. The ratio of nickel isotopes in fuel and near the core of the KV3 reactor before and after reactor operation.

Percentage	^{58}Ni	^{60}Ni	^{61}Ni	^{62}Ni	^{64}Ni
Initial fuel	65.93	27.98	1.19	3.98	0.91
Fuel after work	65.74	28.17	1.20	3.98	0.91
Substance between tubes	66.66	27.33	1.30	3.79	0.91
Ceramics	67.65	27.37	0.82	3.26	0.91
Natural ratio	68.27	26.10	1.13	3.59	0.91

$$^{62}\mathrm{Ni} + {}^{1}\mathrm{H} \rightarrow {}^{63}\mathrm{Cu} + 6.125\ \mathrm{MeV}, \qquad {}^{64}\mathrm{Ni} + {}^{1}\mathrm{H} \rightarrow {}^{65}\mathrm{Cu} + 7.450\ \mathrm{MeV}. \tag{4}$$

About 200 MJ are released as a result of reactions (4), when 20 mg of copper is formed. This energy release does not contradict the total excess heat release in the KV3 reactor (about 400 MJ). In addition to heat generation, the appearance of such a quantity of copper should cause a decrease in the relative content of ^{62}Ni by 0.8% and ^{64}Ni by 0.4%. The data presented in Table 6 does not show such changes. It should be noted that the predicted changes lie within the limits of a possible measurement error, and the ^{64}Ni content is generally difficult to measure reliably due to uncontrolled additions of ^{64}Zn.

Undoubtedly, in the reactors described here, in addition to nuclear transmutations, ordinary physical and chemical processes occur. These processes require further study because of their extreme complexity. But the excess energy release, which is much higher than a chemical reaction can produce, proves that the processes in the reactors cannot be explained only by conventional chemistry.

8. Conclusions

(1) The isotopic and elemental composition of the substance in four nickel-hydrogen reactors of various designs with an excess energy output from 100 to 790 MJ has been analyzed. Not only the changes in fuel but also the materials adjacent to the active zone have been investigated. In addition, the composition of the substance accumulating in the cavity of the reactor near the active zone has been studied.
(2) There were no significant changes in the isotopic composition of nickel and lithium, except for the analysis of the fuel of the AP2 reactor at Uppsala University (Sweden).
(3) A significant increase in the concentration of impurities of a number of nuclides has been detected not only in the fuel, but also in structural elements adjacent to the active zones of the reactors. In addition to tungsten and rhenium, the appearance of which can be explained by migration from the heater coil, the content of boron increased greatly, as well as nuclides with atomic masses of 43–53, 64–83, 107–130, and 198–208.
(4) In the substance that was found in the cavity of the reactor near the active zone, in addition to tungsten, a lot of iron, sodium, potassium, nickel, silicon, calcium, scandium and a number of other elements accumulated.

References

[1] G. Levi, E. Foschi and B. Höistad, Observation of abundant heat production from a reactor device and of isotopic changes in the fuel. http://www.sifferkoll.se/sifferkoll/wp-content/uploads/2014/10/LuganoReportSubmit.pdf.
[2] A.G. Parkhomov, Report of the international commission on the test of high-temperature heat generator Rossi, *IJUS* **2** (6) (2014) 57–61 (in Russian). http://www.unconv-science.org/pdf/6/parkhomov2-ru.pdf.
[3] A.G. Parkhomov, Nickel–hydrogen reactors created after publication of the report on experiment in Lugano, *IJUS* **4** (11) (2016) 58–62 (in Russian). http://www.unconv-science.org/pdf/11/parkhomov-ru.pdf.

[4] K.A.Alabin, S.N. Andreev and A.G. Parkhomov, Results of analysis of isotopic and elemental composition of the fuel of nickel–hydrogen reactors, *IJUS* **3** (10) (2015) 49–53 (in Russian). http://www.unconv-science.org/pdf/10/alabin-ru.pdf

[5] A.G. Parkhomov, Investigation of new version of the device similar to high-temperature Rossi heat generator, *IJUS*, **8**(3) (2015) 34–38. http://www.unconv-science.org/pdf/8/parkhomov-en.pdf.

[6] A.G. Parkhomov, Long-term tests of nickel–hydrogen heat generators in water flow calorimeter, *IJUS* **4** (12–13) (2016) 74–79 (in Russian). http://www.unconv-science.org/pdf/12/parkhomov-ru.pdf.

[7] I. Grigoryev and E.Z. M. Meilikhova (Eds.), *Physical Magnitudes*, *Directory*, Energoatomizdat, 1991, 1232 p. (in Russian).

J. Condensed Matter Nucl. Sci. 26 (2018) 45–53

Research Article

Cold Nuclear Transmutations. Distribution of Binding Energy within Nuclei

Philippe Hatt*,†

Route Gouvernementale 154, B-1950 Kraainem, Belgium

Abstract

In 1936 Bethe and Bacher and in 1938 Hafstad and Teller predicted that α particle structures could be present in atomic nuclei. In the course of developing a theory of nuclear structure based on the assumption of closest packing of clusters of nucleons, Linus Pauling found that the magic numbers have a very simple structural significance. He assumed that in nuclei the nucleons may, as a first approximation, be described as occupying localized 1s orbitals to form small clusters. These small clusters, called spherons, are usually helions (i.e. α particles), tritons and dineutrons. In nuclei containing an odd number of neutrons, an He^3 cluster or a deuteron may serve as a spheron. The close-packed-spheron model differs from the conventional liquid-drop model of the nucleus in having spherons rather than nucleons as the units. This is a simplification: Gd^{154}, for example, is described in terms of 45 spherons, rather than 154 nucleons. This enables to determine the binding energies in a much simpler way than the approach based on individual nucleons. I developed that idea, i.e. having clusters as basic bricks within the nucleus instead of nucleons. These clusters are the same than Pauling's ones, i.e. α particles and deuterium, tritium, He^3 and dineutrons like clusters. Nevertheless, on the method, my approach differs from that one of Pauling. I tried a simple method of mind experiments, approaching the problem step by step, nucleus after nucleus, isotope after isotope, looking each time at the preceding nucleus or isotope binding energy to compare with the next nucleus binding energy. My purpose is about LENR, i.e. looking for differences of binding energies between elements at the beginning and the end of the LENR process in order to determine the energy release. Indeed, my approach is looking for the distribution of binding energy within each element and each isotope, comparing their values, rather than researching for an internal structure of these elements. So, my approach is not about 3D structure of the nuclei but is rather based on an unidimensional value of their binding energy, looking for the internal distribution of that energy and trying to find distribution similarities between elements and isotopes. As a result, I could determine in a coherent way the binding energy of all stable nuclei and their isotopes on basis of the five clusters mentioned above and which are the same as those retained by Pauling. Indeed, I do not care about the geometrical structure of the packing of spherons, but rather about the organization of these spherons in order to determine for each element and isotope the binding energy characterizing it.
 ISSN 2227-3123

Keywords: Alpha particle, Deuterium, Dineutron, He^3, Tritium

*E-mail: pcf.hatt@gmail.com.
†Independent researcher.

 ISSN 2227-3123

1. Introduction

In 1936 Bethe and Bacher [1] and in 1938 Hafstad and Teller [2] predicted that α particle structures could be present in atomic nuclei. In line with Pauling [3] view on the nuclear structure, allowing him to determine some clusters within the nucleus he called spherons, I tried to organize the nucleus in a similar way. The sub nuclei I took into consideration are the α particles. These particles are linked together with four types of bonds determined in the following way.

- Deuterium like bond, called NP with value 2.2246 MeV, linking a neutron of one α particle with a proton of a second α particle, or a neutron or proton outside an α particle to that α particle.
- Tritium like bond, called NNP with value 8.4818 MeV, linking three nucleons of three different α particles, or one or two nucleons outside an α particle to one or two α particles.
- He^3 like bond, called NPP with value 7.718 MeV, having a similar function as NNP.
- A dineutron bond, I called NN, with value 4.9365 MeV and linking two neutrons not being located within the same α particle. This bond and its value are deduced from the α particle binding energy (for details see www.philippehatt.com).

So, the binding energy (E_B) of an element is composed with E_B of α particles (28.325 MeV each) together with the E_B's of the various four bonds determined above.

With Pauling's model, the difficulty was the arbitrary decisions he made about which structures are "real nuclei" and which are not. I was confronted with the same problem. It is the reason why I studied first the n α nuclei as certain authors predict that α particle structures could be present in atomic nuclei. This could be in particular the case of the light nuclei like O^{16}, Ne^{20}, Mg^{24}, Si^{28}, S^{32}, Ar^{36}, and Ca^{40}. This is my first assumption or hypothesis. So, everything considered, I made that choice which could be seen as arbitrary. In the frame of that hypothesis, there are by definition only α particles within the nucleus. The problem to solve is then how they are bound together. For instance, Be^8 is not stable as there is no room for bonds between the two α particles, the E_B of that element being more or less equal to the E_B of its two α particles. It is not the case of O^{16} containing four α particles and having a global E_B superior to the E_B of these four α particles together. This difference represents the E_B between the four α particles.

2. Composition of Inter Alpha Binding Energy

I assumed that the bonds between α particles should link one α to another α in case of NN and NP involving only two nucleons, and three α in case of NNP and NPP. I eliminated the bonds of type NNN and PPP as non "realistic" and accepted NP, NNP, and NPP because they are equivalent to deuterium, tritium and He^3 bonds already existing before the α particle is constituted.

As far as NN and PP are concerned, these constituting the α particle binding energy, I accepted only NN for the following reasons.

- With exception of He^3 there is no stable element or stable isotope containing more protons than neutrons. So, outside the α particles there is only one proton possible and not more in a given nucleus. There could of course be more neutrons. This excludes proton–proton bonds outside α particle.
- Coming back to O^{16} and to the binding energy in excess to that one of the α, I noticed the following. The four α could be linked by minimum three bonds between each time two α or by one NNP or NPP bond and one NN or one NP bond. The only suitable values were two NP's together with the neutron–neutron binding energy within α particle. Actually, four $E_B\alpha$, two NP and the "neutronic" part of α particle E_B is equal to E_B of O^{16}.

These are the assumptions concerning the four bonds NN, NP, NNP, and NPP. To simplify I merged NP and NN in one bond called A = NN/2+NP/2.

3. Examples of Nuclei Binding Energy

With these five bonds: α, NN, NP, NNP, and NPP, I could determine the binding energy of the $n\alpha$ nuclei mentioned above, and later of all stable nuclei.

Examples:

E_B of O^{16} = 4 E_B α+ 4A,

E_B of Ne^{20} = 5 E_B α+ 5A + NP/2 (or A + 2NPP),

E_B of Mg^{24} = 6 E_B α+ 2A + NN + NNP + NPP,

E_B of Si^{28} = 7 E_B α+10A + NN/2,

E_B of S^{32} = 8 E_B α+ 4A + 4NPP,

E_B of Ar^{36} = 9 E_B α+ 8A + 3NPP,

E_B of Ca^{40} = 10 E_B α+ 6A + NN + 2NNP + 2NPP.

Moreover, one can see the kinship between these nuclei, for example, see Figs. 1–3:

E_B O^{16} versus E_B S^{32}

E_B Ca^{40} versus E_B O^{16} and E_B Mg^{24}.

$^{32}_{16}$S		8α	E_B in MeV = 271.7801
	E_B	8α	226.6000 MeV
		2NN	9.8730
		2 NP	4.4492
		4 NPP	30.8720
			271.7942 MeV
			+0.014

E_B = 8 E_B α+ 4A + 4NPP = 271.7942 MeV (+0.014).

The core of this structure is the same than that one of O^{16}. Four NPP bonds linking each time three α particles are completing this core structure. The S^{32} contains eight α particles, the double of O^{16}. Nevertheless, the bonds of S^{32}

supplementary to O^{16} have a higher value: 4 NPP = 8A + NP instead of 4A. The excess value is then equal to 4A + NP. A tentative transmutation process between two O^{16} nuclei with outcome S^{32} is shown in Fig. 2. 4A bonds of second O^{16} structure interact with the four α particles of first O^{16} structure.

Result: 4NPP bonds are created as there are four interactions between each time three α particles.

Total: eight α particles, 4A bonds and 4NPP bonds, i.e. the structure of S^{32} (see Fig. 1).

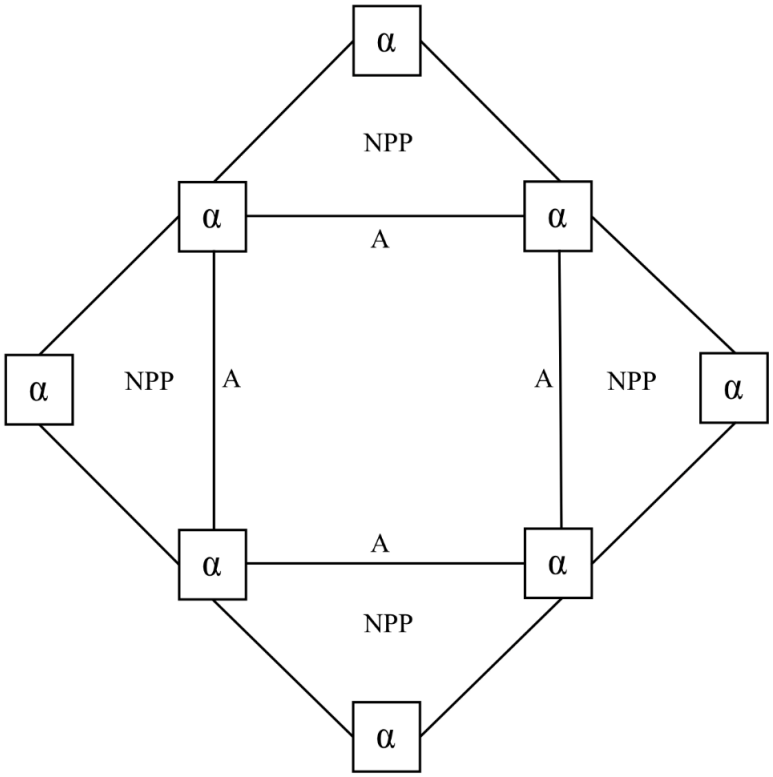

Figure 1. Distribution. of E_B $^{32}_{16}$S between α particles.

$^{40}_{20}$Ca 10 αE_B in MeV = 342.0522.

E_B	10	α	283.2500	MeV
	4	NN	19.7460	
	3	NP	6.6738	
	2	NNP	16.9636	
	2	NPP	15.4360	
			342.0694	MeV
			+0.017	

E_B = 10 E_B α+ 6A + NN + 2NNP + 2NPP = 342.0694 MeV (+ 0.017).

This structure has a core equal to that one of O16.The rest is similar to Mg^{24}. Actually, the addition of O^{16} bonds and Mg^{24} bonds is the following:

O^{16}	4A			
Mg^{24}	2A	NN	NNP	NPP
	6A	NN	NNP	NPP

The bonding of Ca^{40} is the following: Ca^{40} 6A NN 2NNP 2NPP. Ca^{40} bonds represent the O^{16} bonds plus the Mg^{24} bonds with addition of one NNP and one NPP bonds (see Fig. 3).

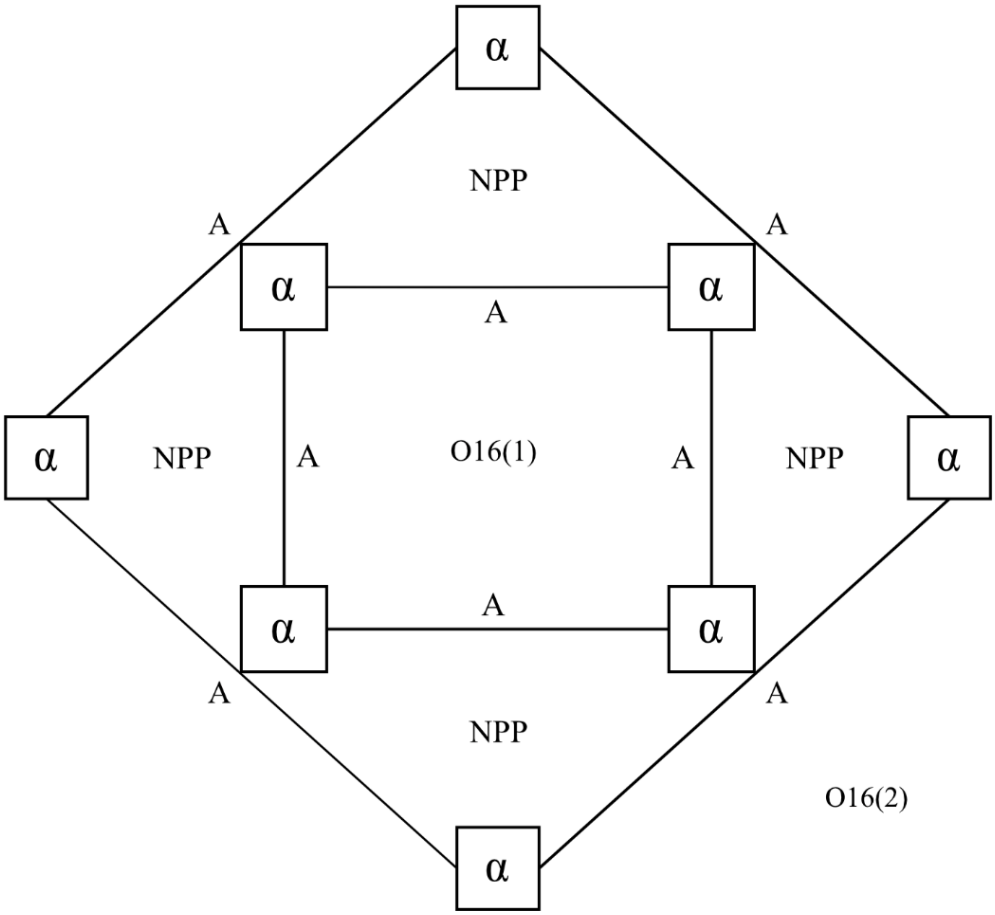

Figure 2. Tentative transmutation process. Basis: Two structures of O^{16} with each 4A bonds.

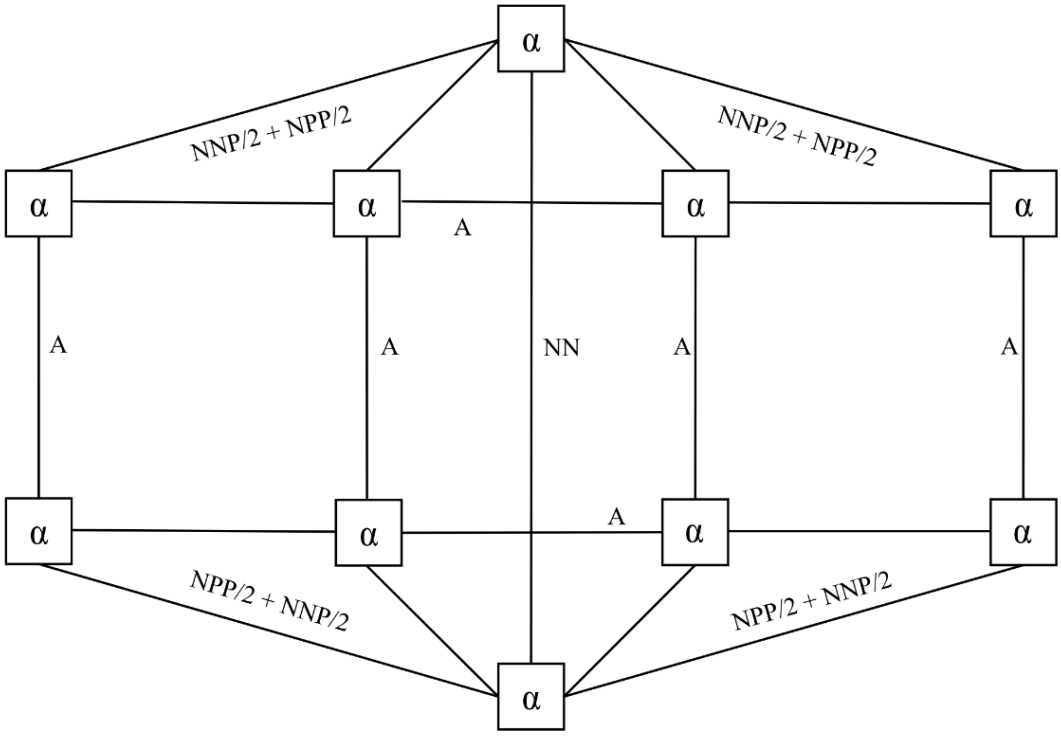

Figure 3. Distribution of E_{B} Ca^{40} between α particles.

4. Discussion

The key idea of my theory is to find a common distribution of binding energy within the various nuclei which could in turn help to understand the LENR process. It is about finding a kinship between the various nuclei. According to my theory there is the following sequence in binding energy:

NP | bonds pre-existing
NNP ⇒ NPP | to α particle bond
α particle

So, in case of two α and more, it is assumed that the binding energy between these α is based on binding energy between their nucleons and that the value of these bonds is related to the values of NP, NNP, NPP and on the value of NN which part of α binding energy is.

4.1. Progression of binding energy

4.1.1. *Basic values*

NP = 2.2246 MeV,

NNP = 8.4818 MeV,
NPP = 7.7180 MeV. Difference between NNP and NPP = 0.7638 MeV,
α particle = 28.325 MeV = 2NN + PP = 9.873 MeV + 18.452 MeV (for details see www.philippehatt.com).

4.1.2. *Determination of binding energy values based on preceding values*

He^5 = He^4+ neutron (N),
$E_B = E_B\ \alpha -$ NNP + NPP = 28.325 − 0.7638 = 27.5612 MeV,
Li^6 = He^4+ N + P (proton),
$E_B = E_B\ \alpha -$ NNP + NPP + 2NP = 28.325 − 0.7638 + 4.4492 = 32.01 MeV,
Li^7 = He^4+ 2N + P,
$E_B = E_B\ \alpha +$ 3NP + NNP/2 = 28.325 + 6.6738 + 4.2409 = 39.2397 MeV,
Be^9 = 2 He^4+ N,
$E_B = 2\ E_B\ \alpha +$ 1.5/2 NN + 1.5/2 NP − NPP/2 = 56.65 + 3.7024 +1.6685 − 3.859 = 58.162 MeV,
B^{10} = 2 He^4+ N + P,
$E_B = 2\ E_B\ \alpha +$ NNP/2 + NPP/2 = 56.65 + 4.2409 + 3.859 = 64.7499 MeV,
B^{11} = 2 He^4+ 2N + P,
$E_B = 2\ E_B\ \alpha +$ 1.5 NN +2 NP + NPP = 76.222 MeV.

4.2. Other examples of nuclei binding energy

$E_B\ C^{12}$ =3 $E_B\ \alpha +$ NN + NP = 92.136 MeV,
$E_B\ C^{13}$ =3 $E_B\ \alpha +$ NN + NP + NP/2 + NPP/2 = 97.107 MeV,
$E_B\ C^{14}$ =3 $E_B\ \alpha +$ 1.5 NP + 2NNP = 105.274 MeV,
$E_B\ C^{15}$ =3 $E_B\ \alpha +$ NP + 2.5 NPP = 106.495 MeV,
$E_B\ C^{16}$ =3 $E_B\ \alpha +$ NP + 2.5 NPP + NNP/2 = 110.735 MeV.

$E_B\ N^{14}$ =3 $E_B\ \alpha +$ NNP/2 + 2 NPP = 104.652 MeV,
$E_B\ N^{15}$ =3 $E_B\ \alpha +$ 2NN + 2NP + NNP + NPP = 115.497 MeV,
$E_B\ N^{16}$ =3 $E_B\ \alpha +$ 1.5NN + 2.5NP + NNP + 1.5NPP = 118.000 MeV.

$E_B\ O^{16}$ =4 $E_B\ \alpha +$ 2NN + 2NP = 127.622 MeV,
$E_B\ O^{17}$ =4 $E_B\ \alpha +$ 1.5NN + 1.5NP + NPP = 131.760 MeV,
$E_B\ O^{18}$ =4 $E_B\ \alpha +$ 2NN + 4NP + NPP = 139.789 MeV.

Remark: for all these results the differences between experimental and calculated values are less than 0.026 MeV (source: "The AME 2012 atomic mass evaluation").

5. Conclusion

5.1. Determining the binding energy

These results are obtained by comparing binding energy values of several nuclei, especially isotopes of the same element and by breaking down these values in NP, NNP, NPP, and α particle binding energy values. The α particle binding energy value was also broken down in 2 NN and PP values. Only NN is active outside α particle, PP being active only within α particle. One single process is used, i.e. looking step by step, isotope element after isotope

element, for binding energy differences between the various elements and their isotopes. One should also consider that the mass differences in binding energy values could be positive or negative, the negative values showing a mass recreation. Having this in mind one can determine the binding energy value of every element or its isotopes. See the figures displayed in www.philippehatt.com.

My geometrical schemas are not designed to build a structure of nucleons but are destined to be a visual support for my research, especially to see the kinship between the binding energy distribution within the various nuclei. For instance, in case of O^{16} the figure is based on four α particles bound by four equal bonds I call "A", actually a simplification for NN/2 + NP/2. If a neutron is added it becomes O^{17}. So, I look for a bond implying the new neutron and two nucleons located within two α particles. This is the state the closest to O^{16}. I have the choice between NNP and NPP. It is NPP which fits, so I take that one arbitrarily. I am aware of that "theoretical failure", my purpose being not to build a theory on strong nuclear force but rather to find simplicity in the "jungle" of hundreds of nuclear bonds in order to explain better the LENR process. Actually, I use three bonds which pre-exist to the α bond, i.e. NP, NNP, NPP, and a fourth one deducted from α bond, i.e. NN.

So, my method is not based on a theory. Instead, I make mind experiments. As said above I have the choice to use a few bonds each time a new neutron or proton is entering a nucleus. I choose that one which "fits". This unconventional way is comparable to the work of a chemist looking for several solutions in his experiments and validating that one which fits best. Moreover, I am looking at the compliance of the solution for one nucleus with the solution for another nucleus in order to avoid discrepancies, especially between isotopes. I am also taking care of symmetry within a given nucleus and between nuclei. Indeed, my work is not addressing the three-dimensional model of nuclei in the sense that I am not looking for a structure of these nuclei but rather for the distribution of binding energy within them. Nevertheless, my work could be complementary to those dealing with this topic. My work is trying to explain the LENR processes where energy release is a direct consequence of nuclear transmutations, i.e. modification of binding energy values between elements present at the beginning and at the end of the LENR reaction.

So, in my approach to the problem the 2D drawings just illustrate the bonds between α particles and nucleons or between nucleons, and not the 3D structure of the nuclei.

5.2. Calculation of binding energy

As seen, my system for determining the binding energy of the nuclei is based only on calculations.

I found that E_B α is equal to E_B of NP + NNP + NPP + 2 NN, where NP = E_B of Deuterium, NNP = E_B of Tritium, NPP = E_B of He^3 and 2NN being a dineutron of mass value = (mass of neutron − mass of 1800 electrons)/2. The whole is equal to 28.296 MeV.

This is for a free α particle. In a nucleus the NP, NNP, NPP bonds are replaced by a PP bond equal to the mass of proton − mass of 1800 electrons. The whole is equal to 28.325 MeV. So, I tried to determine the E_B of all the nuclei. I could find them for all the stable nuclei and have issued a book on that discovery (see www.philippehatt.com).

Example of calculation: E_B of Be^8 versus E_B of Be^9:

Be^8	$2 \times 28.325 = 56.6500$	$2 \times 28.325 = 56.6500$
	NN/2 = 2.4683	−NNP/2 = −3.8590
	NP/2= 1.1123	
	60.2306 MeV	52.7910 MeV

Average: 60.2306/2 + 52.7910/2 = 56.511 MeV (+0.011 MeV compared with AME 2012 value)

Explanation: the balance between (NN/2 + NP/2) and NNP/2 is negative ($2.4683 + 1.1123 - 3.8590 = -0.2784$ MeV). As a consequence, there is no bond between the two α particles and the nucleus is instable.

Be^9	$2 \times 28.325 = 56.6500$	$2 \times 28.325 = 56.6500$
	3 NN/2 = 7.4048	$-$NPP $= -7.7180$
	3 NP/2 $= 3.3369$	
	67.3917 MeV	48.9320 MeV

Average: 67.3917/2 + 48.9320/2 = 58.1640 (+0.002 MeV compared with AME 2012 value).

Explanation: the introduction of one neutron has occurred two more A bonds and also a negative NPP bond double as for Be^8. Nevertheless, the balance is positive ($7.4048 + 3.3369 - 7.7180 = 3.0237$ Mev). The nucleus is stable.

References

[1] H.A. Bethe and R.F. Bacher, *Rev. Mod. Phys*. **8** (1936) 82.
[2] L.R. Hafstad and E. Teller, *Phys. Rev*. **54** (1938) 681.
[3] L. Pauling, *Science* **150** (1965) d 297.

J. Condensed Matter Nucl. Sci. 26 (2017) 54–68

Research Article

Deepening Questions about Electron Deep Orbits of the Hydrogen Atom

Jean-Luc Paillet*
Aix-Marseille University, France

Andrew Meulenberg†
Science for Humanity Trust Inc., USA

Abstract

In previous works, we analyzed and countered arguments against the deep orbits, as discussed in published solutions. Moreover, we revealed the essential role of Special Relativity as source of electron deep orbits (EDOs). We also showed, from a well-known analytic method of solution of the Dirac equation, that the obtained EDOs have a positive energy. When including the magnetic interactions near the nucleus, we observed a breakthrough in how to satisfy the Heisenberg Uncertainty Relation (HUR) for electrons confined near the nucleus, in a radial zone of only a few fm. Here we chose a different method, by directly facing the HUR for such confined electrons, from which we deduce the coefficient γ of these highly relativistic electrons. Then we show the effective Coulomb potential due to a relativistic correction, can maintain the electrons in containment. Next we resume and deepen our study of the effects of EM interactions near the nucleus. We first obtain computation results: though approximate, we can effectively expect high-energy resonances near the nucleus. These results should be confirmed by using QFT-based methods.
 ISSN 2227-3123

Keywords: Confinement, Deep electron levels, Heisenberg uncertainty relation, Highly relativistic electrons, LENR, Magnetic interaction, Relativistic quantum physics

1. Introduction

The concept of nuclear, or near-nuclear, electrons goes back nearly 100 years (Appendix A). After being acceptable for a decade, it was rejected for several reasons and buried. The deep-orbit-electron aspect periodically resurfaced for various reasons, but was always rejected in subsequent publications. With the advent of cold fusion and the possibility of experimentally testing for these levels (Appendix B), the arguments against such orbits have been actively countered in this context (Appendix A). In earlier papers [1–4], we have analyzed works on electron deep orbits (EDOs) [5–7]

*E-mail: jean-luc.paillet@club-internet.fr.
†E-mail: mules333@gmail.com.

 ISSN 2227-3123

obtained by means of relativistic quantum equations (Dirac and Klein–Gordon) and answered the principal criticisms found in the literature and some indicated by colleagues. In particular, we have verified, extended, and improved the results of [7], obtained with a modified nuclear potential to take into account the finite dimension of the proton.

In our most recent paper [8], we answered a recent criticism by proving that the sign of the energy of EDO's solutions of the Dirac equation is positive. We also recalled the essential role of Special Relativity in the existence of the EDO's. This latter point was already indicated in [4] and particularly analyzed in [9]. Nevertheless, the studied methods used to find EDO's have imperfections that make them disputable on some important questions, e.g. the satisfaction of the Heisenberg uncertainly relation (HUR). Therefore, we began to address the EDO question from another angle, by starting a study on the role of magnetic interactions.

First, we analyzed several works on this subject from Barut [10–13] as well as the subsequent works on the so-called "Barut-Vigier model" [14–18] on the hydrogen atom. These latter papers were developed in a non-relativistic context, unlike those of Barut himself. Finally, while computing magnetic interactions near the nucleus, we obtained a first positive answer about the essential question of the HUR satisfaction. Then, we addressed another important question: the stability of an electron resonance near the nucleus. For doing this, we first used a well-known [19,20] classical approximation: to look for a local minimum of energy (LME) near the nucleus, while respecting the HUR. However, the results were not conclusive, insofar as the computed LME appeared deep inside the proton, i.e. where the relations used for computing it are no longer correct.

Here, we completely change strategy:

- We start from the HUR, to determine a size order of the momentum p for an electron confined in a region of mean radius $\langle r\rangle$ around the nucleus.
- From p we can directly deduce an approximate expression for the relativistic coefficient γ as a function of r.
- As γ is very high for the expected region of the EDO's, we take into account the relativistic corrections to the Coulomb potential, yielding an effective dynamical electric potential energy V_{eff} [1,21,22].This potential is strong enough to confine highly relativistic electrons to very deep orbits. Moreover, this new method allows progress into further questions, in particular for the computation of the LME. Now, we obtain interesting results: though these computations are approximate, they allow us to expect stable resonances for EDO's.

The HUR, which began as a big problem, leads us not only to find its proper solution but also to progress in the solution of the next questions. This study confirms the central role of the Relativity. Special Relativity is not only the source of EDO's, but as already felt previously, it also appears that relativistic methods may be necessary to prove the existence of EDO's.

2. Relativistic Confinement Energies and the Relativistic Coefficient γ

We take up and deepen elements discussed in Section 6 of [8], by starting from the Heisenberg Uncertainty Relation, (HUR) to be satisfied by an electron confined to a very small volume around the nucleus. In particular, we previously saw that electrons on deep orbits are *strongly* relativistic. Under these conditions, instead of computing the well-known relativistic coefficient γ for such electrons indirectly, as previously, we *directly deduce an approximate minimum value for* γ for an electron confined in a region corresponding to an average radius $\langle r\rangle$ around the proton.

To make such a computation using HUR, it is usual [19,23] to consider that the dispersion ("uncertainty") on the norm of the momentum |**p**| satisfies $\Delta|\mathbf{p}|\Delta r \geq \hbar/2$; to accept $\Delta|\mathbf{p}|$ as an average estimate of the momentum; and to attribute $\langle r\rangle$ to Δr. So, we write $p \geq \hbar/2r$, where p stands for |**p**| and r for $\langle r\rangle$, in order to simplify notation. Then, we consider the relativistic expression of momentum: $p = \gamma mv$, where m is the mass of the electron and v its velocity. Thus, we have to satisfy the relation $\gamma mv \geq \hbar/2r$, i.e. $\gamma v \geq \hbar/2mr$. We put $s = \hbar/mr$, a quantity of physical dimension "speed", which gives the inequality $\gamma v \geq s/2$, and thus $(\gamma v)^2 = (cv)^2/(c^2 - v^2) \geq s^2/4$.

After some simple algebraic transformations[a], we obtain $\gamma^2 \geq 1+\hbar^2/4(mcr)^2 = 1 + \lambda_c^2/4r^2$, where λ_c is the "reduced" Compton wavelength of the electron $\hbar/mc$. As $\lambda_c \sim$386 F and for the EDOs r is of order a few F, one has $\lambda_c^2/4r^2 \gg 1$, so one can write the following inequality deduced from the HUR:

$$\gamma \geq \lambda_c/2r. \tag{1a}$$

We note that the introduction of the Compton wavelength allows us to simplify the relation. Of course this expression (and the involved approximations) is valid only under the condition above on r, i.e. $r \ll \lambda_c/2$.

In the previous references [19,23] the coefficient "1/2" is removed to give an order of size for the momentum p : $p \sim \hbar/r$. Under this condition, one can show the following relation:

$$\gamma \sim \lambda_c/r. \tag{1b}$$

It is rather remarkable to obtain such a relation involving the Compton wavelength, even if the principle used for the computations is coarse.

To give a size order of γ for EDOs: if computing γ with (1b) and for $r = 2$ F, we can expect a relativistic coefficient of order $\sim$193, i.e. close to 200 (!), and if we consider the inequality relation $\gamma \geq \lambda_c/2r$, we have γ_{min} near 100.

3. Consequences on the Effective Coulomb Potential Energy V_{eff}

In [8], while seeking to resolve important physical questions for EDOs, such as the satisfaction of the HUR and the existence of a resonance near the nucleus thanks to a local minimum of the energy, we have principally considered magnetic interactions, because we expect them to yield high potential energy. But here, because of the high level of the relativistic coefficient γ, it is interesting to consider the effects of the relativistic correction of the static Coulomb potential, indicated in [21,22], under the resulting form of an effective dynamical potential noted V_{eff}, and already considered in [4]. In this latter reference, the coefficient γ was computed on a very different basis, and the energy shifts were not negligible but moderate.

We recall the general form of V_{eff}, (Eq. (2)), comes from the development of relativistic quantum equations (Dirac and Klein–Gordon) with the expression of the relativistic energy of a particle in a central field for a Coulomb potential energy V:

$$V_{eff} = V(E/mc^2) - V^2/2mc^2. \tag{2}$$

Nevertheless, in the case of the atomic electrons in light elements, one has $E \sim mc^2$ and $V \ll mc^2$, so the corrective term is always neglected and one has $V_{eff} = V$.

In the case of a relativistic electron, one can show V_{eff} takes the following form:

$$V_{eff} = \gamma V + V^2/2mc^2, \tag{3}$$

With the expected expression of γ as function of r indicated above, the expression of V_{eff} reads:

$$V_{eff} \sim -(\hbar/mcr)(\alpha c\hbar/r) + (\alpha c\hbar/cr)^2/2m = -(\alpha\hbar^2/mr^2)(1-\alpha/2) \sim -\alpha\hbar^2/mr^2. \tag{4a}$$

If we take the inequality $\gamma \geq \lambda_c/2r$ (as in Eq. (1a)), one obtains:

[a] From $(cv)^2/(c^2-v^2) \geq s^2/4$. We deduce $(cv)^2 \geq [(cs)^2-(vs)^2]/4$, $v^2(c^2 + s^2/4) \geq (cs)^2/4$, $(v/c)^2 \geq (s^2/4)/(c^2 + s^2/4)$. With $S = (s^2/4)/(c^2 + s^2/4)$, $\gamma^2 = 1/1-(v/c)^2 \geq 1/1-S = (c^2 + s^2/4)/c^2 = 1+s^2/4c^2$

$$|V_{\text{eff}}| \geq \alpha\hbar^2/2mr^2. \tag{4b}$$

With this last relation, and for any radius $r \leq \lambda_c/2 \sim 193$ F, we can show the three following results for the relativistic potential:

(1) V_{eff} is always attractive.
(2) $|V_{\text{eff}}| \geq |V|$. So one has a strengthening of the static Coulomb potential.
(3) V_{eff} has a behavior in K/r^2 when r decreases (and thus $|V|$ increases), with $K \sim 9 \times 10^{-41}$ in SI units. Previously [4], these results were obtained only for quasi-circular orbits, but with no condition on the radius.

To have an idea of the size order of V_{eff} near the nucleus, by computing it for $r = 2$ F, we obtain the following approximate values:

V_{eff} of order –140 MeV, whereas the kinetic energy KE $= (\gamma - 1)mc^2 \sim 98$ MeV.

With such a high value, V_{eff} can confine an electron in this region. We showed previously that Special Relativity is the source of the EDO's. Here we have shown that the HUR, which seemed an impediment for the EDO's, provides its proper resolution thanks to Relativity.

4. The Question of Stability of the EDOs. Seeking a Local Minimum of the Energy

4.1. Principles

We use a well-known approximation to estimate the possibility of a stable resonance near the nucleus before applying more complex and complete tools to solve the problem. We proceed so because the area near the nucleus is a region where several strong interactions must be considered under different conditions. Nevertheless, we expect to determine which interactions have greatest importance in the generation of resonance. For doing this, we consider the relativistic expression of energy, in which the norm of momentum $|\mathbf{p}|$ is replaced by $\hbar/r$, in order to respect the HUR and to obtain the following term noted E_{H} ("H" for Heisenberg):

$$E_{\text{H}} = \sqrt{\frac{\hbar^2 c^2}{r^2} + m^2c^4}. \tag{5}$$

At E_{H}, we add a term V representing a potential energy, where V is a function of the radius. Thus we obtain the total energy E, represented by the following relation:

$$E = E_{\text{H}} + V. \tag{6}$$

Then, we look for a local minimum of energy E for various combinations of potentials included in the term V and we determine the radius of this local minimum. In fact, a potential is "interesting" for the resonance, i.e. to be kept for the rest of the study, not only by considering the energy levels, but also if the (average) radius in the approximation for the local minimum is acceptable, i.e. near and maybe outside the nucleus (here it is a proton).

Of course, V includes the electric Coulomb potential, but we recall that, earlier in this study [8], we considered potential energies of magnetic interactions, after analyzing the works referring to the "Vigier-Barut Model" [14–18]. These interactions include Spin–Orbit (SO) and Spin–Spin (SS), taken in their attractive form, as well as a repulsive term in $1/r^4$ coming from the square of the nuclear vector potential $\mathbf{A}$. More precisely, this term comes from an expression $(\mathbf{P} \pm e\mathbf{A})^2$, associated with the minimal coupling between one charged particle and an "exterior" EM field, as e.g. in a Pauli equation. $\mathbf{P}$ is the kinetic momentum of the particle, e its electric charge, m its mass, and $\mathbf{A}$ the vector

potential of the EM field. $\mathbf{P} \pm e\mathbf{A}$ is sometimes called the "canonical" or the "dynamical" momentum. The vector potential produced by a magnetic moment **m** can be expressed by using:

$$\mathbf{A}(r) = \frac{\mu_0}{4\pi}\frac{\mathbf{m}\times\hat{r}}{|\mathbf{r}|^2}.$$

The complete energy term associated with $\mathbf{A}^2$ has the form $e^2\mathbf{A}^2/2m$ and is considered [24,25] to be expressing a "diamagnetic" energy with a behavior in $1/r^4$. Although it is usually negligible at atomic levels, it has a considerable importance here, not only because it is strongly increasing near the nucleus but also, as it is repulsive, it avoids a "fall at the center." This fall is almost inevitable in "macrocospic" (non-quantum) computation, if keeping only attractive interactions, and would give a result with questionable physical meaning.

There are actually two similar diamagnetic terms to consider, as we can see when considering the Hamiltonian of a two-body system electron + proton, as in [16,18]:

(1) One is caused by the interaction of the electric charge of the electron with the intrinsic magnetic moment of the proton spin.
(2) The other is caused by the symmetric interaction: between the electric charge of the proton and the intrinsic magnetic moment of the electron spin.

In spite of this apparent symmetry, the strength of both terms is very different because of the great difference between the values squared of the electron and proton magnetic moments. In fact, the term #2 is equal to ∼240 times the #1 and "absorbs" completely this term. Finally, its coefficient C is computed by the following expression:

$$C \sim (\mu_0/4\pi)[e^4\hbar^2/(4m_e^2 m_p)] \sim 1.3\times10^{-71} \quad \text{in SI units.} \tag{7}$$

Further repulsive potentials include the well-known "centrifugal term" in $1/r^2$, which is available only if the angular momentum L, as determined by its quantum number l, is not null. On another hand, the *SO* interaction is also available only if $l \neq 0$. The lesser known Spin–Orbit interaction, S_pO, involving again the orbital momentum of the electron, but with the nuclear spin instead of the electron spin, also needs $l \neq 0$. Nevertheless, the magnetic moment of the proton μ_p is of order 10^3 (in fact ~660) smaller in absolute value than that of the electron, μ_e. So, the S_pO interaction, in either its attractive or repulsive version, is completely "absorbed" by the *SO* interaction and can be neglected. Note finally that the "Heisenberg" term E_H (5), having a positive sign, is also repulsive, but with a $1/r$ behavior for r very small and tending towards 0. Under these conditions, it can be surpassed by attractive terms in $1/r^3$, such as the magnetic potentials *SO* and *SS*, when $r \to 0$.

To put some order in all these terms possibly involved in the computations, we list them below while specifying some associated conditions, possible eliminations by "absorption", and their computation expressions. (Further refinements are mentioned in Section 4.2.2.ii.)

(1) E_H: relativistic energy taking into account the HUR for an electron confined at a radius r.

Nature: repulsive. Expression defined in (5). Always Taken into Account (ATIA)

(2) The Coulomb potential. Nature: attractive.

In the previous study, we considered only the static potential energy $V_{Cb} = \alpha c\hbar/r$, as the relativistic coefficient γ was computed afterwards, after inserting further attractive potential energies coming from magnetic interactions. But now, as we have a high value of γ, derived beforehand from the HUR, we can directly take the effective potential V_{eff} (3), (4b) ATIA.

(3) SO interaction: available only if $l \neq 0$. Nature: we choose the *attractive* version, derived from rules on composition of angular momenta: here, $j = l - 1/2$. We use the expression of energy given in [8], by taking $l = 1$ and thus $j = 1/2$. In order to establish this calculation expression, we suppose that one can use the same quantum rules for deep orbits as for atomic orbitals, based on the quantum $\hbar$, to evaluate $L \cdot S$. Initially, in not considering a possible relativistic correction for E_{SO} (see Section 4.2), we had $\langle E_{\text{SO}} \rangle \sim (-1.7 \times 10^{-53}/\langle r^3 \rangle)$ J $\sim (-1.1 \times 10^{-34}/\langle r^3 \rangle)$ eV.

(4) SS interaction: always "available." Nature: first, we choose the *attractive* version, corresponding to a singlet state. The approximate expression [8] is derived by extrapolation from the atomic case: the total energy shift between the singlet state (attractive, $s = 0$) and the triplet state (repulsive) is $A \sim 5.87 \times 10^{-6}$ eV [26] for the fundamental state, i.e. for $r \sim 53 \times 10^{-12}$ (Bohr radius), and the energy shift is equal to (–3/4) A. We deduced $\langle E_{\text{SS}} \rangle \sim (-10^{-55}/\langle r^3 \rangle)$ J $\sim (-0.64 \times 10^{-36}/\langle r^3 \rangle)$ eV. With a $1/r^3$ dependence, as for the SO interaction, SS is *taken into account only if the former is not*, since $|E_{\text{SS}}| \ll |E_{\text{SO}}|$ unless $l = 0$.

(5) V_{centr}: "Centrifugal term." Nature: repulsive. Expression: $V_{\text{centr}} = l(l+1)\hbar^2/2mr^2$. One supposes simply $l = 1$, which gives $V_{\text{centr}} = \hbar^2/mr^2$. As for $E_{\text{SO}}, V_{\text{centr}}$ has value $\neq 0$ only for $l > 0$. V_{centr} even dominates V_{eff}, which is also in $1/r^2$ when r becomes very small: V_{eff} has order $10^{-40}/r^2$, whereas V_{centr} has order $\sim 10^{-38}/r^2$. Despite its very weak coefficient (of order 10^{-52}) only E_{SO} (for point particles), as it is in $1/r^3$, can surpass V_{centr}.

(6) V_4: "Diamagnetic" term coming from the square of the vector potentials $\mathbf{A}^2$. Nature: repulsive. Approximate expression in SI units: $V_4 = 1.3 \times 10^{-71}/r^4$, as indicated above in Section 4.1 ATIA.

To summarize, we look for a local minimum of energy $E = E_{\text{H}} + V$, with $V = \text{CbPot} + V_4 + \text{OptPot}$, where

- CbPot was the static potential V_{Cb} in previous computations, and is now V_{eff} in the new ones.
- OptPot is a combination (possibly empty) of "optional" potential energy terms #3, #4 and #5.

4.2. Analysis of the computation results for a local minimum of energy near the nucleus

4.2.1. *Quick recall of the previous computations*

- Trial with OptPot $= E_{\text{SO}}$, and thus $E = E_{\text{H}} + V_{\text{Cb}} + E_{\text{SO}} + V_4 \sim E_{\text{H}} - \alpha c\hbar/r - 1.7 \times 10^{-53}/r^3 + 1.3 \times 10^{-71}/r^4$.

The LME is at ~ 0.001 F. Of course this result has no physical meaning for electron orbitals. Moreover, if we compute E at $r = 2$ F, we find $E \sim E_{\text{SO}} \sim -13$ GeV. Such a "hadronic" value seems unreasonable unless we are considering very high-energy particle resonances. We had also noted that even with adding the (repulsive) centrifugal term V_{centr} to OptPot, one obtains almost the same excessive energy result.

Moreover, as $\gamma \gg 1$, one has to take into account a *relativistic expression* of the SO interaction including γ. The SO interaction energy is proportional to the "difference" between the Larmor and the Thomas precessions. The Larmor precession ω_{L} depends on the effective magnetic field seen by the electron as it orbits the charged nucleus. The Thomas precession ω_{T} is a relativistic geometric effect on the electron spin axis, in the opposite direction of the Larmor precession. The relativistic Larmor precession is $\omega_{\text{L}}' = \gamma\omega_{\text{L}}$, where ω_{L} is the usual precession at low speed, i.e. when $\gamma \sim 1$. The full relativistic expression of the Thomas precession corresponds to $\omega_{\text{T}} = -[\gamma^2/(\gamma+1)]\omega_{\text{L}}$ (see, e.g. [27]) $= -[\gamma/(\gamma+1)]\omega_{\text{L}}'$. The total precession rate is thus equal to the following expression:

$$\omega_{\text{tot}} = \omega_{\text{L}}' + \omega_{\text{T}} = [\gamma - \gamma^2/(\gamma+1)]\omega_{\text{L}} = [\gamma/(\gamma+1)]\omega_{\text{L}}. \tag{8}$$

Because of the high value of γ for EDO electrons (estimated to be $\gamma > 100$ near the nucleus), we have $\omega_{\text{tot}} \sim \omega_{\text{L}}$. Thus, the total SO interaction energy for the highly relativistic EDO electron is functionally twice that for the well-known

usual precession $\omega_L/2$ at atomic levels, which increases with electron proximity to the nucleus. Surprisingly, other than within this factor of 2, relativity has no effect on the net precession rates.

This change would increase, in the same ratio, the value of SO computed in the trial above, which was already unrealistically high. Then we decide, for the time and as working hypothesis for the sequel, not to take into account a SO interaction. Of course, this amounts to putting $l = 0$.

- Trial with OptPot $= E_{SS}$, i.e. $E = E_H + V_{Cb} + E_{SS} + V_4 \sim E_H - \alpha c\hbar/r - 10^{-55}/r^3 + 1.3 \times 10^{-71}/r^4$. Of course, we must suppose $l = 0$, which implies $E_{SO} = 0$ and $V_{centr} = 0$. The LME is reached at $r \sim 0.17$ F, i.e. again inside the proton, albeit less deeply than with E_{S0}. Moreover, at $r = 2$ F, we had $E_{SS} \sim -81$ MeV, to compare (while assuming a quasi-circular orbit) with a kinetic energy order ∼76 MeV, and γ ∼150.

To summarize, we conclude that, without major adjustments, neither above trial can determine a realistic LME.

4.2.2. *Present results of computations*

Now, the static potential is replaced by the effective V_{eff} due to relativistic dynamical corrections, the sum with any "optional" attractive potential energy gives an even greater attractive strength than determined previously. It is thus useless to try a combination with OptPot including E_{SO} or even $E_{SO} + V_{centr}$. For the same reason, with OptPot including the attractive E_{SS}, we obtain again an LME inside the nucleus, at $r \sim 0.16$ F, very near the previous result with E_{SS}.

(i) Results of a potential including a repulsive *SS* interaction.

We can test a simulation with the *repulsive* version of the SS interaction, corresponding to a triplet state ($s = 1$). At $r =$ Bohr radius, the energy shift is positive and equal to (1/4) A. One deduces the repulsive version of the interaction, noted E_{SSR} : $E_{SSR} = |E_{SS}|/3 \sim 3.4 \times 10^{-56}/r^3$ J $\sim 2.2 \times 10^{-37}/r^3$ eV.

- Trial with $E = E_H + V_{eff} + E_{SSR} + V_4 \sim E_H + V_{eff} + 3.4 \times 10^{-56}/r^3 + 1.3 \times 10^{-71}/r^4$, and $l = 0$.

This time, Fig. 1, the LME is reached at $r \sim 1.07$ F, with $E \sim -61$ MeV. So the LME is outside the proton. We have also the following results: $\gamma \sim 365$, kinetic energy KE ~ 185 MeV, total potential energy PE ~ -250 MeV. Moreover, the potential wall due to the HUR is of order ~ 20 MeV, at $r \sim 5$ F. The curve of E is plotted on the Fig.1, with the radius in the interval [0.9 F, 4 F].

One finds also a LME (not included in Fig. 1) corresponding to the Bohr radius, but the energy E does not agree with the classical value. To simplify the reason, V_{eff} is computed here with an expression of γ as a function of r, which is relevant only for very small value of r, i.e. $r \leq \lambda_c/2 \sim 193$ F, whereas V_{eff} for a non-relativistic electron is practically equal to the static Cb potential. Of course, this result about a local minimum of energy, with a potential well outside the nucleus, is just a coarse approximation; but it gives size orders and an "interesting" combination of potentials capable of obtaining a realistic resonance for EDO, without yet using quantum equations.

Note that for an electron to be inside the nucleus would not be scandalous per se, since one knows the electron of an orbital s has a finite probability to be inside the nucleus. In a more-extreme case, if considering a muonic atom of lead, where the muon plays the role of an electron, one knows [28] the muon is more inside the nucleus than outside, in a region where the potential, according to a classical approximation, is parabolic. But, similar to this last example, the expressions of the potential energies are completely different inside the nucleus from the ones outside. Thus the computations of local minima such as those indicated in Section 1, with LME inside, are simply erroneous, since they are computed with incorrect expressions and thus must be modified in a yet-to-be-determined manner.

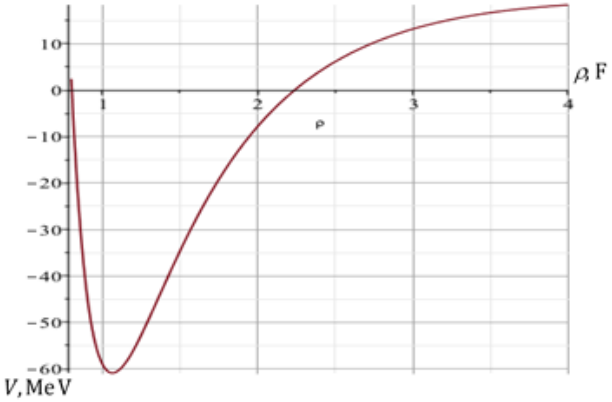

Figure 1. Plot of E in MeV as a function of ρ in F, for $E_{\mathrm{SO}} = 0$ and a repulsive E_{SSR}

- Now, we can try computations with a modified electro-static potential inside the nucleus, by using the expression

$$V_i(r) = -\left[\frac{3}{2} - \frac{1}{2}\left(\frac{r^2}{R_0^2}\right)\right]\frac{e^2}{R_0}[7],$$

for $r < R_0$, the charge radius of the proton taken equal to ~ 0.84 F. By using the usual expression for $r \geq R_0$, we determine a Cb potential, V_{mod}, modified for any radius r. Next, by replacing V by V_{mod} in the expression (3) of V_{eff}, we define an "effective Cb potential" with relativistic correction, V_{effmod}. While taking account of the repulsive SS interaction, i.e. with $E = E_{\mathrm{H}} + V_{\mathrm{effmod}} + E_{\mathrm{SSR}} + V_4$, it is interesting to note a slight shift of the LME, which passes from ~ 1 to 1.1 F.

(ii). Taking into account a relative weakening of strong EM interactions near the nucleus.

On one hand, some EM interactions become very strong when the radius decreases, because of behavior in inverse powers of r, mostly in powers –2,–3 and –4. Nevertheless, one also has to take into account effects that can weaken the Coulomb potential before even arriving at the proton. In particular, we consider some radiative corrections derived from QED, such as the electron self-energy and the vacuum polarization, which generates a cloud of virtual pairs of electrons and positrons confined in a localized region around the electron, smearing its charge. In fact, self-energy decreases the binding energy, while vacuum polarization tends to increase it, but the sum of both effects gives a repulsive action. At atomic levels, this causes the well-known "Lamb shift" on the order of a few 10^{-5} eV. This is of intermediate importance between the fine and the hyperfine structure shifts. Moreover, it acts on the spin g-factor of the electron, leading to the so-called "anomalous magnetic moment".

As the effects of QED increase with the intensity of the electric field that the electrons are exposed to, one can expect these corrections to become much stronger for an electron localized near the nucleus. Observations on heavy atoms can already give an idea of the size of these corrections. For example, for the ground state of a H-like uranium ion (U^{91+}), one observes a Lamb shift of almost 1/2 keV [29]. Effective calculations using QED and other considerations for near-nuclear effects are beyond the scope of this paper, but will certainly be involved in future work.

There is another possibility of weakening, that for interactions involving the spin. Indeed, about the solutions of Dirac equation for a free electron, one can note [30] that a velocity transverse to the spin affects the direction of the spin. To summarize: as the general expressions of the Dirac spinors involve the momentum **p** of the particle, if its spin

at rest was in an eigenstate, it will become a linear combination of eigenstates when $\mathbf{p} \neq 0$; in fact, when $|\mathbf{p}|$ increases, the direction of the spin "bends" in the direction of $\mathbf{p}$, and as the velocity approaches c, the spin tends to be aligned with the helicity. Except for the cited reference, the phenomenon seems practically passed over in the literature. In the case of a relativistic bound electron, one would therefore expect a weakening of the interactions and a source of new resonances involving the electron spin ($\mathbf{s}_1 \cdot \mathbf{s}_2$ and $\mathbf{l} \cdot \mathbf{s}$). But, because of the orbital acceleration experienced, it is much more difficult to evaluate possible "bending" effects in the case of a bound electron than a free one. Both effects have consequences for spin interactions, and mostly without a signature in the expression of the wavefunction. In the literature, it seems that authors [24] note rather a strengthening of the SO interaction for relativistic s electrons of heavy atoms at the same time as a shrinkage of the considered orbital, thus expressing a strengthening of the binding energy. Concerning the spin–spin interaction, there are works about relativistic calculations of spin–spin constants (principally in nuclear resonance spectra). For example, in a very complete and complex study [31] involving possible interactions between electrons, the authors consider multi-electron atoms. Nevertheless, it is difficult to deduce a numerical weakening of the SS interactions near the nucleus from it. In future work, we will reexamine assumptions and more strictly apply relativity in the nuclear region.

Under these conditions, and for the present, we make simple simulations of weakening for V_{eff}, E_{SSR} and V_4, while computing localization of an LME near the nucleus. For V_{eff}, we first consider a weakened version (due to QED effects) of the static Cb potential, noted V_{Cbw} and defined in the following way:

we choose a radius $r_1 > r_0$, where r_0 is the charge radius ~ 0.84 F, and we suppose

- at $r = r_1$, $V_{\text{Cbw}}(r) \sim -\alpha c\hbar/r$, the usual Cb potential V_{Cb},
- at $r = r_0$, $V_{\text{Cbw}}(r) = KV_{\text{Cb}}$, where K is a coefficient < 1.

To simplify, we suppose a linear weakening of V_{Cb} when going from r_1 to r_0, and we do not specify what happens for $r < r_0$, since we are only interested in values of LME outside the nucleus.

So, $V_{\text{Cbw}}\,(r)$ can be defined by:

- $V_{\text{Cbw}}(r) = V_{\text{Cb}}(ar + b)$, when $r_0 < r < r_1$, where $a = (1 - K)/(r_1 - r_0)$ and $b = 1 - ar_1$,
- $V_{\text{Cbw}}(r) = V_{\text{Cb}}(r)$ for $r \geq r_1$. In fact, it is unnecessary to consider this case.

Next we deduce the expression of a lessened version of V_{eff} (i.e., V_{effw}) by using V_{Cbw} for V in the expression (3), i.e. $V_{\text{effw}} = \gamma V_{\text{Cbw}} + (V_{\text{Cbw}})^2/2mc^2$. For the expression of energy E, we take $E = E_{\text{H}} + V_{\text{effw}} + E_{\text{SSR}}/C + V_4/D$, where C and D are constants > 1. We made several computations with various values of r_1, K, C, and D, resulting in LME outside the nucleus. Here we report only the following example.

For $r_1 = 2.5$ F, $K = 0.55, C = 1.8$ and $D = 2$, we have an LME at $r \sim 1.6$ F, where $E \sim -5$ MeV. Moreover, $\gamma \sim 235$, and the potential energy is ~ -125 MeV, corresponding to the potential well at the LME. The "dynamic" potential wall due to the HUR is order ~ 18 MeV at ~ 8 F. In Fig. 2, we plot the curve of E as a function of the radius taken in the interval [1.3 F, 2.5 F].

While looking at the indicated parameters (K, C, D), the weakening of the energies can seem small; nevertheless for $r = 1.6$ F, i.e. at the LME, the weakening $V_{\text{eff}} - V_{\text{effw}}$ is equal to ~ -49 MeV; the weakening of E_{SSR} is ~ 22 MeV, and for V_4, it is ~ 6 MeV. In fact, these weakenings are considerable in absolute values.

5. Analysis of the Results and Conclusions

(1) We can make a first important remark: contrary to what was observed in the Barut–Vigier works, where the region near the nucleus was characterized by a pre-eminence of the magnetic interactions, whereas the "atomic region" was characterized by the electric interactions, now *both types of interactions are entangled in the nuclear region* and they have similar importance.

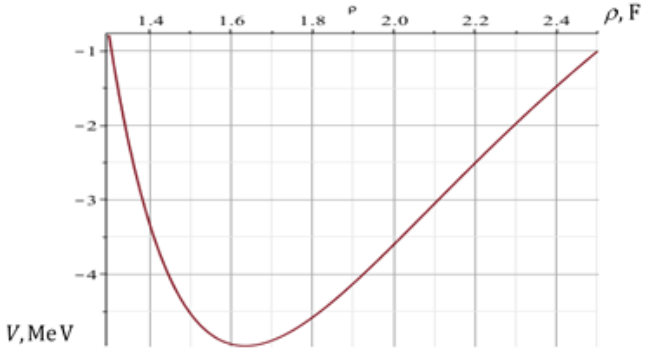

Figure 2. Plot of E (in MeV as function of ρ in F) based on weakenings of the potentials inside the nuclear region (see text).

A pure mathematical exercise (where values are non-significant) is shown in Fig. 3.

(2) The computations have been carried out with coarse approximations: we used $\gamma \sim \lambda_c/r$, but one could as well multiply/divide this expression by 2 or by π. This is only a size order, which must be taken into account. Nevertheless,

(i) By combining in some ways the different potentials, we easily find a local minimum of energy outside the nucleus, for very deep electron orbits.
(ii) This LME is associated with a potential well, which is strong enough to respect the HUR.

(3) The combinations of potentials, which yield a positive result, lead to the following choices and requirements for future studies:

(i) As the confined electrons are highly relativistic, we have to take into account the effective Coulomb potential V_{eff}.
(ii) We discard the spin–orbit interaction and this amounts to confine the angular momentum to $l = 0$. As a consequence, the term expressing the centrifugal barrier also vanishes.

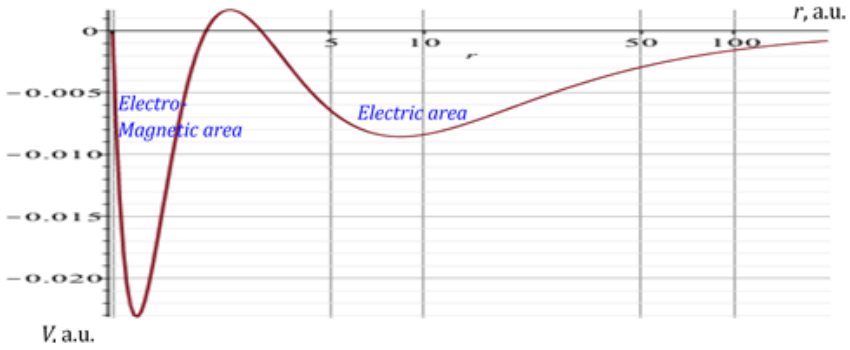

Figure 3. Simulation of two potential wells.

(iii) Concerning the spin–spin interaction, the repulsive version seems more propitious to the existence of EDO's. (The attractive version hints at quarks and higher-energy nuclear resonances.) Either way, this interaction makes it necessary to take into account the magnetic moment and spin of the proton and not just assume a point charge. Under these conditions, the Dirac equation for one particle in an "external" electric field is not adequate to the task.

(iv) We take into account the repulsive "diamagnetic" potential energy, V_4, which is caused by an interaction between the magnetic moment of the electron with the charge of the proton (and not the symmetric interaction) and involves the squared norm of the magnetic vector potential of the electron. The only constraints are to take into account the electron spin and its magnetic moment in the near presence of the nuclear electric-charge field.

For future continuation of the study on EDO's, the points cited above could lead us to use at least relativistic 2-body quantum equations involving spins. Moreover, works on QED are necessary to evaluate the radiative corrections evoked above in Section 4.2.2 (ii), which have certainly a significant action on the strength of the different interactions near the nucleus. In a QED context, it seems that the Two Body Dirac Equation of (Dirac) Constraint Dynamic [32] [33] could usefully be tested, for the following reasons:

- The initial two-body Dirac equation involves 16-component spinors, since they have the dimension of tensor products of 4-D spinors. Nevertheless, the Constraint Dynamic allows one to reduce it to a 4-component equation, if one mass is (relatively) very large as is the case for the proton mass relative to the mass of the electron.
- This method is fully relativistically covariant and it eliminates some problems of non-interaction for highly relativistic particles [34].
- The equations lead to the expression, in a consistent relativistic way, of numerous magnetic interactions at short distance as "quasi-potentials," including all the possible interactions.

Acknowledgement

This work is supported in part by HiPi Consulting, Ashland, VA, USA; by the Science for Humanity Trust, Bangalore, India; and by the Science for Humanity Trust Inc., Tucker, GA, USA.

Appendix A. Electron Deep Orbits (EDOs)

Beginning in 1920, with Rutherford's suggestion of electrons combining with protons to form neutral particles within the nucleus, a decade followed where the concept of a "nuclear electron" was acceptable [35]. The concept fell out of favor toward the end of the decade with the Heisenberg Uncertainty Relation (HUR), the Klein Paradox, and the fact that the intrinsic spin of the proton, electron and neutron do not add up. This was despite developments of the relativistic Klein–Gordon and Dirac equations. The next few years saw the discovery of the neutron and the development of proton-neutron models of the nucleus. Thus, the concept of a nuclear electron became unnecessary and was largely forgotten.

Periodically, in later decades, the concept of the deep-electron orbits was revisited for various reasons, but outside of the neutron. In this case, the objection of the intrinsic-spin disparity no longer was of concern. However, other (mathematical) problems, along with the HUR, became the dominant mode of rejection. Early (1994 and 1995) in the development of cold fusion, after electron screening was identified as a major requirement, EDOs were analyzed in the Klein–Gordon and Dirac equations to a much greater extent than previously. Unfortunately, this work was all but ignored for over a decade.

In 2005, the EDO of the Klein–Gordon equation was again explored. However, this time it was in the context of Randall Mills' fractional orbits rather than in that of cold fusion. Nevertheless, it opened the eyes of one of the present authors (AM) when he viewed the paper in 2009. This revelation of relativistic quantum mechanics predicting deep-electron orbits began the series of papers on the topic in Items (b) and (c) from Meulenberg, Sinha, and Paillet. Item (a) below contains the EDO papers from other authors that have contributed to this concept in cold fusion.

(a) EDO Works within the Context of Cold Fusion

J.A. Maly, J. Vavra, Electron transitions on deep dirac levels I, *Fusion Technol.* **24** (1993) 307.

J. Maly and J. Va'vra, Electron transitions on deep dirac levels II, *Fusion Technol.* **27** (1995) 59–70.

J. Va'vra, On a possibility of existence of new atomic levels, which were neglected theoretically and not measured experimentally, presented at Siegen University, Germany, November 25, 1998.

J. Naudts, On the hydrino state of the relativistic hydrogen atom, http://arxiv.org/abs/physics/0507193.

J. Va'vra, A new way to explain the 511 keV signal from the center of the Galaxy and some dark matter experiments, *Astronomy & Astrophys*. (2013) http://arxiv.org/abs/1304.0833.

V.K. Ignatovich, A missed solution for an atom: a gate toward cold nuclear fusion, *Infinite Energy Magazine* issue 117 (2014) 33–36.

V.K. Ignatovich, A Singular solution for a hydrogen atom as a way toward cold nuclear fusion, *Open Sci. J. Modern Phys.* 2015 – academia.edu

(b) EDO works by A. Meulenberg and K.P. Sinha

Tunneling beneath the ^{4}He$*$ fragmentation energy, AM-KPS, 239th ACS Nat. Meeting *JCMNS* 4.

From the naught orbit to ^{4}He ground state, AM, *ICCF-16*, *JCMNS* 10.

Deep-electron orbits in cold fusion, AM-KPS, *ICCF-16*, *JCMNS* 13.

Deep-orbit-electron radiation emission in decay from ^{4}He* to ^{4}He, AM-KPS, *ICCF-16*, *JCMNS* 13.

Femto-atoms and transmutation, AM, *ICCF-16*, *JCMNS* 13.

Lochon and extended-lochon models for LENR in a Lattice, AM-KPS, *Infinite Energy Magazine,* Issue 112, November/December 2013, pp. 29–32.

Femto-atom and femto-molecule models of cold fusion, *AM, Infinite Energy Magazine,* Issue 112, November/December 2013, pp. 41–45.

Femto-helium and PdD transmutation, AM, *ICCF-18*, *JCMNS* 15.

Deep-orbit-electron radiation absorption and emission, AM, *ICCF-18*, *JCMNS* 15.

Pictorial description for LENR in linear defects of a lattice, AM, *ICCF-18*, *JCMNS* 15

(c) EDO works by J.-L. Paillet and A. Meulenberg

Arguments for the anomalous solutions of the Dirac equations, JLP-AM, *JCMNS 18*.

Basis for electron deep orbits of the hydrogen atom, JLP-AM, *ICCF19, JCMNS 19*.

Nature of the deep dirac levels, AM-JLP, *ICCF1, JCMNS 19*.

Basis for femto-molecules and -ions created from femto-atoms, AM-JLP, *ICCF19. JCMNS 19*.

Electron deep orbits of the hydrogen atom, JLP-AM, *11^{th} Int. WorkShop, Airbus, Toulous*e. *JCMNS 23* .

Special relativity, the source of the electron deep orbits, JLP-AM, *Found. Phys.* ***47****(2*).

Relativity and electron deep orbits of the hydrogen atom, JLP-AM *RNBE I, Avignon, JCMNS 21*.

Advance on electron deep orbits of the hydrogen atom, JLP-AM, ICCF20, Sendai.

Implications of the electron deep orbits for cold fusion and physics, AM-JLP, *ICCF20.*

Physical reasons for accepting the Deep-Dirac Levels, AM-JLP, *ICCF20*.

Appendix B. Application of Electron Deep Orbit (EDO) Models to Cold Fusion Predictions and Experimental Results

Why an EDO model – It was created to explain the D + D $\Rightarrow{}^4$He results of CF.

(1) It does so by transferring energy (mass) from a nucleus to a bound relativistic electron orbiting within femtometers of the nucleus. *This transfer occurs (for different reasons) prior to, during, and after fusion*.
(2) The DO electron, in forming a femto-H atom, eliminates the Coulomb barrier of a hydrogen nucleus.
(3) The extra kinetic energy of the DO electrons lowers the mass defect Q of the fusing deuteron pair to below the ^{4}He* fragmentation or other excited-nucleon levels.
(4) If fragmentation or gamma decay is not possible, other decay modes must lower ^{4}He* to ^{4}He.
(5) Application of this model and its consequences readily explain most, or all, CF experimental results.

What is the EDO model – Electrons are Coulomb-bound in deep orbits about a nucleus

(1) The existence of deep orbits is predicted by the *relativistic* Klein–Gordon and Dirac equations.
(2) For H, the predicted orbits are in the femto-meter range with a binding energy $|\mathrm{BE}| \geq 507$ keV.
(3) Kinetic energy of DO electrons are predicted to be in the KE $= 1$ MeV range (e.g., [36] and references therein) and the 100 MeV range (above).
(4) H or ^{4}He with DO electrons are *femto-atoms*, which are near-nuclear-size neutral objects with properties to explain most of CF experimental results.
(5) KE $= 1$ MeV DO electrons violate Heisenberg Uncertainty Relation (a problem not yet resolved). The $\sim 100\,\mathrm{MeV}$ electrons do not.
(6) Nuclear mass reduction is key to D–D $\Rightarrow{}^4$He CF results:
    - A change of 1 MeV may not be noticeable. ^{4}He with a DO electron would appear to be H with strangely shifted spectral lines; so, EDOs would be confirmed, but cause(s) of the exact shift might not be obvious.
    - A change of 100 MeV would be clearly identifiable in spectroscopic data as a nuclear mass shift.
(7) Known example of such energy/mass transfer – energy conservation in the atomic hydrogen system. Emitted photons from decaying electrons carry away excess Coulomb energy from the nuclear-mass.

EDO model predictions – How does the model fit with Cold Fusion models and experiment?

(1) It is a natural extension of Sinha's Lochon model that has published calculations of interaction probabilities for the D^+ - D^- fusion reaction in a solid-state lattice.
(2) It is a natural consequence of both the linear-H molecule model and Takahashi's Tetrahedral Symmetric Condensate.
(3) It works for both D–D and H–H cold fusion results and explains the observed differences.
(4) It predicts transmutation results consistent with those observed in CF results.

(5) It predicts the CF results of nuclear energy transfer to the lattice without the energetic particles or gamma radiation of hot-fusion and neutron-activation experiments.
(6) It predicts selective attraction of femto-atoms to radioactive isotopes for nuclear waste remediation.

References

[1] J.L. Paillet and A. Meulenberg, Arguments for the anomalous solutions of the Dirac equations, *J. Condensed Matter Nucl. Sci.* **18** (2016) 50–75.
[2] J.L. Paillet and A. Meulenberg, Basis for electron deep orbits of the hydrogen atom, *Proc. of ICCF19, 19th Int. Conf. on Cond. Matter Nuclear Science*, Padua, Italy, 13–17 April 2015, *J. Condensed Matter Nucl. Sci.* **19** (2016) 230–243.
[3] J.L. Paillet and A. Meulenberg, Electron deep orbits of the hydrogen atom, *Proc. 11th Int. Workshop on Hydrogen Loaded Metals,* Airbus Toulouse, 15–16 Oct. 2015, *J. Condensed Matter Nucl. Sci.* **23** (2017) 62–84.
[4] J.L. Paillet and A. Meulenberg, Relativity and electron deep orbits of the hydrogen atom, *Proc. of the 1st French Symp*., RNBE-2016 on Cond. Matter Nucl. Sc., Avignon, 18–20 March 16, *J. Condensed Matter Nucl. Sci.* **21** (2016) 40–58.
[5] J. Naudts, On the hydrino state of the relativistic hydrogen atom, arXiv:physics/0507193v2.5, 2005.
[6] J.A. Maly and J. Va'vra, Electron transitions on deep Dirac levels I, *Fusion Sci. Technol.* **24**(3) (1993) 307–318, http://www.ans.org/pubs/journals/fst/a_30206.
[7] J.A. Maly and J. Va'vra, Electron transitions on deep Dirac levels II, *Fusion Sci. Technol.* **27**(1) (1995) 59–70, http://www.ans.org/pubs/journals/fst/a_30350.
[8] J.L. Paillet and A. Meulenberg, Advance on electron deep orbits of the hydrogen atom, *Proc. of ICCF20*, *20th Conf. on Cond. Matter Nuclear Science*, Sendai, Japan, 2–7 October 2016.
[9] J.L. Paillet and A. Meulenberg, Special relativity, the source of the electron deep orbits, *Found. Phys.* **47**(2) (2017) 256–264.
[10] A.O. Barut and J. Kraus, Resonances in e+ – e$^-$ System due to Anomalous Magnetic Moment Interactions , *Phys. Lett.* **59B**(2) (1975) 175–178.
[11] A.O. Barut and J. Kraus, Solutions of the Dirac equation with Coulomb and magnetic moment interactions, *J. Math. Phys.* **17**(4) (1976) 506–508.
[12] A.O. Barut, Prediction of new tightly-bound states of H_2^+ (D_2^+) and cold fusion experiments, *Int. J. Hydrogen Energy* **15**(12) (1990) 907–909.
[13] A.O. Barut, Stable particles ad building block of matter, Int. Centre for Theoretical Physics Lib., Miramare-Trieste, IAEA, 1979.
[14] J.P. Vigier, New hydrogen(deuterium) Bohr orbits in quantum chemistry and cold fusion processes, *Proc. of ICCF4*, 3–6 Dec. 1993, Lahaina, Maui, Hawaii, TR-104188-V4 Section 7 (1994) 1–25.
[15] A. Dragic, Z. Maric and J.P. Vigier, *Phys. Lett*. A **237** (1998) 349–353.
[16] N.V. Samsonenko, D.V. Tahti and F. Ndahayo, On the Barut–Vigier model of the hydrogen atom physics, *Phys. Lett.* A **220** (1996) 297–301.
[17] S. Ozcelik and M. Simsek, *Phys. Lett.* A **152** (1991) 145–149.
[18] R.L. Amoroso and J.P. Vigier(Posth), Evidency 'Tight Bound States' in the hydrogen atom, Unified Field Mechanics, *9th Int. Symp. Honoring Math.*, *Physicist J.*-P. Vigier, Dec. 2014.
[19] Cl. Cohen-Tannoudji, B. Diu and Fr. Laloë, *Quantum Mechanics*, Vol. 1, C_I, Wiley-VCH, Hoboken (New Jersey), 1977.
[20] A. Messiah, *Quantum Mechanics*, Vol. 1, North-Holland, Amsterdam, 1967.
[21] S.V. Adamenko and V.I. Vysotskii, Mechanism of synthesis of superheavy nuclei via the process of controlled electron-nuclear collapse, *Found. Phys. Lett.* **17**(3) (2004) 203–233.
[22] S.V. Adamenko and V.I. Vysotskii, Evolution of annular self-controlled electron–nucleus collapse in condensed targets, *Found. Phys.* **34**(11) (2004) 1801–1831.
[23] R. Kwok, Phys. 53, Soln.Homew. Ch 39#4, Charles W.Davidson Coll. Of Engineering, 4-Jul-2010, San Jose State Univ. http://www.engr.sjsu.edu/rkwok/Phys53/soln53_Ch39.pdf.

[24] W.H.E. Schwarz, *An Introduction to Relativistic Quantum Chemistry, Relativistic Methods for Chemists*, Chapter 1, Challenges and Advances in Comp. Chem. and Phys. Series, J. Leszczynski (Ed.), Vol. 10, M. Barysz (Ed.), Yasuyuki Ishikawa, Springer.
[25] Cl. Cohen-Tannoudji, B. Diu, Fr. Laloë, *Quantum Mechanics*, Vol. 2, D_{VII}, Wiley-VCH, Hoboken (New Jersey), 1977.
[26] M. Bellac, *Quantum Physics*, Université de Nice, Sophia Antipolis, Jan 2006, Cambridge University Press, Cambridge.
[27] H. Kleinert, *Particles and Quantum Fields*, Book on line, Nov. 19, 2016, Freie Universität of Berlin.
[28] Cl. Cohen-Tannoudji, B. Diu, Fr. Laloë, *Quantum Mechanics*, Vol. 2, D_{XI}, Wiley-VCH, Hoboken (New Jersey), 1977.
[29] GSI-Modern Atomic Physics: Experiment and Theory, Lect. 3, April 29th Working Group pf Prof. Thomas Stöhlker, GSI-Darmstadt. http://web-docs.gsi.de/~stoe_exp/lectures/SS2015/archive/15_05_29-lecture_modts.pdf.
[30] R. Klaubert, *Student Friendly Quantum Field Theory*, 2nd Edn., Sandtrove Press, Fairfield, Iowa, 2013.
[31] L. Rusakova Irina, Yu Yurii, Rusakov, B. Krivdin Leonid, Theoretical grounds of relativistic methods for calculation of spin–spin coupling constants in nuclear magnetic resonance spectra, *Russian Chem. Rev.* **85**(4) (2016) 356–426.
[32] H.W. Crater, R.L. Becker, C.Y. Wong, P. Van Alstine, A detailed study of nonperturbative solutions of two-body Dirac equations, Oak Ridge National Laboratory (ORNL), Central Research Lib., Martin Marietta, D.O.E, Dec. 1992.
[33] H.W. Crater and C.Y. Wong, Magnetic states at short distances, *Phys. Rev.* D **85** (2012) 116005.
[34] D.G. Currie, T.F. Jordan and E.C.G. Sudarshan, Relativistic invariance and hamiltonian theories of interacting particles, *Rev. Mod. Phys.* **34** (1963) 350–375.
[35] https://en.wikipedia.org/wiki/Neutron#Discovery.
[36] A. Meulenberg, Extensions to physics: what cold fusion teaches, Special Section: Low Energy Nuclear Reactions, M. Srinivasan and A. Meulenberg (Eds.), *Current Science*, Vol. 108, No. 4, 25 Feb. 2015. http://www.currentscience.ac.in/cs/php/feat.php?feature=Special%20Section:%20Low%20Energy%20Nuclear%20Reactions&featid=10094.

J. Condensed Matter Nucl. Sci. 26 (2018) 69–75

Research Article

On the Heat Transfer in LENR Experiments

T. Toimela*

Vaasa University of Applied Sciences, Wolffintie 30, 65200, Vaasa, Finland

Abstract

Thermal conduction is considered in deuterated palladium. We assume that the energy released in a single LENR event thermalizes in a region that has a typical dimension on the order of a hundred nanometers. It is shown that thermal conductivity enables the heat transfer of the energy released in repeated events without causing the lattice to melt. Consequently, continuous power is possible. It is argued that power of close to one watt can arise from a single nuclear active environment, NAE. Both the experimental and theoretical consequences of the results are discussed.
 ISSN 2227-3123

Keywords: Heat transfer, LENR, Theory

1. Introduction

In the LENR research there are two important – and unsolved – problems. Firstly, what is the mechanism which allows detectable energy production even though the interparticle distances between hydrogen nuclei remain much larger compared to the nuclear distances. Secondly, how is the nuclear energy, that is released, transferred to the heat without penetrating radiation. Several different approaches have been proposed to solve either or both of these questions [1–8]. However, the discussion on these problems have shown practically no convergence over the years. The total lack of agreement in these principal questions forces us to skip these principal questions here and to proceed further on more general grounds, in order to extract some useful information anyway. Therefore, in this article we will consider the issue, how the heat is transferred away after the thermalisation has taken place.

It is possible that initially the energy released in a fusion reaction is in the form of the energies of the initial energy carriers which can be phonons, photons, electrons or hydrogen nuclei (protons or deuterons), depending on the theoretical model. In the first stage these energy carriers may have a non-thermal energy distribution. Due to collisions the thermalisation of the hydrogen loaded metal will be reached. We shall assume here that this thermalisation takes place in a submicron region, of order hundred nanometers, large enough that no melting of the lattice will occur.

*E-mail: tuomo.toimela@vamk.fi.

 ISSN 2227-3123

2. Heat transfer

Considering how the heat is transferred, we need to use the thermal diffusion equation [9]

$$\frac{\partial T(\mathbf{x},t)}{\partial t} = D\,\nabla^2 T(\mathbf{x},t)\,, \tag{1}$$

where the thermal diffusion constant D is defined by the thermal conductivity κ and the specific heat per unit volume

$$D = \frac{\kappa}{C/V} = \frac{\kappa}{c_{\mathrm{p}}\,\rho}. \tag{2}$$

Here c_{p} is specific heat per unit mass and ρ is the mass density.

Assume here that the temperature is large compared to the Debye temperature, which is clearly true as we are dealing with temperatures corresponding to the room temperature or above it. The specific heat of the metal increases with hydrogen loading due to the additional vibration modes corresponding to the hydrogen atoms. However, the same is also true for the thermal conductivity. The thermal conductivity is proportional to the number of free electrons in metal [10]. This increases with loading due to the additional free electrons associated with the loaded hydrogen atoms. Therefore we can use, as the first approximation, the known values of the thermal conductivity and the specific heat of the host metal to calculate the thermal diffusion constant. To be specific, we shall here consider (fully loaded) palladium metal. For palladium we get the value of the thermal diffusion constant $D = 2.5 \times 10^{-5}\,\mathrm{m}^2/\mathrm{s}$.

In the standard solution of the diffusion equation (1) the thermal distribution at some later time t_0, $T(\mathbf{r},t_0)$, can be expressed by the initial temperature distribution, $T(\mathbf{x},0)$

$$T(\mathbf{r},t_0) = \frac{1}{(4\pi D t_0)^{3/2}} \int \mathrm{d}^3\mathbf{x}\,\mathrm{e}^{-(\mathbf{r}-\mathbf{x})^2/4Dt_0}\,T(\mathbf{x},0). \tag{3}$$

In the case of the spherical symmetry this reads

$$T(r,t_0) = \frac{1}{r\sqrt{4\pi D t_0}} \int_0^\infty \mathrm{d}x\,x\,\left[\mathrm{e}^{-(r-x)^2/4Dt_0} - \mathrm{e}^{-(r+x)^2/4Dt_0}\right] T(x,0). \tag{4}$$

Now, assume that the initial state is ambient temperature T_0 plus (due to a fusion reaction) a temperature increase by an amount of ΔT inside a sphere of radius r_0:

$$T(x,0) = T_0 + \Delta T\,\theta(r_0 - x)\,. \tag{5}$$

Then the temperature distribution becomes

$$T(r,t_0) = \frac{1}{r}\int_0^\infty \mathrm{d}x\,x\,f(r,x)\,[T_0 + \Delta T\,\theta(r_0 - x)] = T_0 + \frac{\Delta T}{r}\int_0^\infty \mathrm{d}x\,x\,f(r,x)\,\theta(r_0 - x), \tag{6}$$

where a shorthand notation has been used:

$$f(r,x) = \frac{1}{\sqrt{4\pi D t_0}}\left[\mathrm{e}^{-(r-x)^2/4Dt_0} - \mathrm{e}^{-(r+x)^2/4Dt_0}\right] \tag{7}$$

Assume now that the next fusion reaction takes place at the same sphere at the time t_0, leading to another temperature increase ΔT in the sphere. The temperature distribution at the time $2t_0$ can be written then

$$T\left(r,2t_0\right) = \frac{1}{r}\int_0^\infty \mathrm{d}x_2\, x_2\, f\left(r,x_2\right)\, \left[T\left(x_2,t_0\right)\right]$$
$$= \frac{1}{r}\int_0^\infty \mathrm{d}x_2\, x_2\, f\left(r,x_2\right)\, \left[T_0 + \frac{\Delta T}{x_2}\int_0^\infty \mathrm{d}x_1\, x_1\, f\left(x_2,x_1\right)\, \theta(r_0 - x_1) + \Delta T\, \theta\left(r_0 - x_2\right)\right]. \quad (8)$$

By renaming the integration variable x_2 to x_1 in the last term this can be written

$$T\left(r,2t_0\right) = T_0 + \frac{\Delta T}{r}\left\{\int_0^\infty \mathrm{d}x_1\mathrm{d}x_2\, f\left(r,x_2\right)\, f\left(x_2,x_1\right)\, x_1\, \theta\left(r_0 - x_1\right) + \int_0^\infty \mathrm{d}x_1\, f\left(r,x_1\right)\, x_1\, \theta\left(r_0 - x_1\right)\right\}. \quad (9)$$

Assuming several consequent fusion reactions, so that the temperature inside the sphere of the radius r_0 increases by the amount ΔT after every time interval t_0. Then the above solution can be iterated, leading to the thermal distribution

$$T\left(r,nt_0\right) = T_0 + \Delta \mathrm{T}\left\{\frac{1}{r}\left[\int_0^\infty \mathrm{d}x_1 \cdots \mathrm{d}x_n\, f\left(r,x_n\right) f\left(x_n,x_{n-1}\right) \cdots f\left(x_2,x_1\right)\, x_1\, \theta\left(r_0 - x_1\right)\right.\right. \quad (10)$$
$$\left.\left. + \cdots + \int_0^\infty \mathrm{d}x_1\, f\left(r,x_1\right)\, x_1\, \theta\left(r_0 - x_1\right)\right] + \theta\left(r_0 - r\right)\right\}$$

where the temperature increase at the time $t = nt_0$ has been also included. Every term in this sum (10) represents a separate fusion reaction; the first term corresponding to the reaction occurred at zero time, and so on, the last one corresponding to the last reaction at the time $t = nt_0$.

The temperature has its largest value in the center. Noting that

$$\lim_{r \to 0} \frac{f(r,x)}{r} = \frac{x}{Dt_0}\, \frac{\mathrm{e}^{-\frac{x^2}{4Dt_0}}}{\sqrt{4\pi D t_0}}, \quad (11)$$

we get

$$T\left(0,nt_0\right) = T_0 + \Delta T\left\{\int_0^\infty \mathrm{d}x_1 \cdots \mathrm{d}x_n\, \frac{x_n}{Dt_0}\, \frac{\mathrm{e}^{-\frac{x_n^2}{4Dt_0}}}{\sqrt{4\pi D t_0}}\, f\left(x_n,x_{n-1}\right) \cdots f\left(x_2,x_1\right)\, x_1\, \theta\left(r_0 - x_1\right)\right.$$
$$\left. + \cdots + \int_0^\infty \mathrm{d}x_1 \frac{x_1}{Dt_0}\, \frac{\mathrm{e}^{-\frac{x_n^2}{4Dt_0}}}{\sqrt{4\pi D t_0}}\, x_1\, \theta\left(r_0 - x_1\right) + 1\right\}. \quad (12)$$

By using the dimensionless variables

$$z_i = \frac{x_i}{\sqrt{4\pi D t_0}}, \quad (13)$$

this can be written

$$T\left(0,nt_0\right)=\,T_0+\,\Delta T\left\{4\int_0^\infty\frac{\mathrm{d}z_1\cdots\mathrm{d}z_n}{\pi^{n/2}}\,z_n\,\mathrm{e}^{-z_n^2}\,g\left(z_n,z_{n-1}\right)\cdots\,g\left(z_2,z_1\right)\,z_1\,\theta\left(\frac{r_0}{\sqrt{4\pi Dt_0}}-\,z_1\right)\right.$$
$$\left.+\cdots\,+4\int_0^\infty\frac{dz_1}{\pi^{\frac{1}{2}}}\,z_1\,e^{-z_1^2}z_1\,\theta\left(\frac{r_0}{\sqrt{4\pi Dt_0}}-\,z_1\right)+1\right\} \tag{14}$$

with

$$g\left(z_n,z_{n-1}\right)=\,\mathrm{e}^{-\left(z_n-z_{n-1}\right)^2}-\,\mathrm{e}^{-\left(z_n+z_{n-1}\right)^2}. \tag{15}$$

Now, consider the integral

$$I=\,\frac{1}{k^{3/2}\sqrt{\pi}}\int_0^\infty\mathrm{d}z\,z\,\,\mathrm{e}^{-z^2/k}\left(\mathrm{e}^{-(z-w)^2}-\,\mathrm{e}^{-(z+w)^2}\right). \tag{16}$$

This integral can be written

$$I=\,\frac{1}{k^{3/2}\sqrt{\pi}}\int_0^\infty\mathrm{d}z\,z\left(\mathrm{e}^{-\frac{k+1}{k}\left(z-\frac{k}{k+1}w\right)^2}-\,\mathrm{e}^{-\frac{k+1}{k}\left(z+\frac{k}{k+1}w\right)^2}\right)\,\mathrm{e}^{-w^2/(k+1)}. \tag{17}$$

Substituting in the latter integral $z\,\rightarrow\,-z$, we obtain

$$I=\,\frac{\mathrm{e}^{-w^2/(k+1)}}{k^{3/2}\sqrt{\pi}}\,\int_{-\infty}^\infty\mathrm{d}z\,z\,\mathrm{e}^{-\frac{k+1}{k}\left(z-\frac{k}{k+1}w\right)^2}. \tag{18}$$

This can be evaluated analytically [11] giving

$$I=\,\frac{w\,\mathrm{e}^{-w^2/(k+1)}}{\left(k+1\right)^{3/2}}. \tag{19}$$

Comparing this to Eq. (16) we find that in Eq. (14) all the multiple integrals can be evaluated analytically one by one (except the last one) the integer k just increasing by one in every integration, leading to the sum

$$T\left(0,\infty\right)=\,T_0+\,\Delta T\,\left\{1+\,\frac{4}{\sqrt{\pi}}\,\sum_{k=1}^\infty\frac{1}{k^{\frac{3}{2}}}\,\int_0^\infty\mathrm{d}x\,x^2\,\mathrm{e}^{-\frac{x^2}{k}}\,\theta\left(\frac{r_0}{\sqrt{4\pi Dt_0}}-\,x\right)\right\} \tag{20}$$

or

$$T\left(0,\infty\right)=\,T_0+\,\Delta T\,\left\{1+\,\frac{4}{\sqrt{\pi}}\,\sum_{k=1}^\infty\int_0^{\frac{r_0}{\sqrt{4\pi Dt_0k}}}\mathrm{d}x\,x^2\,\mathrm{e}^{-x^2}\,\right\}. \tag{21}$$

In these equations a continuous power is assumed by letting $n\,\rightarrow\,\infty$. For numerical calculations this sum converges relatively fast. Even faster convergence can be obtained if the exponential function is expanded as a Taylor expansion and the integrations are performed. We get then

$$T\left(0,\infty\right) = T_0 + \Delta T \left\{ 1 + \frac{4}{\sqrt{\pi}} \sum_{n=0}^{\infty} \frac{\left(-1\right)^n \xi\left(\frac{2n+3}{2}\right)}{\left(2n+3\right)\, n!} \left(\frac{r_0}{\sqrt{4\pi D t_0}} \right)^{2n+3} \right\}, \tag{22}$$

where the Riemann zeta function is

$$\xi\left(z\right) = \sum_{k=1}^{\infty} \frac{1}{k^z}. \tag{23}$$

The temperature increase ΔT depends on energy released Q and the number of the host metal atoms in the volume of the sphere inside which the energy thermalizes.

$$\Delta T = \frac{Q}{C} = \frac{Q}{6Nk} = \frac{Q}{8\pi r_0^3 \rho_n k}, \tag{24}$$

where ρ_n is the particle density of the host metal atoms. In Eq. (24) we have used the Dulong–Petit equation to express the heat capacity:

$$C = 6\, N\, k, \tag{25}$$

where k is the Boltzmann constant and N is the number of Pd atoms in the r_0-sphere

$$N = \frac{4\pi}{3}\, r_0^3 \rho_n. \tag{26}$$

The extra factor 2 in Eq. (25) arises from the doubled vibration degrees of freedom in the fully loaded palladium metal, $\mathrm{D/Pd} \approx 1$. In Eq. (25) the contribution from the degenerated electron gas is neglected as a small change, at most on the order of a few per cent. The time interval between the consequent fusion reactions can be written by the excess power P

$$t_0 = \frac{Q}{P}. \tag{27}$$

Now, demanding that the central temperature will remain below the melting temperature, we get an equation relating the maximum excess power P_{max} to the thermalisation sphere radius r_0:

$$T_m > T\left(0,\infty\right) = T_0 + \frac{Q}{8\pi r_0^3 \rho_n k} \left\{ 1 + \frac{4}{\sqrt{\pi}} \sum_{n=0}^{\infty} \frac{\left(-1\right)^n \xi\left(\frac{2n+3}{2}\right)}{\left(2n+3\right)\, n!} \left(\frac{r_0}{\sqrt{4\pi DQ/P_{\mathrm{max}}}} \right)^{2n+3} \right\}. \tag{28}$$

We assume here the deuterium-deuterium to He-4 fusion, so that $Q = 23.85$ MeV. T_0 is assumed to be room temperature, $+20^{\circ}$C. Inserting also the values of the thermal diffusion constant and the particle density of palladium, we can calculate numerically the maximum power that can arise from a single spot while still leaving the central temperature below the melting point. This maximum power is shown in Fig. 1. as a function of the radius r_0.

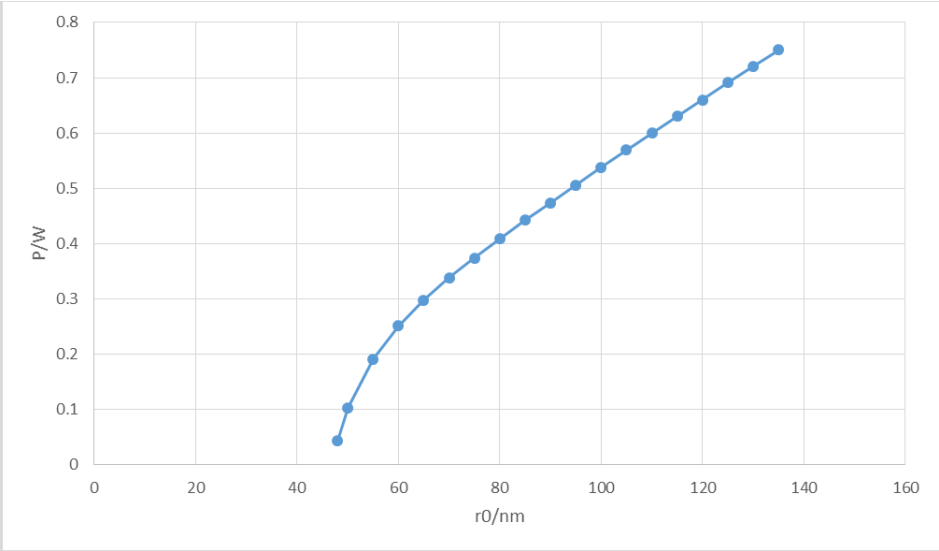

Figure 1. Maximum power as a function of the radius.

3. Discussion

As we can see in Fig. 1, the thermal conductivity of loaded Pd-metal is large enough to allow continuous excess power to exist up to the order of, or close to, one watt, provided that the thermalization takes place in submicron range (on the order 100 nm). Or, to put it other way around, it is possible to have continuous excess power on the order of one watt originating from a single spot of about 100 nm. It should be noted, however, that the exact relation between $P_{\max}$ and r_0 depends on the specific assumptions about the power production (i.e. does it originate as discrete events, as assumed here, or for example as constant power).

In roughly half of the electrochemical experiments in LENR research the excess power reported has been on the order of one watt. So, it is possible that in those experiments the excess power has originated from a single spot (or a single NAE [12]). Or if not just from a single spot - then from a very small number of spots. This notion can be regarded as compatible with the fact that LENR is a very rare phenomenon. It is possible that in the evolution of the surface region during electrolysis, the critical properties of NAE do not appear anywhere, leading to a null result. Sometimes, the requirements of NAE are met in only a single place (or in very few places) leading to excess power of 1 W or less. And only occasionally will several NAE emerge, leading to larger values of excess power.

The results of the above calculation also suggests that surface studies may have rather limited value. In surface studies, typically only the average values are considered. Now, if the critical requirements of NAE are met only in a single spot on the order 100 nm, they will remain hidden, because we cannot have control over the whole cathode surface within 100 nm accuracy.

As a final remark, we can note that the results shown here may be used to restrict possible theoretical models by their ability to reproduce the behavior found here. Especially the results may be used to restrict the possible energy carriers in the first stage.

References

[1] E. Storms, *The Science of Low Energy Nuclear Reaction*, World Scientific, Singapore, 2007, and references cited therein.

[2] Y.N. Bazhutov, Erzion model interpretation of the experiments with hydrogen loading of various metals, *J. Condensed Matter Nucl. Sci.* **13** (2015) 29–37.

[3] J.C. Fisher, Outline of polyneutron theory, *Proc. 8th Int. Workshop on Anomalies in Hydrogen/Deuterium Loaded Metals*, J. Rothwell and P. Mobberley (Eds.), 2008, InstantPublisher, Collierville, USA, pp. 70–93.

[4] P.L. Hagelstein, Bird's EyeView of phonon models for excess heat in the Fleischmann–Pons experiment, *J. Condensed Matter Nucl. Sci.* **6** (2012) 169–180.

[5] Y.E. Kim, Bose–Einstein condensation nuclear fusion: theoretical predictions and experimental tests, *Proc. 15th Int. Conf. on Condensed Matter Nuclear Science*, V. Violante and F. Sarto (Eds.), 2009, ENEA: Rome, Italy, pp. 286–296.

[6] E. Storms, Explaining cold fusion, *J. Condensed Matter Nucl. Sci.* **15** (2014) 29–304.

[7] A. Takahashi, Progress in condensed cluster fusion theory, *J. Condensed Matter Nucl. Sci.* **4** (2011) 269–281.

[8] T. Toimela, Multiple resonant scattering, *Proc. 8th Int. Workshop on Anomalies in Hydrogen/Deuterium Loaded Metals*, Rothwell, J. and P. Mobberley (Eds.), 2008, InstantPublisher, Collierville, USA, pp. 328–340.

[9] See any standard textbook, for example, M. Alonso and E.J. Finn, *Fundamental University Physics,* Vol. II, Addison-Wesley, Reading, Massachusetts, USA, 1974.

[10] E.M. Lifshitz and L.P. Pitaevskii, *Physical Kinetics (Course in Theoretical Physics)*, Vol. 10, Pergamon Press, Oxford, 1981.

[11] I.S. Gradshteyn and I.M. Ryzhik, *Table of Integrals, Series and Products,* Academic Press, New York, 1965.

[12] E. Storms, The nature of the energy-active state in Pd–D, *Infinite Energy*, Issues 5 and 6 (1995) 77.

J. Condensed Matter Nucl. Sci. 26 (2018) 76–97

Research Article

Reanalysis of an Explosion in a LENR Experiment

Jacques Ruer*

Jean-Paul Biberian

Aix-Marseille University, France

Abstract

An electrolytic cell operated with a hollow Pd cathode exploded in 2004. The violence of the explosion was surprising. We decided to re-analyze this event. The examination of the cell remnants indicate that the explosion occurred in the gas phase, and the electrodes seem unaffected. The stoichiometric H_2–O_2 mix can explode following different mechanisms that are briefly reviewed. A particular phenomenon called Shock Wave Amplification by Coherent Energy Release (SWACER) is able to produce strong detonations. A gas quantity similar to the original cell ignited by a hot spot or a spark produces only weak explosions that do not break the glass tube. Strong detonations are reproducibly obtained with a setup designed to induce the SWACER. The re-analysis of the event shows that the explosion was probably triggered by the SWACER resulting from a reaction in the hollow Pd cathode. In order to avoid accidents in the future during the operation of closed electrolytic cells, it is advised in addition to the conventional safety measures to avoid the presence of hollow, gas-filled metallic pieces in the reactor gas space, like a tube or a folded sheet.
 ISSN 2227-3123

Keywords: Deflagration, Detonation, Electrolytic cell, Explosion, Pd cathode, SWACER

1. Introduction

In 2004 Jean-Paul Biberian conducted an electrolytic Low Energy Nuclear Reaction (LENR) experiment with a mass flow calorimeter. The purpose of this experiment was to measure the abnormal heat during the electrolysis of heavy water with a palladium cathode. The reactor used has been described in a previous paper [1], see Fig. 1. The experiment ended with a strong explosion. The glass tube was shattered into many small pieces.At that time, the strength of the explosion seemed strange, because the quantity of explosive gas mixture in the reactor was limited. Biberian made some additional tests. An identical reactor was filled with a H_2–O_2 stoichiometric gas mix and ignited by a hot wire. These chemical explosions were relatively weak and unable to break the glass reactor. Therefore, the question was raised about a potential LENR mechanism to explain the explosion.

*E-mail: jsr.ruer@orange.fr.

 ISSN 2227-3123

Because of the significant implications of this hypothesis, it was considered desirable to further investigate the possibility that the phenomenon is of chemical origin. This is the purpose of the present paper.

The paper is organized as follows:

(1) The experimental setup is briefly presented together with the examination of the pieces recovered after the explosion.
(2) In order to provide a useful discussion of the problem, the basics of the different phenomena that take place during the reaction of H_2 and O_2 are reviewed. The whole series of phenomena ranging for ignition to detonation are briefly described.
(3) Explosions of H_2–O_2 stoichiometric gas mix were tested. They made it possible to demonstrate that the glass tube may be broken or not depending on the conditions of the experiment, in accordance with the theories mentioned in Section 2.
(4) The theoretical and the practical explanations allow the elaboration of a plausible mechanism of the event that occurred in the test reactor.
(5) Some similar events reported in the literature are re-examined under the light of the findings.
(6) Finally, some recommendations are offered in order to avoid accidents in the future.

2. Description of the 2004 Event

Electrolysis was performed in a Dewar to minimize undesirable heat losses. The reactor was built as a mass flow calorimeter. A controlled flow of water in the central condenser removed the heat as illustrated in Fig. 1. The geometrical characteristics are summarized in Fig. 2.

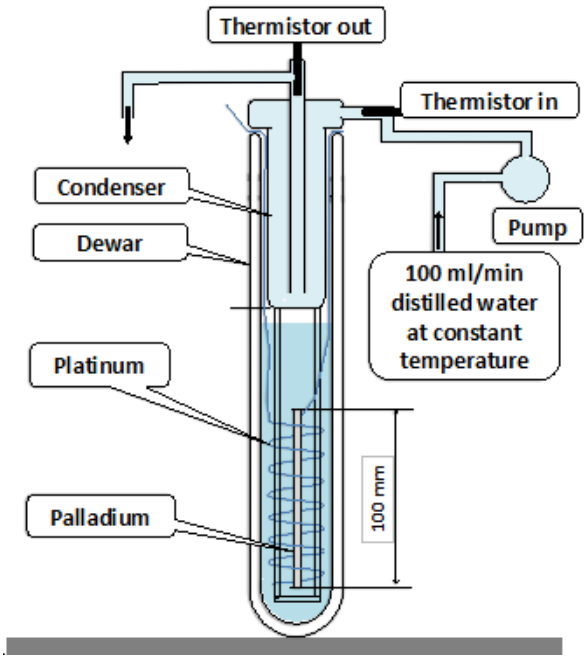

Figure 1. Schematic of the electrolytic cell.

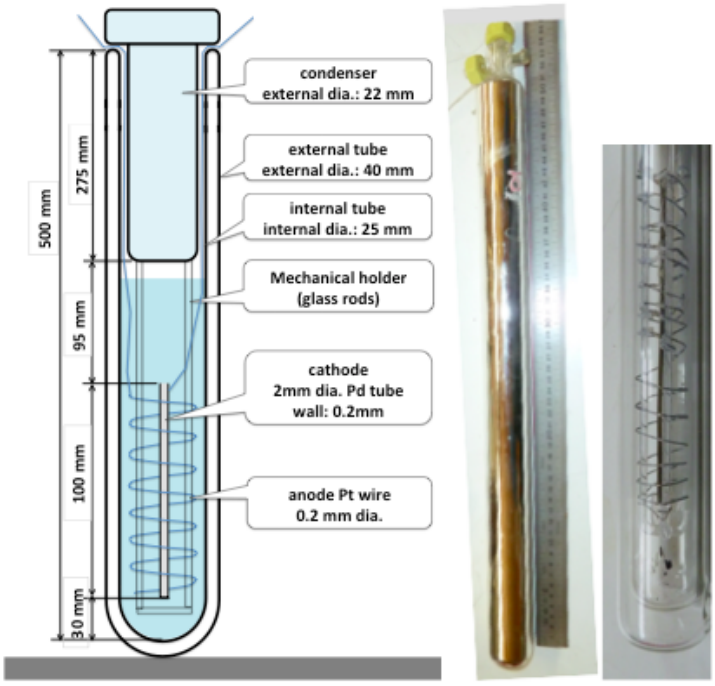

Figure 2. *Left*: Schematic geometry of the reactor used during the test with the precise dimensions as shown – *Middle*: The reactor glass tubes were silver coated on the inner faces. *Right:* The electrodes utilized during the test are shown inserted in a similar non-silver coated reactor.

Figure 3 shows the reactor after the explosion. Figure 4 shows the electrodes after the event. The cathode was a 100 mm Pd tube 2 mm outer diameter and 200 μm wall thickness closed at the bottom and opened at the top. The

Figure 3. Photograph of the reactor after the explosion. The bottom parts remained in place, some liquid was left inside.

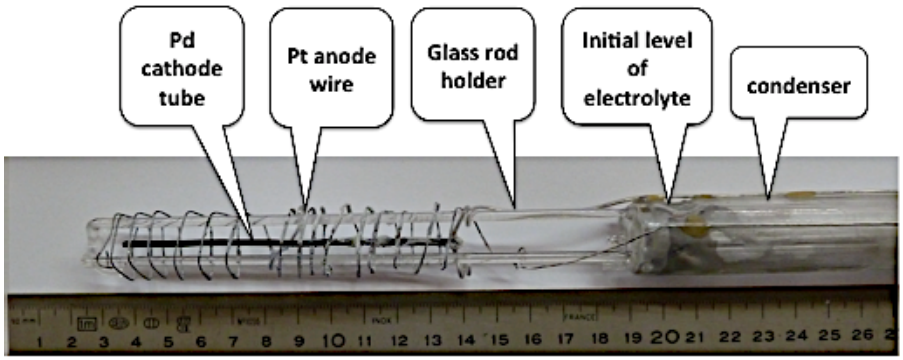

Figure 4. Photograph of the electrodes. The ruler shows the altitude over the bottom of the inner reactor tube. Note the trace at 200 mm probably corresponding to the initial level of the electrolyte.

anode was a platinum wire wrapped around glass rods.

An examination of the electrodes leads to the conclusion that they are relatively unaffected.

The glass reactor was broken into many fragments. Many of them were small pieces in the millimeter size or less. Some others had a size in the centimeter range and were carefully recovered (see Fig. 5).

The bottom part of the outer tube was broken into four pieces that can be fitted together. The bottom part of the inner tube punched the outer tube that was resting on the table. It seems likely that the bottom sections of both tubes were struck nearly simultaneously by the shock wave. The bottom sections were not shattered in small fragments probably because the electrolyte reflected the shock wave.

The elements available for examination lead us to consider that the explosion occurred in the gas phase. This is the hypothesis considered in this paper.

3. Review of the Explosion Mechanisms

The main phenomena are briefly reminded here. The reader interested in more details is invited to refer to the literature.

Figure 5. *Left*: Pieces from the outer tube. *Right*: Pieces from the inner tube. The cylinders visible on the left of both pictures are parts of the outer and the inner tubes and give the scale.

3.1. Chemical reaction

The H_2–O_2 stoichiometric gas mix can readily react according to the equation:

$$2H_2 + O_2 \rightarrow 2H_2O \ + 572\,\text{kJ mol}^{-1}. \tag{1}$$

In standard conditions, this energy equates to 8.5 J/cm^3 of gas mix. The internal volume is 100 cm^3. Therefore, the maximum chemical energy available in the explosive mixture is at most 850 J.

3.2. Reaction initiation

The simplest method to ignite a combustible mixture is to create a hot spot. This may be done with a heated surface. In the case of the H_2–O_2 stoichiometric gas mix, the temperature of the hot surface must be higher than 833 K [2]. Another solution is to trigger an electrical spark with sufficient energy. For the H_2–O_2 stoichiometric gas mix, the critical energy is low: 3 μJ. Such a weak spark may result from an electrostatic discharge. This explains why this stoichiometric mixture can so easily ignite.

There are other ways to ignite the reaction. One important possibility for the present discussion is the presence of chemical radicals on or close to the vessel surface [3]. This has been demonstrated by the initiation of the reaction (and subsequently of the detonation, as will be seen later) by UV irradiation of chemically sensitive gases, like H_2–O_2 with addition of Cl_2 [4]. The Cl radicals resulting from the photo-dissociation of Cl_2 molecules are able to ignite the gas mixture.

It is also well known that a metallic surface like Pt catalyzes the recombination of H_2 with O_2, to the point that an explosion may occur [5]. Therefore, a high temperature spot created by an external energy input is not necessarily required to initiate the H_2–O_2 reaction.

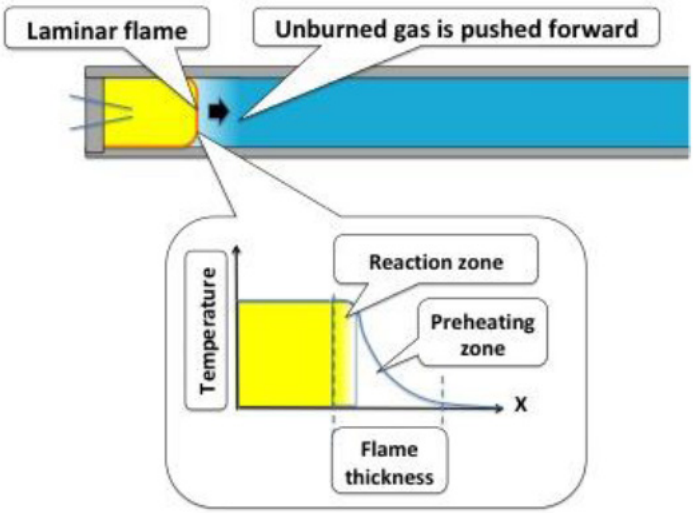

Figure 6. Schematic of the laminar combustion and detail of the flame front.

3.3. Laminar flame

Once combustion is initiated, a flame propagates through the gas mixture [6]. Let us consider Fig. 6. This sketch represents a flame travelling along a tube closed at one end, filled with a combustible gas mixture. The gas is ignited near the closed end. Shortly after the ignition, the flame is laminar. It has typically the shape of a flat front moving at a speed called the laminar flame speed.

Figure 6 also shows a schematic of an enlargement of the flame structure. The reactive zone itself is very thin. The heat released by the combustion diffuses towards the fresh gas adjacent to the front, elevating its temperature to the point that it reacts in turn. The flame moves ahead and the process continues. The flame velocity is governed by heat diffusion. For a stoichiometric H_2–O_2 mix at atmospheric pressure and ambient initial temperature, the flame propagates at a speed of 11 m s^{-1} [6]. This velocity is called the laminar flame speed. The flame thickness for H_2–O_2 is 0.32 mm. Dividing this value by the flame speed, we find that there is an induction time of 30 μs to initiate the reaction locally.

If now we observe the flame propagating along the tube, the hot gas resulting from the combustion creates a movement of the unburned gas ahead of the flame front [7]. The gas movement is sufficiently rapid to induce a turbulent flow of the unburned gas in the tube (Fig. 7).

The flame front is unstable and distorted by the turbulence eddies. Combustion proceeds over an increased surface that has a larger area than the flat laminar front. The heat release rate in the zone where combustion is taking place is increased. Therefore, the velocity imparted to the fresh mixture is also increased, and this further reinforces the turbulence of the gas flow [7,8]. This process is self-accelerated. The flame velocity increases progressively to supersonic speeds (e.g. 1000 m s^{-1}) [6–14]. This process is called deflagration.

3.4. Deflagration Detonation Transition (DDT)

Once the flame velocity approaches the speed of sound in the unburned gas, a pressure wave is formed ahead of the flame. As the velocity nears the speed of sound, the pressure wave steepens into a primary shock wave. The temperature of the unburned gas is rapidly raised when the primary shock wave passes. In other words, the unburned gas is preheated before the combustion starts. It is clear that because of the preheating, the combustion process is reinforced. The flame becomes supersonic and accelerates further.

At some point, called the detonation kernel, the preheating is such that an explosion arises directly within the combustion front creating a new local detonation shock wave (Fig. 8). The flame and the new shock wave are now coupled. There is a transition of the deflagration into a new phenomenon called detonation [7–14].

If we consider a detonation wave travelling in a stabilized manner along the tube, the flame parameters are well described by the theories of Chapman–Jouguet (CJ) and Zeldovich–von Neuman–Döring (ZND) [7–15].

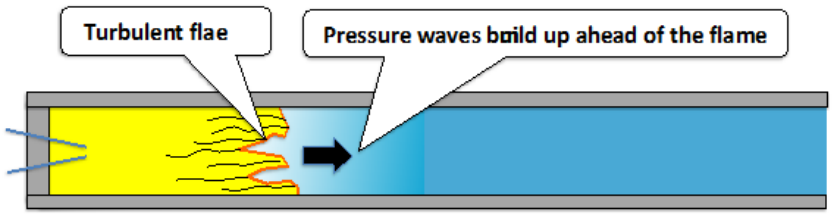

Figure 7. Propagation of a deflagration. The flame front surface is enlarged by the instabilities, this increases the combustion rate.

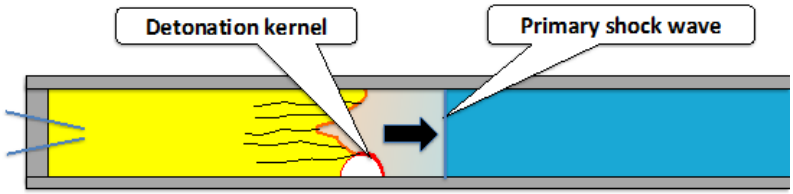

Figure 8. Onset of detonation.With sufficient preheating of the gas by the supersonic primary shock wave, an explosion occurs locally (detonation kernel). The detonation velocity is much larger than the primary shock wave velocity. The detonation propagates rapidly through the unburned gas.

The CJ theory makes it possible to calculate the main characteristics of the detonation. For the stoichiometric H_2–O_2 mix, the pressure in the burned gas is 18.4 bar and the temperature 3400 K. The wave velocity is 2900 ms^{-1}.

The ZND theory takes into account the fact that the reactants cannot be consumed instantly, but that the reaction requires a minimum duration (induction time). Within the wave front, there is a pressure peak P_{ZND} that is typically twice the pressure P_{CJ}, see Fig. 10. The compression results in the instantaneous heating of the gas to a temperature level of roughly $T_{CJ}/2$, sufficient to get the combustion within a short induction time. In the case of H_2–O_2, the reaction time is 80 ns and P_{ZND} is 41 bar [15]. In a 38 mm tube, the time between flame ignition and onset of the detonation is 500 μs for the stoichiometric H_2–O_2 mix [9]. The run-up distance between the point of ignition and the onset of the detonation is 60 mm [15].

The turbulence has a strong influence on the DDT. The run-up distance can be reduced by the introduction of devices able to increase the level of turbulence in the tube. The reader interested in the details of these theories is invited to refer to the relevant literature.

The detonation is in fact a very complicated process. Many shock waves are created, travel back and forth, and interact with each other (Fig. 9). Reflection of the detonation wave on a closed wall may double or triple the pressure shock [16–18]. Values exceeding 80–100 bar are reported [17–19]. Once the detonation front is established, the unburned gas remains unaffected until the arrival of the supersonic front. At the onset of the detonation, the unburned gas ahead of the flame front is already preheated by the shock waves that were running ahead of the flame while the

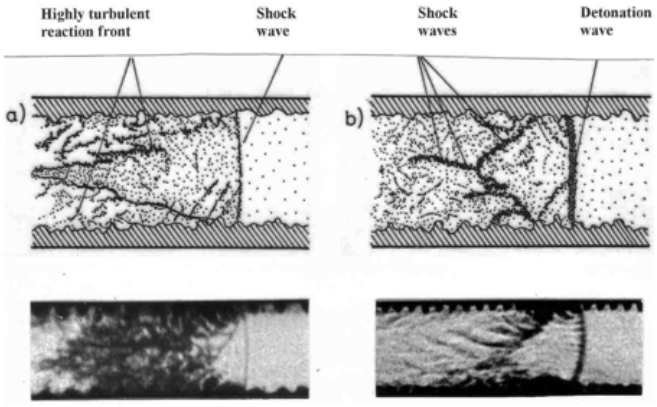

Figure 9. Shadowgraphs after [7]. (a) Before the onset of the detonation, the turbulent distorted reaction front and the supersonic primary shock wave are visible. (b) After the onset of detonation, the detonation front is clearly visible, as well as several secondary shock waves.

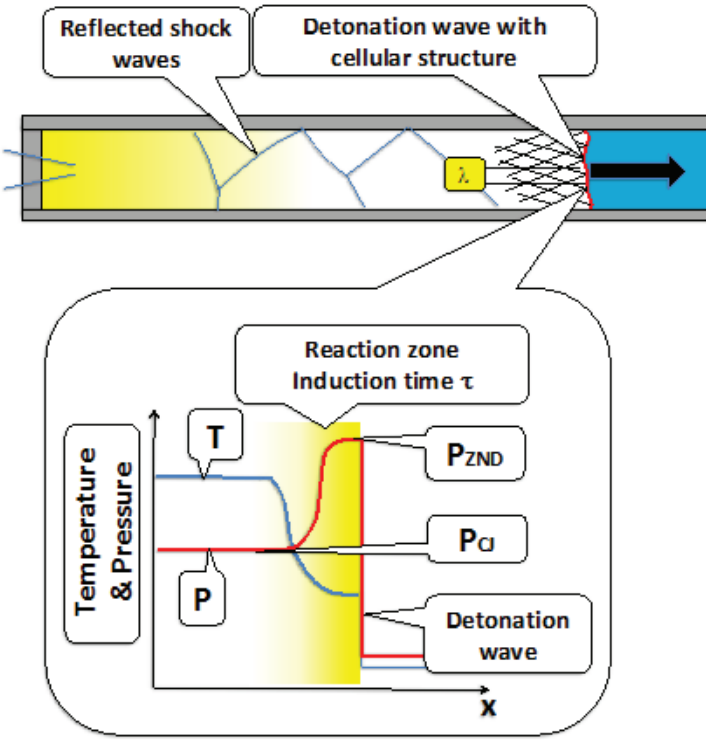

Figure 10. Detonation. The front has a cellular structure. The peak pressure within the front is about twice the pressure of the reacted gas.

flame was still subsonic. Therefore, the reaction is more violent than at a later moment, once the detonation wave is fully established. This is called overdriven detonation and the pressure is temporarily much higher than P_{CJ} [20].

Another fact to be mentioned here is that the reaction front is not a stable uniform structure, but exhibits a cellular structure (Fig. 10). The reader may refer to the literature for details. It is sufficient to mention here that in the case of H_2–O_2 the cell size λg is about 2.4 mm [8,15,21].

3.5. Direct initiation of a detonation

If the ignition energy is large, the shock can directly trigger the detonation without the intermediate deflagration phase (Shock Detonation Transition or SDT). In the case of the H_2–O_2 mix, an energy amount of about 6 J (e.g. a strong spark) is able to directly induce the detonation [8,21].

3.6. Combustion in a small diameter tubes and gaps

In large diameter tubes, the turbulence that can be fully developed is often considered as an important factor to accelerate the flame leading to the DDT. Conversely, in small diameter tubes the role of the turbulence is reduced. The flame is stretched along the boundary layers, and the elongation of the flame accelerates the local combustion, in a similar manner as the turbulence in large tubes. It is generally accepted that no detonation can propagate itself in a tube with a diameter smaller than λ/π [9,21]. However, experience shows that detonation is readily obtained when the reaction

takes place in small dimension tubes [22–25]. Detonation is obtained in tubes as small as 0.5 mm. It is also observed when the gases react between two parallel plates (Fig. 11). A gap of 0.26 mm is sufficient for the ethylene–oxygen mix [23]. Computations make it possible to simulate the phenomena at play. The run-up distance between ignition and DDT is three times shorter in a 3D tube than in a 2D gap [24].

When a small tube opens into a larger one, the detonation is transmitted in the large one only if some conditions are satisfied [9,15,19,23,24]. In particular, the diameter of the small tube must be larger than 13λ. Otherwise, the expansion of the flame decouples the shock wave from the reaction front and the detonation is changed into a deflagration, or even extinguished. However, the deflagration exiting from a small tube or gap may trigger a large explosion in some cases, as explained in the next paragraph.

3.7. Shock wave amplification by coherent energy release

When certain conditions are present in the explosive gas, initially weak shocks can amplify extremely rapidly to form detonations. There is a universal initiation mechanism called SWACER. The general requirement is the existence of a gradient of induction time in the explosive gas [3,4,10,20]. Of particular interest in the present discussion is the possibility to create the induction time gradient via a temperature gradient [3,25,26]. Consider Fig. 12a. A pre-chamber filled with an explosive mixture is connected through an orifice to a large volume of explosive gas. A deflagration is initiated in the pre-chamber. The temperature rise pushes a hot gas brush into the large volume. The hot jet is mixed with the initially quiescent gas by turbulent eddies. This shows that several outcomes are possible depending on the degree of turbulence:

- If the hot jet velocity is low because the orifice is large, the degree of turbulence is limited and the deflagration flame is transmitted to the gas in the large volume. No detonation occurs immediately (it may later, because of a DDT in the large volume).
- If the orifice is too small, the hot jet velocity is very large. The hot gas is strongly mixed with the cold gas. The temperature of the gas particles falls below the ignition temperature and the flame is extinguished.
- If the orifice section has an appropriate size, the turbulent mixing results in the buildup of a temperature gradient, see Fig. 12b. The hottest gas is located just at the tube orifice, and the temperature decreases as the distance increases. When the temperature at the orifice reaches the gas ignition temperature, the reaction starts in the large volume. The heat released reinforces the flame. Part of this heat is transmitted to the next gas layer that was at a slightly lower temperature but at the verge of ignition (Fig. 12c). If the heat imparted by the previous layer more than compensates for the temperature gradient, this layer reacts as well and amplifies further the flame energy (Figs. 12d and 12e). This process continues until a shock wave is formed (Fig. 12f). If the conditions are correct a detonation occurs (Fig. 12g).

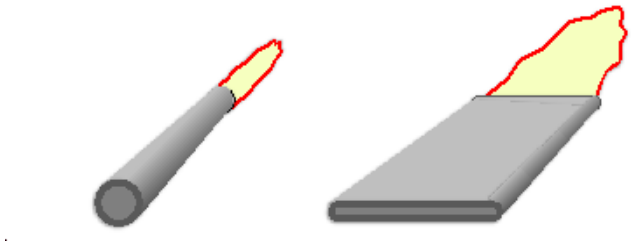

Figure 11. Combustion in small diameter tubes or gaps may transit into deflagration or detonation.

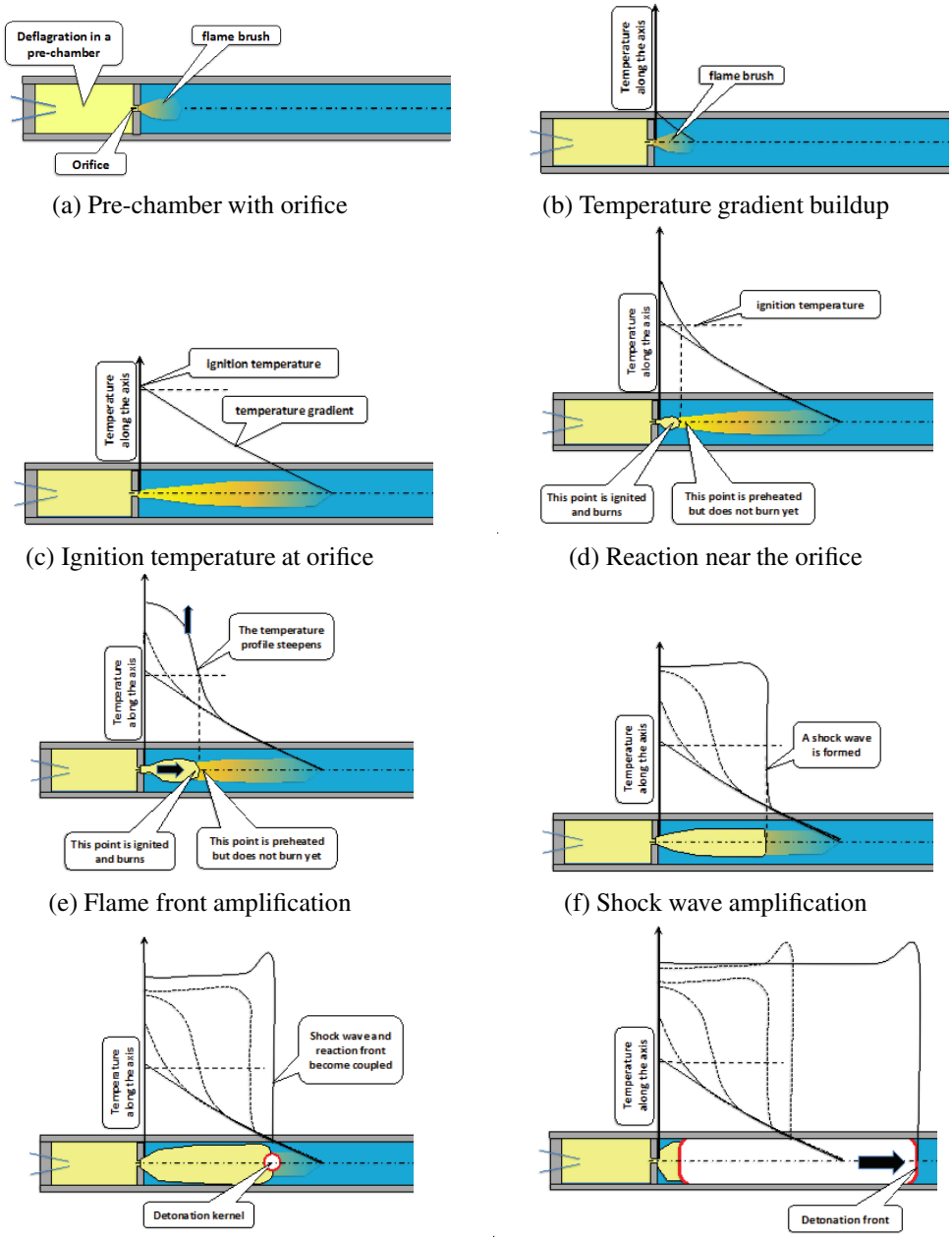

(a) Pre-chamber with orifice

(b) Temperature gradient buildup

(c) Ignition temperature at orifice

(d) Reaction near the orifice

(e) Flame front amplification

(f) Shock wave amplification

(g) Detonation onset

(h) Detonation wave

Figure 12. The SWACER detonation mechanism.

The SWACER is a powerful mechanism to detonate an explosive gas mixture. In the case of the H_2–O_2 stoichiometric mix, the detonation occurs in less than 100 μs [26]. It is interesting to note that the detonation in a small diameter tube does not always induce a detonation in the large volume, while a deflagration can sometimes do that via the SWACER process.

4. Explosions Tests

4.1. Experimental setup

In order to develop a better understanding of the explosion mechanism that destroyed the reactor in 2004, we decided to perform different experiments with the H_2–O_2 stoichiometric mix.

The following experiments have been conducted.

- A first series of tests was made in glass tubes with dimensions similar to the original reactor. The aim was to check if a simple explosion would be able to break the tube. Several modes of ignition were utilized (hot wire, high voltage spark, and exploded wire).
- A second series of tests were made in steel tubes. The objective was to evaluate the explosion damaging pressure following the setup configuration. One particular test showed by serendipity the influence of the SWACER mechanism.
- A third series involved ignition in a pre-chamber connected by a long small diameter tube to the test tube to investigate the SWACER phenomenon.

In total, 28 shots were performed.

4.2. Explosions in glass tube

The tube in Pyrex glass has an external diameter of 25 mm similar to the internal tube of the original reactor. The wall thickness is 1 mm and the length 200 mm (Duran® from Schott).

The stoichiometric H_2–O_2 gas mix was produced by the electrolysis of light water added with some NaOH at the bottom of the Pyrex tube. The electrodes were made of iron.

Several modes of ignitions were utilized. Movies were recorded at 30 frames/s.

4.2.1. *Ignition by a hot wire*

The ignition was obtained by a small coil of 200 μm diameter Constantan wire, heated by an auxiliary current source. As explained in Section 3.2, the hot spot temperature must exceed 833 K (560°C) to initiate the reaction.

Figure 13 shows three successive photos taken from a movie. On the left-hand side, the heated wire is red hot. The brightness of the wire seems to correspond to a temperature higher than 833 K, although a precise evaluation is not possible. The middle picture 33 ms later is a snapshot of the flame travelling up the tube. This shows that the flame velocity is low. The silicone plug is still in place. 33 ms later, the flame is already extinguished and the silicone plug is thrown clear of the tube. It is clear that in this case a deflagration was observed, not a detonation. The glass tube was never broken in this series of shots. An evaluation of the pressure developed by the explosion was not possible.

4.2.2. *Ignition by a high voltage spark*

In order to observe detonations, the energy of the ignition was increased. This was obtained by a spark triggered between an auxiliary electrode and the bath (Fig. 14). The length of the spark was 5 mm. In a movie taken at 30

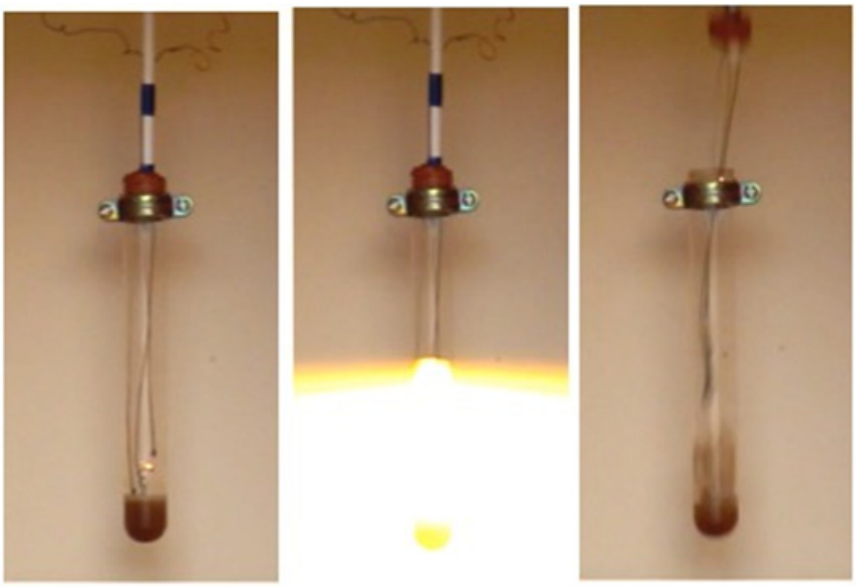

Figure 13. Deflagration ignited by a hot Constantan wire. Photographs at 33 ms intervals.

frames/s, the flame is visible in only one the pictures. The flame fills the whole tube indicating that the flame velocity is high. The explosion was much noisier and stronger. This probably corresponds to a detonation. However, the glass tube was never broken in this series of shots. An evaluation of the pressure developed by the explosion was not possible.

4.2.3. *Ignition by an exploded wire*

Another setup was tested in an attempt to quantify the peak pressure during the explosion. The tube was closed by a cover free to lift under the influence of the high gas pressure in the gas space. The cover weight was increased by a lead mass of 1100 g.

A high voltage 1 μF capacitor loaded up to 6 kV was discharged through a small coil of 70 μm diameter copper wire. Tests were performed with the exploded wire located at different heights along the tube axis. The explosions were likely detonations. The cover loaded by a 1100 g weight is lifted 20–30 mm, as shown on the right picture of Fig. 15. A 30 mm lift corresponds to an initial vertical velocity of 0.8 m s^{-1}. The momentum of the cover was then 0.88 kg m s^{-1}. Assuming very roughly that the impulse of the explosion lasted 1ms, the force exerted by the hot gases is 880 N. The section of the tube is 4.5 cm^2. The ratio of the force to the section gives a pressure of 19 bar. This is close to the P_{CJ} value (see Section 3.4), however this method can only give a rough estimate. In spite of the large pressure rise, the glass tube was never broken in this series of shots. In fact, the same glass tube was re-used for all the tests discussed in the above (10 shots).

4.3. Tests in steel tubes

These tests were done in 21 mm internal diameter steel tubes in order to evaluate the damaging pressure of the explosion, as explained in [17]. Aluminum disks at both ends close the steel tube. The internal pressure developed during

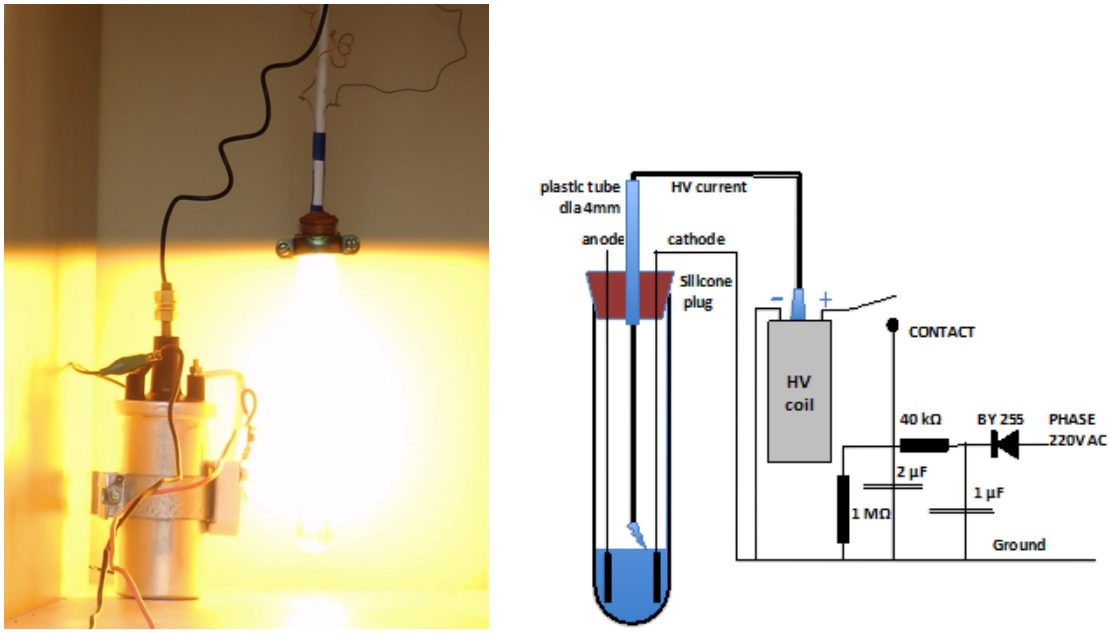

Figure 14. Explosion ignited by a high voltage spark.

the explosion deforms the disks permanently. This raises the possibility that we can estimate what the pressure peak was during the reflection of the shock wave at the tube end face. The aluminum disks thickness was 0.5 mm. The disks were annealed at 320°C before use to obtain reproducible mechanical characteristics. The relationship between

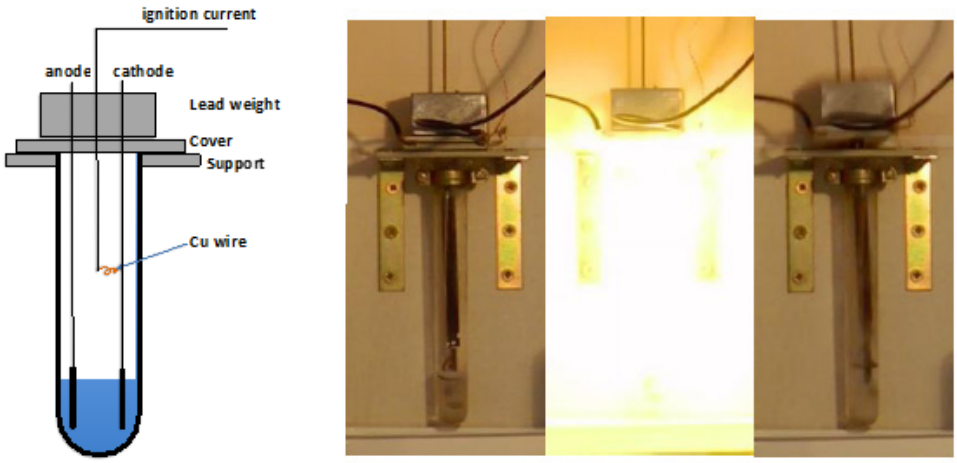

Figure 15. Ignition by an exploded wire. The tube is plugged by a lead weight, free to lift under the influence of the gas pressure. Pictures are taken at 33 ms intervals. The maximum altitude reached by the weight makes it possible to obtain a rough estimate of the gas pressure.

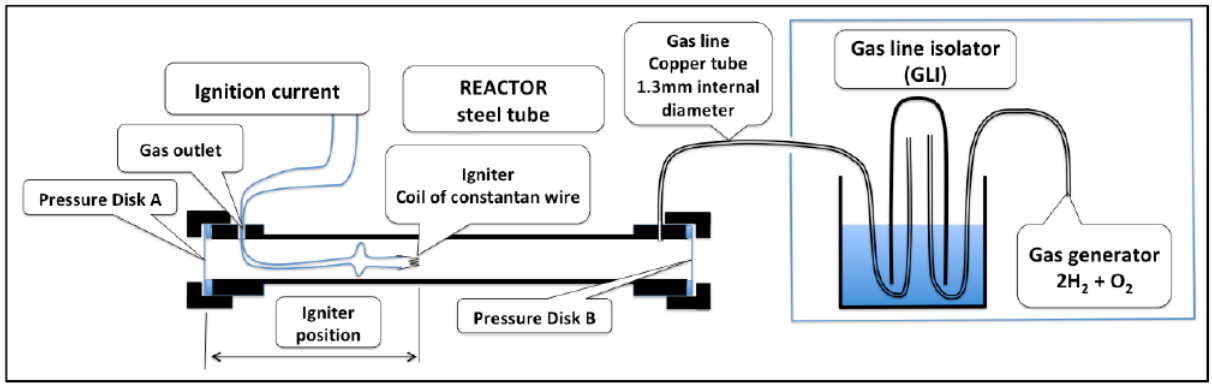

Figure 16. Sketch of the experiment in a steel tube.

the disk deformation and the pressure was established by hydraulic tests. Figure 16 presents the principle of the experiment. The stoichiometric H_2–O_2 gas mix is fed by a 1.3 mm copper tube. Ignition was done by a hot wire or a HV spark. Figure 17 shows examples of disks before and after the test.

A test was prepared by a prolonged purge of the tube with the H_2–O_2 mix. The glass tube of the gas line isolator (GLI) was removed and the shot promptly fired to limit the effect of the leakage by the gas outlet hole.

Different tube lengths were used from 160 to 640 mm. Pressure peaks of about 40 bar were measured in the long tubes, in accordance with the P_{ZND} value mentioned in Section 3.4. This clearly demonstrates that full detonations were obtained.

The location of the igniter in the tube has an influence on the pressure peaks observed on the end plates. This is illustrated by the results shown in Fig. 18. In 160 mm long tubes, the igniter was located at different distances from the tube end. One can see that the pressure peaks developed on the opposite ends are different. The pressure is higher at the end opposite the igniter. However, the figure is not symmetric. This may be due to the influence of the igniter

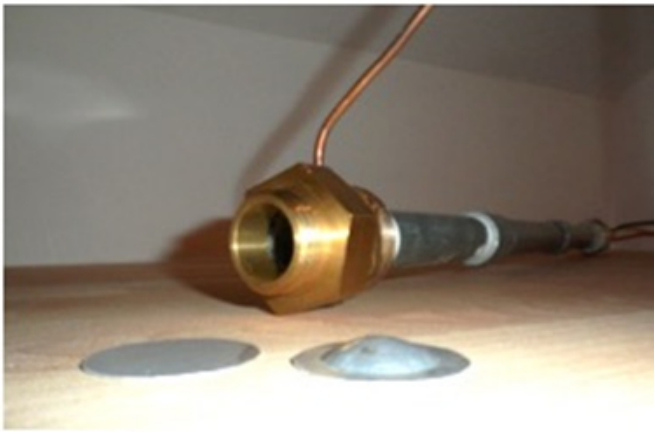

Figure 17. Picture of the reactor steel tube and of aluminum disks before and after a shot.

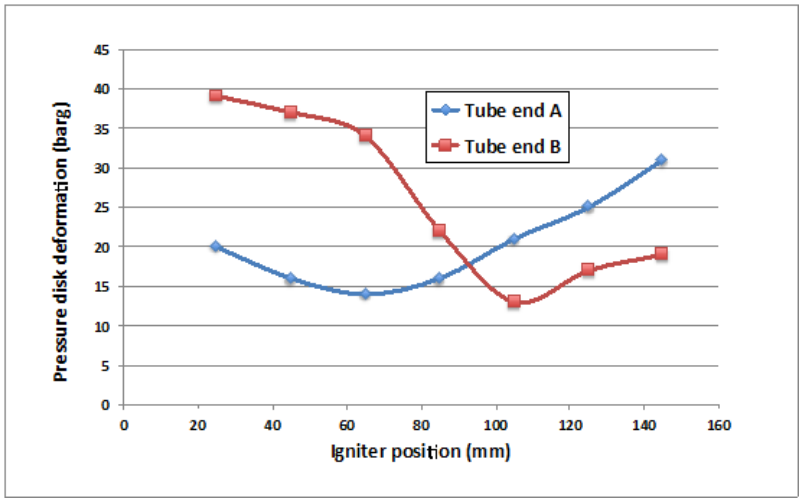

Figure 18. Influence of the igniter position on the pressure peaks at both ends of a 21 mm diameter 160 mm long steel tube.

connection wires on the turbulence within the tube.

The last test of this series was performed differently. The gas flow through the GLI was maintained in order to compensate the gas leakage until the shot (Fig. 19). Therefore, in the last test the isolator glass tube was left in place. The explosion was transmitted along the feeding line. The GLI glass tube was completely shattered, and the water bath glass container also broken. This experiment proved that a deflagration propagating along a small diameter tube could lead to a strong detonation, most probably via the SWACER mechanism. The explosion was not transmitted to the electrolyzer.

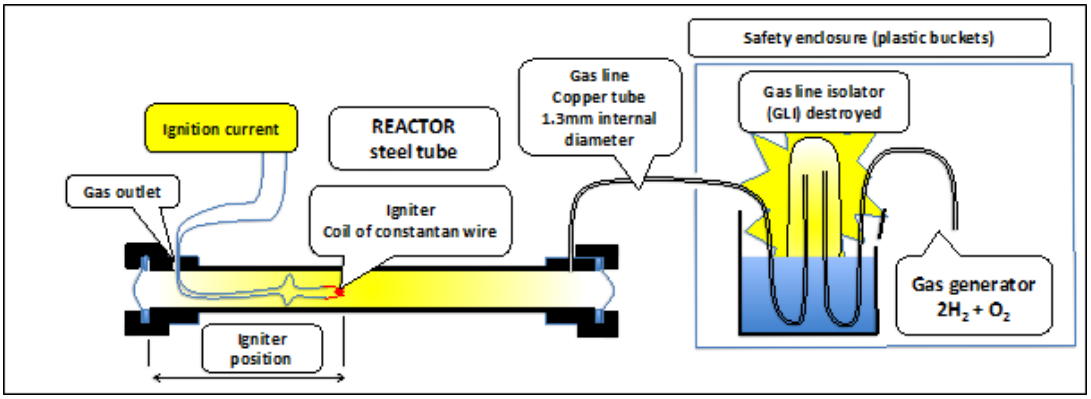

Figure 19. Last test of the series in steel tubes. The explosion is transmitted to the GLI and induces an SWACER in the glass tube that is shattered.

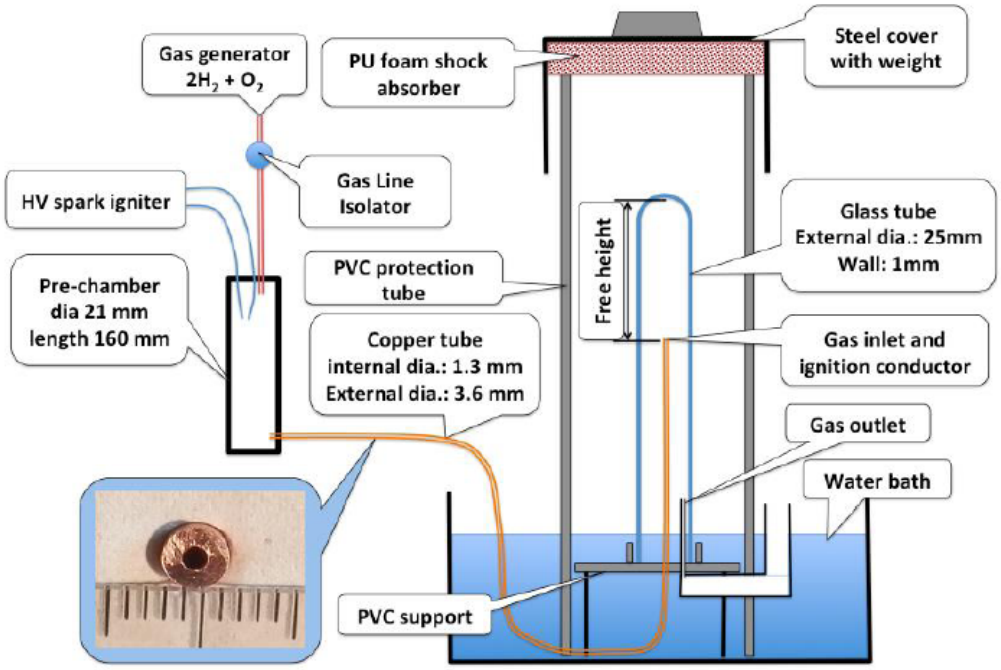

Figure 20. The gas is ignited in the pre-chamber. The deflagration propagates along the copper tube to the glass tube. A protection is provided in order to avoid the projection of glass debris by the detonation. The insert shows a cut of the copper tube.

4.4. Ignition in a pre-chamber

This series of tests is a direct consequence of the unexpected result described above. The aim was to explore some of the parameters that lead to the SWACER mechanism. In particular, it was decided to investigate the influence of the

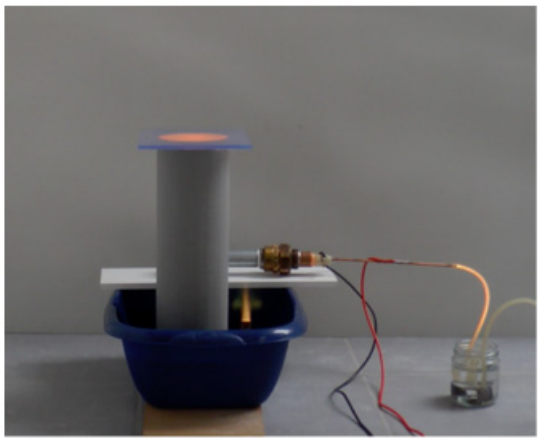

Figure 21. Picture taken during a shot. In this case there was no detonation. The protection cover with a foam shock absorber was replaced here by a transparent plastic sheet. The pre-chamber is the steel tube in background. The flame is visible through the cover, as a jet through the gas outlet, and in the transparent gas feeding line up to the gas line isolator on the right of the image.

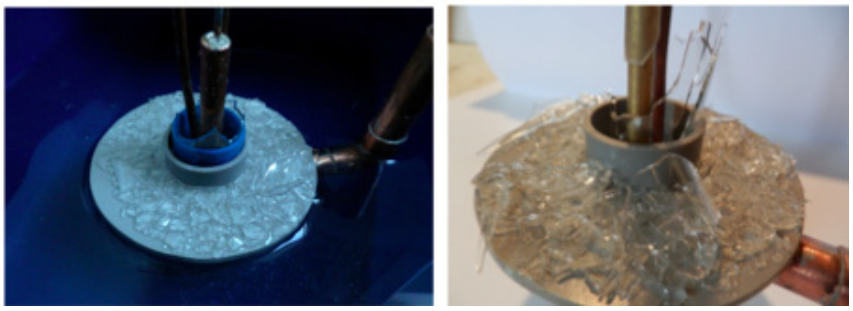

Figure 22. Examples of glass debris settled on the tube support after strong detonations. On the left picture, the protection tube has been removed and the water level lowered to make the support visible. On the right picture the assembly has been taken out of the bath. Note that the glass tube section that was immersed in water during the shot is not completely pulverized.

position of the small tube opening inside the glass tube. Figure 20 presents the corresponding setup.

The photo of Fig. 21 is taken from a movie made during a test that led to a simple deflagration, just at the time of the flame flash. The glass tube was not broken in this case but thrown-up onto the cover.

Figure 22 shows the results of full detonation experiments. After removal of the protection tube, glass debris were found on the tube support. Small glass fragments were also encrusted on the internal surface of the protection tube by the force of the explosion.

Different distances between the glass bottom and the copper tube opening have been tested. The results are summarized in Fig. 23. The SWACER occurred for 60 and 90 mm. The tube was left intact for 30 and 140 mm. It was broken into a few large pieces for a distance of 110 mm. This demonstrates that the precise configuration of the setup is a decisive factor to trigger the SWACER mechanism or not. This is probably linked to the presence of turbulent eddies within the tube, more or less favorable for the occurrence of the SWACER mechanism.

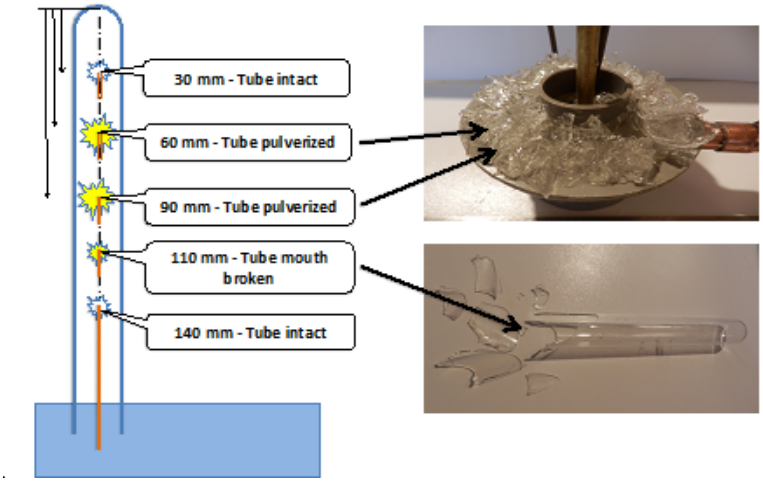

Figure 23. Tests with the small ignition tube located at different height along the glass tube center line. Pictures of the glass tube debris after different shots.

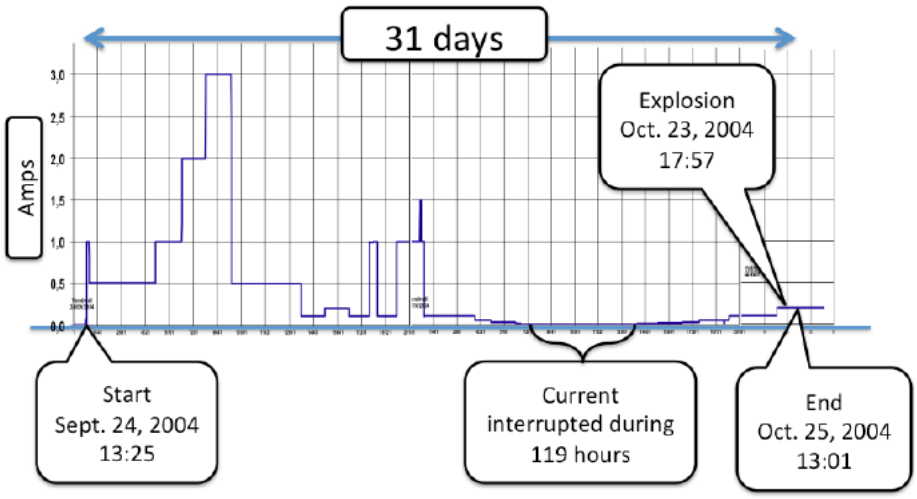

Figure 24. Electrical current during the experiment.

5. Scenario of the Reactor Explosion

The above explanations and tests invite one to consider the following scenario to explain the event that occurred in 2004.

Figure 24 shows the current recorded during the 31 days of the experiment. The current was varied several times. It was interrupted during 119 h. No addition of D_2O was done during the whole duration of the experiment. The explosion happened on a Saturday evening. Although the reactor was broken, there was sufficient electrolyte left at the bottom to maintain the 0.2 A current. The problem was discovered on the following Monday.

The following scenario is proposed (see Figs. 25a–f).

At the start of the experiment, the reactor is filled with 100 cm^3 of D_2O added with LiOD. (A trace of the initial level is still visible on the condenser, see Fig. 4.) During this phase of the experiment the Pd cathode is loaded with deuterium. The surplus of D_2 and O_2 escapes between the condenser and glass tube.

The liquid level drops progressively. The top of the Pd cathode emerges. The Pd and the Pt surfaces catalyze the recombination of a part of the gas mix, slowing down the loss of liquid. The current is interrupted. During that period, the Pd loses a part or all of the dissolved deuterium.

The gas space is filled again by D_2–O_2. The D_2–O_2 mix diffuses inside the Pd tube because its opening is exposed to the gas space. The Pd metallic wall of the cathode is reloaded with deuterium. The deuterium diffuses through the Pd tube wall and builds up in the Pd wall in the bottom part still immersed in the electrolyte.

The deuterium dissolved in the palladium diffuses across the wall and comes to the inner tube face. The Pd catalyzes the recombination of the D atoms with the oxygen present inside the tube void. The local reaction creates a hot spot inside the Pd cathode at the bottom

The local reaction ignites a flame inside the Pd tube, leading to a deflagration. The deflagration in the small hollow cathode triggers the SWACER mechanism in the gas space. The reactor explodes. This sequence based on prosaic phenomena may explain the explosion event observed in the reactor in 2004. If confirmed, then it would mean that non-conventional reactions are not required.

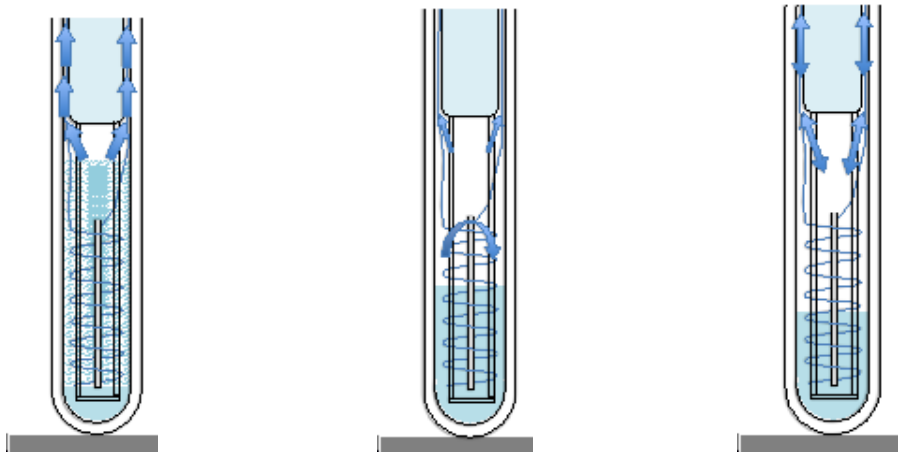

(a) Initial electrolysis period (b) Prolonged electrolysis period (c) Current interruption

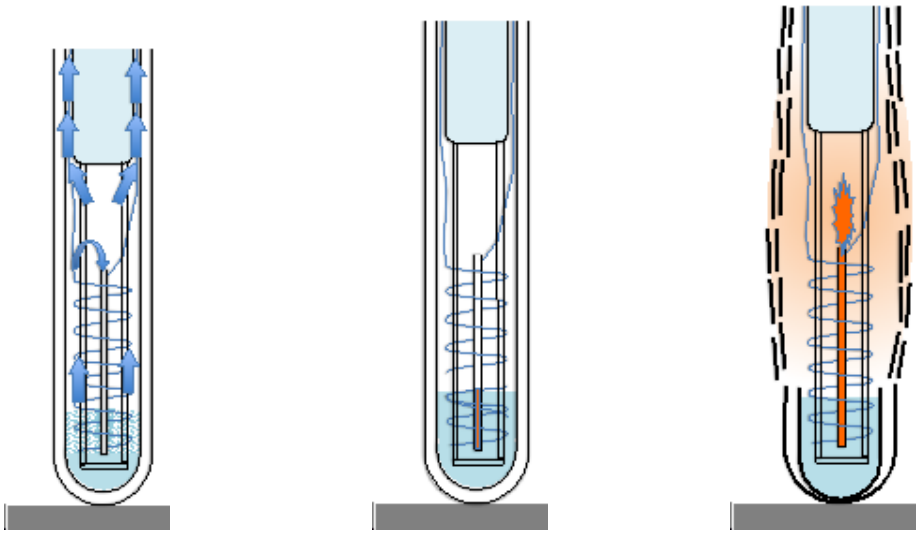

(d) Electrolysis is resumed (e) Reaction in the hollow cathode (f) Explosion of the reactor

Figure 25. Proposed scenario of the explosion.

6. Review of Similar Events

The literature reports other experiments that also ended with explosions. Three of them are discussed here.

6.1. Experiences at Beijing National Laboratory for molecular sciences [27,28]

The experimental system included a glass tube (23 mm int. dia.) a Pd tubular cathode (1.07 mm int. dia., 80 mm long) in heavy water. Three explosions occurred. The initial liquid level in the cell was 94 mm. It is then possible that after some hours of operation the top of the Pd tube emerged. The explosions might then be explained by a sequence of phenomena similar to that presented in the last section.

6.2. Accident at SRI [29,30]

The cell 4″ dia. × 6″ height was designed for high pressure. The cathode was a Pd plate shaped 1 cm^3 electrode. The cell exploded after the disconnection, while it was removed from the water bath. Because of leaks, the pressure was close to ambient. A hypothetical explanation may be the formation of a concentration gradient, resulting in the SWACER phenomenon. Unfortunately, this accident resulted in the death of a researcher.

6.3. Experiences at Hokkaido University [31,32]

The cell had a volume of 1000 cm^3 and was closed by a tight cover. It contained 700 cm^3 of light-water based electrolyte to study plasma electrolysis. A plasma discharge was conducted with a tungsten cathode wire 1.5 mm in diameter. The explosion occurred after about 10 s of normal electrolysis under a voltage of 15 V and a current of 1.5 A. Many parameters were recorded, including the bath temperature and the flow of hydrogen that was much higher than for normal electrolysis because of the pyrolysis of the water. Oxygen was also produced by the same reactions. The temperature increased from 20°C to more than 70°C just before the explosion. The amount of energy responsible for the fast heating is much larger than the electrical input and might result from non-conventional reactions. The accident report acknowledges: “It is possible that the tungsten cathode may have been exposed to the gas in the headspace”. In that case, the explosion itself of the H_2–O_2 may have resulted from a phenomenon that took place in the gas phase, the SWACER triggered by non-homogeneities in the gas composition and a spark.

7. Safety Recommendations

The occurrence of powerful explosions in electrolytic systems is a problem that should not be ignored. Even a limited amount of explosive gas may result in an accident if the conditions for the SWACER mechanism are unfortunately satisfied.

Safety measures must be observed. Some of them make common sense:

- Keep a safe distance, remote control is best.
- Place a protective screen between the cell and the operators.
- Wear appropriate personal protection: eyes goggles, gloves, ear plugs, non-flammable clothes.
- Make sure the safety measures are obeyed by all attendants.

The possibility of occurrence of the SWACER mechanism should be minimized. The following precautions are advised.

- If not required by the setup, do not confine the explosive gases in the cell.

- If you need to confine the gases (e.g. because the setup includes a recombiner in the gas space) make sure that pieces of catalytic metal like Pd or Pt electrodes are never exposed to the gas phase and remain submerged in the liquid.
- If pieces of such metals must be in the gas phase, make sure there is no hollow structure like a small diameter tube or a folded foil with a narrow gap.

8. Conclusions

The re-analysis of the explosion that occurred in 2004 at J.-P. Biberian's laboratory is done via a review of the literature and dedicated experiments. It shows that the explosion may result from the SWACER mechanism. This type of reaction may also be responsible for other explosions that happened in similar experimental setups. It must be taken into consideration to employ the correct safety measures in the future.

References

[1] J.-P. Biberian, Unexplained explosion during an electrolysis experiment in an open cell mass flow calorimeter, *J. Condensed Mater Nucl. Sci.* **2** (2009) 1–6.
[2] Inflammabilité et explosivité de l'hydrogène – Mémento de l'hydrogène Fiche 7. 1 – INERIS AFHYPAC (2015).
[3] A.M. Bartenev and B.E. Gelfand, Spontaneous initiation of detonations, *Progr. Energy Combustion Sci.* **26** (2000) 29–55.
[4] R. Knystautas and J.H. Lee, Mechanisms of Initiation of Detonation in Explosive Vapor Clouds, United States Air Force Office of Scientific Research, 1978.
[5] G.J.K. Acres, The Reaction between Hydrogen and Oxygen on Platinum – Progress in establishing kinetics and mechanisms – PM Research Laboratories, Johnson Matthey & Co Limited.
[6] Heinz Pitsch, Laminar premixed flames: kinematics and burning velocity, CEFRC Combustion Summer School, 2014.
[7] Andrzej Teodorczyk, Fast deflagrations, deflagration to detonation transition (DDT) and direct detonation initiation in hydrogen–air mixtures, First European Summer School on Hydrogen Safety, Belfast, 15–24 August 2006.
[8] A.E. Dahoe, Joint European summer school on fuel cell and hydrogen technology, Tutorial on Deflagrations and Detonations (2011).
[9] E. Schultz, E. Wintenberger and J. Shepherd, Investigation of deflagration to detonation transition for application to pulse detonation engine ignition systems, California Institute of Technology, Pasadena, CA 91125, USA, 1999.
[10] Geraint Thomas, Some observations on the initiation and onset of detonation, 2012. http://rsta.royalsocietypublishing.org/content/370/1960/715.
[11] The Chapman, Jouguet condition, Eng. Wikipedia.
[12] Jouguet and Emile, Sur la propagation des réactions chimiques dans les gaz, *J. Math é matiques Pures et Appliquées* **6**(1) (1905) 347–425.
[13] Von Neuman, *Theory of Detonation Waves,* Progress Report to the National Defense Research Committee, Division B, OSRD-549 (April 1, 1942, PB 31090), 34 pages.
[14] D.R. Kirk, MAE 5310: Combustion Fundamentals and Detonation, Mechanical and Aerospace Engineering Department, Florida Institute of Technology.
[15] Rémy Sorin, Etude et optimisation de la Transition Déflagration Détonation (TDD) en tube des mélanges stoechiométriques $H_2/O_2/N_2$ et (CH_4, C_2H_2, C_2H_4 et C_3H_8)/O_2/N_2 et de sa Transmission à un espace de plus grande dimension, Energie électrique. Université de Poitiers, 2005.
[16] J. Damazo and J.E. Shepherd, Reflected detonation waves: comparing theory to measured reflected shock speed, *29th Int. Symp. on Shock Waves*, Madison, WI, July 14–19, 2013.
[17] A.D. Craven and T.R. Greig, The development of detonation over-pressures in pipelines, *I. Chem. E. Symp. Series* No. 25, 1968.
[18] M.P. Moyle, R.B. Morrison and S.W. Churchill, Detonation characteristics of hydrogen–oxygen mixtures, *A. I. Ch. E. J.* March(1960).

[19] Claude Paillard, Personal communication.
[20] Kevin P. Grogan and Matthias Ihme, Weak and strong ignition of hydrogen/oxygen mixtures in shock-tube systems, *Proc. Combustion Institute* **35** (2015) 2181–2189.
[21] Michael Kaneshige and Joseph E. Shepherd, Detonation Database, Graduate Aeronautical Laboratories, California Institute of Technology, Pasadena, CA 91125, Explosion Dynamics Laboratory Report FM97-8, July 30, 1997, Last Revision: September 3, 1999.
[22] Ming-hsun Wu, M.P. Burke, S.F. Son and R.A. Yetter, Flame acceleration and the transition to detonation of stoichiometric ethylene/oxygen in microscale tubes, Proc. Combustion Institute, Volume 31, Issue 2, January 2007.
[23] V'yacheslav Akkerman, Vitaly Bychkov, Mikhail Kuznetsov, Chung K. Law, Damir Valiev and Ming-Hsun Wu, Fast flame acceleration and deflagration-to-detonation transition in smooth and obstructed tubes, channels and slits, *8th US National Combustion Meeting*, May 19–22, 2013.
[24] M.F. Ivanov, A.D. Kiverin, I.S. Yakovenko and M.A. Liberman, Hydrogene–oxygen flame acceleration and deflagration-to-detonation transition in three-dimensional rectangular channels with no-slip walls, *Int. J. Hydrogen Energy* (2013), http://dx.doi.org/10.1016/j.ijhydene.2013.08.124.
[25] M.F. Ivanov, A.D. Kiverin and M.A. Liberman, Flame acceleration and DDT of hydrogene–oxygen gaseous mixtures in channels with no-slip walls, *Hydrogen Energy*, April 2011.
[26] R. Knystautas, J.H. Lee, C. Guirao, M. Frenklach and I.Gg. Waqner, Direct initiation of spherical detonation by a hot turbulent gas jet, *17th Int. Combustion Symposium, Leeds*, August 1978.
[27] X.-W. Zhang, W.-S. Zhang, S.-H. Chen, Y.-B. Fu, D.-X. Fan and W.-J. Chen, *Proc. Third Int. Conf. Cold Fusion*, Nagoya, Japan, 1992.
[28] W.-S. Zhang, X.-W. Zhang, D.-L. Wang, J.-G. Qin and Y.-B. Fu, Thermal analysis of explosion in a open palladium/deuterium electrolytic system, *J. Condensed Mater Nucl. Sci.* **17** (2015) 116–123.
[29] S.I. Smedley, S. Crouch-Baker, M.C.H. McKubre and F.L. Tanzella, The January 2, 1992, Explosion in a deuterium/palladium electrolytic system at SRI international, in *Third Int. Conf. on Cold Fusion, "Frontiers of Cold Fusion"*, 1992, Nagoya, Japan, Universal Academy Press, Tokyo, Japan.
http://lenr-canr.org/acrobat/IkegamiHthirdinter.pdf#page=147.
[30] C. White, Some Issues of the Accident at SRI, EIR News Service, Vol. 19, No. 12 (1992).
[31] T. Mizuno and Y. Toriyabe, Anomalous energy generation during conventional electrolysis, *12th ICCF,* Yokohama, 2005.
[32] T. Mizuno, Accident Report, 2005.
http://newenergytimes.com/v2/news/2005MTExplosion/2005MizunoT-AccidentReport.pdf.

J. Condensed Matter Nucl. Sci. 26 (2018) 98–108

Research Article

Key Principles for Patenting in the Land of LENR

David J. French*

Second Counsel Services, Canada

Abstract

Patents can be obtained in the field of Cold Fusion/LENR but they will be specific to the arrangements that they describe. Proper patent drafting requires close cooperation between the inventor and attorney, with the inventor understanding the principles of claim drafting. Reference is made to the Andrea Rossi patent obtained before the US patent office and to the European patent obtained by Fleischmann and Pons before the European patent office with examples of claims for analysis.
 ISSN 2227-3123

Keywords: Cold fusion, Fleischmann, LENR, Patents, Rossi

1. Why Patent?

The basic reason for patenting is to make more money. The alternative, in the absence of patenting, is to market product in the face of competition. Competition may not be immediate in the case of new technology, but will be inevitable if the new technology is a success. The presence of competitors will eventually force everyone to adopt competitive market prices. This will lower margins and limit the profits of everyone engaged in competition. In the absence of competitors, a company can charge monopoly prices. They can charge what the market will bear and earn profits above those of a competitive marketplace. The result is higher prices for consumers. This is the way the patent system works.

There is a possible contrary argument that patents provide companies with a greater market share, and therefore enable lower prices because of efficiencies of scale. This issue is not addressed here. However, the premise that a company in a monopoly position having efficiencies of scale will price their product to minimize their profit is, in all events, difficult to defend.

2. What Patenting cannot Achieve

The value in the case of a patent is in having the ability to exclude competitors sufficiently to allow a company to enjoy enhanced profits. But there are certain realities that aspiring inventors may find difficult to accept.

Bad news (1). You cannot exclude competitors completely. They can always market "prior art". This means anything previously available to the public can be sold in competition, even if you obtain a patent. The Golden Rule

*Address: 3-60 Hotel de Ville, Gatineau, Québec, Canada J8X 2E2. E-mail: David.French@Second-Counsel.com or david.french@bell.net

 ISSN 2227-3123

of patent law is that a patent cannot take away from the public anything that was previously available. Consequently, even a valid patent cannot exclude competitors who choose to market prior art.

Bad news (2). Patents cannot exclude competitors from inventing something that you did not think of. This is one of the most difficult realities for inventors to accept. They always want to believe that their idea is the best way to do things. They are shocked when they find out that others have thought of other ways to do the job.

Bad news (3). A patent can only exclude competitors to the extent of the protection provided by the patent. What is the extent of patent protection? The answer is: your exclusive rights are defined by your primary "claim" coverage as drafted by you, the inventor, and your patent attorney. Providing the patent office with a claim drafted by the inventor is a core concept of patenting. When you seek a patent by filing an application you must provide a concise statement of the requested scope of your prospective monopoly. For reasons that are lost in time, you must summarize what might infringe in a single sentence. That single sentence, or "claim", must not describe anything that was "previously available to the public". (This includes any obvious variant on things previously available. After all, they were "available to the public" as well.)

Your proposed patent claims may not be effective in excluding others from competing with you in the marketplace. They may be inadequately drafted,

Getting your patent claim, or claims (you are allowed more than one, but focus on Claim 1), right is a job for you, the inventor, and your patent attorney. What should you expect of your patent attorney?

3. Key Question to ask your Attorney

A key question to ask your attorney is: "Am I going to get value for the money that I am paying you?" As a first answer your attorney is likely to say: "That is not for me to say". Actually, your attorney could volunteer a number of more enlightening answers. Here are some samples:

(1) Your invention is trash. It does not work, it is not cost effective or no one will buy it because it has no appeal.
(2) Better alternatives already exist. Some I know about because they been located in the prior art; some are possibly already in existence but we have not discovered them yet.
(3) The scope of your patent protection is limited or is inadequate of necessity. This is a prior art drafting issue. Your patent attorney may have been forced to drop patent claim coverage because otherwise your claims would extend to the prior art. He or she may know that the claims do not adequately cover what you would like to see them cover but this cannot be helped because of the prior art.
(4) Your patent can be avoided because there are loopholes in the way your claims have been drafted. This is a skill issue which your patent attorney should close-off, if he/she is skilled and sees their shortcomings. But you can never expect your attorney to admit that he or she has prepared poorly drafted claims.
(5) New and better ideas may surface. This is a factor that is almost beyond the control of your attorney, a challenge that requires guessing at what the competitors might do. But if your attorney does not know, or is not informed as to what the competitors are likely to do, then they will not be able to draft claims that are free of "loopholes". However, this problem can be addressed, at least in part, through close cooperation between the attorney and the inventor.

This is not to suggest that every patent application deserves every one of these possible answers. Nor is it to suggest that most attorneys would avoid providing any of these answers. The object in listing them is to awaken inventors and patent applicants to the issues that they should be addressing with their attorneys.

4. Loopholes

There are two types of loopholes: claim drafting errors, and failure to anticipate alternate inventions. Who should close loopholes? This is a job for both the attorney and the inventor. They should work together. The secret is to study Claim 1, your first broad claim, from the perspective of a competitor. Ask the question: "If I were a competitor could I enter the market by selling something that does not fit within the language of this claim?"

This key question should be addressed by the inventor before the patent application is finalized. It is all about "completing the invention". Are there other ways of doing the job, than the one that the invention addresses? If you can think of those other ways before the patent is finalized, and put them into the patent, then you will have closed-off at least some loopholes. This is one of the most important exercises in drafting a patent. It is rarely properly addressed by inventors.

Some attorneys will work hard to close-off loopholes. But in all fairness, I have heard an attorney say: "I have not been hired to invent", which is partially true. You can't expect your attorney to invent things that are hard to foresee. Trivial items which are small variations on the invention, yes, your attorney should anticipate that.

For example, if you went to your attorney and said you had invented a revolving door with four panels, then he should see that it works with only three and should make sure that the patent is not restricted to only covering revolving doors with four panels. But what about a revolving door with two panels. I have seen one. How would you make that work? You cannot expect your attorney to think of everything and close-off every possibility.

In order to obtain a commercially valuable patent that will provide you with a "meaningful monopoly" (that you can sell to others), then you have to know the state of the marketplace, what will appeal to consumers, how to put the invention into effect so that it will work, and how to prepare a well-drafted patent application. Also you have to invent prospective advances that might be made by others which you then incorporate into the filing. All of these are key, but the last item is more likely overlooked than the others.

5. Examples of Cold Fusion Patents and Applications

At ICCF-17 in South Korea I wrote a paper which is available in the Journal [1] *J. Condensed Matter Nucl. Sci.* **13** (2014) 118–126, in which I analyzed the then-pending Brillouin Cold Fusion US patent application. I predicted that this application was doomed. Insufficient evidence had been provided to the US patent office that the invention worked. It was, eventually, abandoned and replaced. The story of the problems with that patent filing are addressed in the referenced paper.

At ICCF-18 in Missouri I prepared a paper published in two parts on [2] Cold Fusion Now which addressed in Part 1 a patent obtained on behalf of Melvin Miles by the U.S. Navy. In that particular case, the patent attorney had identified a new composition, a new alloy, as having utility not relating to Cold Fusion. But it was also stated, in passing, that this alloy would support an LENR procedure. The actual use of the composition in an LENR method to produce Cold Fusion excess energy was addressed in a dependent claim in that issued patent. This was an example of a new material that had valid uses that the US patent office had to accept and then they had to apply their internal rule that if you identify one useful application or use for an invention, then you can claim other uses that are more speculative.

The ICCF-18 paper also addresses, in Part 2, a patent filing by a private inventor, James Cook. That patent filing contained claims based on conjectures inspired by what James Cook heard on the radio from a Psychic. The patent was rejected as "not proven to work." It was also rejected as "requiring further research". James had stated in the patent: *"the first and second acoustic wave generators (17, 21) must operate at different frequencies. The specific frequencies required remain to be determined by experimentation."*

It is easy to see why this patent application was rejected. The disclosure of how to make the invention work was incomplete. James is still paying his patent attorney on a monthly basis for the many thousands of dollars it cost to

prepare and present his application to the US patent office.

6. Andrea Rossi US Patent issued August 25, 2015

Andrea Rossi was granted a US patent on August 25, 2015. Here follows an analysis of the key claim of that patent. Claim 1, with its preamble, reads as follows:

Having described the invention, and a preferred embodiment thereof, what I claim as new and secured by Letters Patent is:

(1) An apparatus for heating fluid, said apparatus comprising a tank, an electrical resistor, and a fuel wafer,
   (a) wherein said tank is configured for holding fluid to be heated,
   (b) wherein said fuel wafer is configured to be in thermal communication with said fluid,
   (c) wherein said fuel wafer includes a fuel mixture that includes reagents and a catalyst,
   (d) wherein said electrical resistor is in thermal communication with said fuel mixture and said catalyst, wherein said resistor is configured to be coupled to a voltage source,
   (e) wherein said apparatus further comprises a controller in communication with said voltage source, and a temperature sensor,
   (f) wherein said fuel mixture comprises lithium, and lithium aluminum hydride,
   (g) wherein said catalyst comprises a group 10 element,
   (h) wherein said controller is configured to monitor a temperature from said temperature sensor, and, based at least in part on said temperature, to reinvigorate a reaction in said fuel mixture,
   (i) wherein reinvigorating said reaction comprises varying a voltage of said voltage source.

The subparagraph identifications (a)–(i) have been added for clarification. They do not change the meaning of the claim. The repetition of "wherein" is an eccentricity of the patent draftsman. Normally, this word would appear only once at the top of the list, just before the colon. The draftsman is, of course, Rossi's attorney. Patent Examiners do not draft claims. They only review and approve or reject them.

In this case, Claim 1 is the broadest claim of the patent. It defines everything that Rossi purports to control under the patent. If Claim 1 is valid and infringed, then all the other claims are redundant and unnecessary. This is because all of the other claims are in "dependent form" - they refer-back to Claim 1, adopting all of its limitations. If Claim 1 is not infringed, then none of the dependent claims that refer back to Claim 1 will be infringed. Careful thought should establish that this is true.

In order to be valid, a claim in its totality must not describe anything that was previously known. It must, in the jargon of the trade, be "novel". We assume for the present that Claim 1 is valid. If it were invalid, then the dependent claims would each become relevant on the possibility that, although narrower, they might be valid. Then an infringement assessment would have to be made with respect to each of the dependent claims which appears to be valid. The dependent claims are reproduced in Appendix A.

The primary issue is therefore the type of apparatus that will infringe Claim 1.

In order to infringe a competitor must build, use or sell an apparatus that fits within the entire description of Claim 1. Therefore, Claim 1 is a kind of check-off list for infringement. If a competitor's product lacks the presence of even just one limitation, then they do not infringe this claim.

While we are assuming that this claim is valid, some people will immediately object that a number of elements in the claim were already known. For example, items (a)–(c) appear to describe the things that have already been built. Indeed they do. In fact, every item in the list can probably be found, individually, to have been known previously. All these items are in the "prior art". For validity, however, it is the entire collection of limitations which must avoid

describing the prior art. As the patent examiner issued the claim, there is a likelihood that some feature in this list of limitations provided a distinction over the prior art that allowed the claim to be accepted as being "novel".

In fact, reading the exchange of correspondence between the patent examiner and Rossi's patent attorney (available over the Internet), it is apparent that Rossi was forced to add items (h) and (i) to the claim in order to get it approved. Obviously, adding these to further limitations reduced the scope of coverage of the claim. Not a happy requirement for Rossi.

7. Key Issue for Rossi Claims

Howsoever this claim was allowed, the key question that competitors may now wish to consider is whether they can enter the field and compete without falling within the language of this claim. In other words, does this claim have any loopholes?

The claim could clearly be avoided if a competitor did not include either lithium or lithium aluminum hydride as part of the fuel mixture. What about using lithium borohydride? Would that work just as well? What other substances would do the job? Those are the kinds of question that a competitor would immediately wish to test.

Another way to avoid the claim would be to "reinvigorate" the reaction by providing heat from a source other than by varying the voltage across an electrical resistor that serves as a heater for the fuel. Another possibility would be to provide heat through burning combustible gas. In fact, Rossi has filed an International Application under the Patent Cooperation Treaty (PCT) where he added this alternate method of reinvigorating the reaction in order to close-off this specific loophole. Eventually, this PCT filing will reach the United States and other countries around the world where the claims will be examined afresh.

Extended study of this claim could possibly identify other loopholes. The exercise need not be elaborated presently. The principles have been demonstrated.

Are there flaws in the claims of the Rossi patent? Possibly. If so, could this have been avoided? Possibly, though not necessarily. If there are alternatives to lithium aluminum hydride, then it would have been advisable for Rossi to identify them while his patent application was still in the drafting stage, structuring the claims to cover these alternatives. Perhaps he did research and concluded that lithium aluminum hydride was by far the best key constituent for the fuel. Or, possibly, he did not have the resources to explore alternatives.

This application was filed in the United States on March 14, 2012. Through a unique feature of the US patent law it was kept secret up until it issued on August 25, 2015. As long as the invention was still secret, i.e. not "available to the public" anywhere in the World in any form, then Rossi could have filed an upgraded patent application that closed-off any loopholes of the type discussed. In fact, when the PCT application was filed just before the publication and grant of the US patent the only major change to the disclosure was the inclusion of other forms for heating the fuel in order to rejuvenate the reaction. No change was made to the references to lithium and lithium aluminum hydride.

Was this an oversight? We may never know.

8. Florida Litigation, Leonardo Corporation Versus Industrial Heat

The above-referenced litigation, commenced in Florida in March, 2016, originally alleged that Industrial Heat had infringed this US patent. Bizarrely, the allegation was made that this infringement occurred because Industrial Heat had been engaged in infringing activities in Europe (a territory for which Industrial Heat did not have a license). An American patent cannot be infringed by activities occurring strictly in Europe. Accordingly, the Florida Court in pre-trial procedures struck-out any allegation of infringement of this US patent. The case before the Court in Florida does not include any element of patent infringement. It is largely about breach of contract or possibly illegal use of trade secrets.

One further issue raised in the case is that Industrial Heat filed two patent applications at the US patent office naming one of their staff members and Andrea Rossi as co-inventors. If in fact the invention described in these filings arose from discussions with Andrea Rossi, then he had to be mentioned as a co-inventor of necessity. Whether there has been a violation of the rights of Andrea Rossi by so naming him is an issue relating to the law of confidentiality and is not an issue of patent law.

Whether the August 25, 2015 US patent issued to Leonardo Corporation is valid and whether it can be avoided by a competitor may never be resolved if the patent is never asserted. It may simply be allowed to die a quiet death.

9. A Controlling Patent in the Field of Cold Fusion?

Will there ever be a controlling patent in the field of Cold Fusion? That is not very likely. Nothing can be patented that has already been disclosed publicly. Any future patents based on Cold Fusion effects will have to focus on "arrangements" that are new and unobvious and which deliver useful results. "Arrangements" means physical structures or procedures for manipulating physical things. There can never be a patent on a theory or on the abstract concept of exploiting a theory. Patents have to be directed to new, specific, tangible "arrangements".

Patents are also constrained by the prior art. This is what is meant by saying that patents must be restricted as applying only to things that are new. But a vast amount of literature has been generated on this subject in the years since Fleischmann and Pons made their announcement in March, 1989. If ever there were a chance to obtain patent coverage not fettered by prior art, then it was the 1989 – 1990 patent filings initiated by the University of Utah on behalf of Pons and Fleischmann. The US patent filing never issued due to the policies of the US patent office. But a corresponding European patented did issue and is available at the European patent office website: European patent [3] EP0463089. The "tombstone data" for this patent is available at the following hyperlink: https://register.epo.org/application?number=EP90905756.

A careful review of this tombstone data will show that this European patent originated from a series of 8 United States patents filed over the period from March 13, 1989 to May 25, 1989. A PCT filing [4] was made on March 12, 1990 and the European national entry application made on January 2, 1992. The patent issued at the European patent office on May 22, 1996 and lapsed on 23 October 1998 for failing to respond to a an Opposition proceeding initiated against the patent by Clean Energy Technologies Inc. of Sarasota, Florida, USA.

We can only guess why the patent was not defended in the Opposition proceeding. By then the University of Utah had transferred all of its rights to a private company that presumably did not want to spend funds defending the patent in the Opposition proceedings. Perhaps they were disillusioned if they found they could not get the invention to work according to the directions contained in the patent specification.

Interestingly, we can see in this document some very aggressive claims drafted at the beginning of the LENR era, unfettered by standard prior art. These claims are reproduced in the European patent specification [5] referenced in Appendix B. They are well worth studying as they are the closest that one could ever expect in terms of being a master or dominant patent in the field. They were certainly intended to be that when they were drafted. But they were abandoned.

Claims of 1 and 16 in Appendix B respectively address an apparatus and method and represent the broadest scope of this aspiring set of claims. They can be studied from the viewpoint of a competitor who wishes to exploit a completing system in the marketplace, applying the above-outlined principles.

10. Summary

Why would anyone want to obtain a patent, particularly a patent in respect to Cold Fusion technology?

It is all about profiting from having a monopoly. If you have no monopoly or an inadequate monopoly, you will not be able to earn excess profits. No one will purchase your invention from you if it is not accompanied by protection that

will provide excess profits. Without a patent, once your product is on the market and the secret is out, you have nothing to sell. If you market your invention and thereby disclose your secret to the public, then you will likely eventually be exposed to competition if your product is a success.

If you're going to obtain a patent, then do it right: accept the limitations that are imposed by the prior art, and close the remaining pathways that could be used to get around your patent claims. Close the loopholes! Work closely with your patent attorney to understand the process. And think like your competitor.

References

[1] https://www.iscmns.org/CMNS/JCMNS-Vol13.pdf.
[2] http://coldfusionnow.org/patenting-cold-fusion-inventions-before-the-us-patent-trademark-office-part-2/.
[3] https://register.epo.org/application?number=EP90905756.
[4] https://worldwide.espacenet.com/publicationDetails/biblio?CC=WO&NR=9010935&KC=&locale=en_EP&FT=E#.
[5] https://data.epo.org/publication-server/pdf-document?pn=0463089&ki=B1&cc=EP.

Appendix A

Claims from US patent 9,115,913 issued to Leonardo Corporation (Miami Beach, FL) on an invention of Andrea Rossi.

> *Title*: Fluid Heater.
> *Abstract*: An apparatus for heating fluid includes a tank for holding fluid to be heated, and a fuel wafer in fluid communication with the fluid. The fuel wafer includes a fuel mixture including reagents and a catalyst, and an electrical resistor or other heat source in thermal communication with the fuel mixture and the catalyst.
> 13/420,109 *Filed*: March 14, 2012.
> *Claims*: Having described the invention, and a preferred embodiment thereof, what I claim as new and secured by Letters Patent is:

(1) An apparatus for heating fluid, said apparatus comprising a tank, an electrical resistor, and a fuel wafer,

(a) wherein said tank is configured for holding fluid to be heated,
(b) wherein said fuel wafer is configured to be in thermal communication with said fluid,
(c) wherein said fuel wafer includes a fuel mixture that includes reagents and a catalyst,
(d) wherein said electrical resistor is in thermal communication with said fuel mixture and said catalyst, wherein said resistor is configured to be coupled to a voltage source,
(e) wherein said apparatus further comprises a controller in communication with said voltage source, and a temperature sensor,
(f) wherein said fuel mixture comprises lithium, and lithium aluminum hydride,
(g) wherein said catalyst comprises a group 10 element,
(h) wherein said controller is configured to monitor a temperature from said temperature sensor, and, based at least in part on said temperature, to reinvigorate a reaction in said fuel mixture,
(i) wherein reinvigorating said reaction comprises varying a voltage of said voltage source.

(2) The apparatus of claim 1, wherein said catalyst comprises nickel powder.

(3) The apparatus of claim 2, wherein said nickel powder has been treated to enhance porosity thereof.

(4) The apparatus of claim 1, wherein said fuel wafer comprises a multi-layer structure having a layer of said fuel

mixture in thermal communication with a layer containing said electrical resistor.

(5) The apparatus of claim 1, wherein said fuel wafer comprises a central heating insert and a pair of fuel inserts disposed on either side of said heating insert.

(6) The apparatus of claim 1, wherein said tank comprises a recess for receiving said fuel wafer therein.

(7) The apparatus of claim 6, wherein said tank further comprises a door for sealing said recess.

(8) The apparatus of claim 1, wherein said tank comprises a radiation shield.

(9) The apparatus of claim 1, wherein said reaction in said fuel mixture is at least partially reversible.

(10) The apparatus of claim 9, wherein said reaction comprises reacting lithium hydride with aluminum to yield hydrogen gas.

Appendix B

European Patent Specification of Fleischmann and Pons is (Fig. 1).
https://data.epo.org/publication-server/pdf-document?pn=0463089&ki=B1&cc=EP
Claims of European Patent Specification of Fleischmann and Pons
https://data.epo.org/publication-server/pdf-document?pn=0463089&ki=B1&cc=EP

Claims

(1) A heat-generating apparatus (10, 24, 32, 200) comprising:
   (a) a source (12, 34, 42) of deuterium atoms;
   (b) a lattice material (16, 28, 30, 32, 40, 43, 54, 212) having a crystal structure and being capable of dissolving 55 deuterium atoms such that the concentration of dissolved deuterium atoms achieves a chemical potential which is at or above a predetermined chemical potential at or above which excess heat occurs, excess heat being defined as heat generation which is greater than the joule-heat equivalent used for dissolving deuterium in the lattice material;
   (c) a means (18, 20, 41, 44, 48, 49, 56, 218) for accumulating and compressing deuterium atoms into said lattice material in a quantity which is above the predetermined chemical potential while maintaining integrity of the crystal structure; and
   (d) a thermal conduit (48) for removing heat from said lattice material.

(2) The apparatus according to claim 1, further comprising a container (14, 26) into which said source, lattice material and at least a portion of said accumulating and compressing means are disposed.

(3) The apparatus according to claim 1, wherein said accumulating and compressing means is characterized by means (18, 20, 41, 44, 48, 49) for applying an electric field across said lattice material.

(4) The apparatus according to claim 1, wherein said lattice material comprises at least one metallic element (16, 40).

(19) Europäisches Patentamt
European Patent Office
Office européen des brevets

(11) EP 0 463 089 B1

(12) EUROPEAN PATENT SPECIFICATION

(45) Date of publication and mention of the grant of the patent:
22.05.1996 Bulletin 1996/21

(21) Application number: **90905756.4**

(22) Date of filing: **12.03.1990**

(51) Int Cl.[6]: **G21B 1/00**

(86) International application number:
PCT/US90/01328

(87) International publication number:
WO 90/10935 (20.09.1990 Gazette 1990/22)

(54) METHOD AND APPARATUS FOR POWER GENERATION

VERFAHREN UND VORRICHTUNG ZUR ENERGIEERZEUGUNG

PROCEDE ET APPAREIL DE PRODUCTION DE PUISSANCE

(84) Designated Contracting States:
AT BE CH DE DK ES FR GB IT LI LU NL SE

(30) Priority: **13.03.1989 US 323513**
21.03.1989 US 326693
10.04.1989 US 335233
14.04.1989 US 338879
18.04.1989 US 339646
02.05.1989 US 346079
16.05.1989 US 352478

(43) Date of publication of application:
02.01.1992 Bulletin 1992/01

(60) Divisional application: **95116753.5**

(73) Proprietor: **UNIVERSITY OF UTAH RESEARCH FOUNDATION**
Salt Lake City, Utah 84112 (US)

(72) Inventors:
- **PONS, Stanley**
  Salt Lake City, UT 89019 (US)
- **FLEISCHMANN, Martin**
  Tisbury, Wiltshire SP3 6LJ (GB)
- **WALLING, Cheves, T.**
  New Hampshire 03452 (US)
- **SIMONS, John, P.**
  Salt Lake City, UT 84103 (US)

(74) Representative:
Dost, Wolfgang, Dr.rer.nat., Dipl.-Chem. et al
Patent- und Rechtsanwälte
Bardehle . Pagenberg . Dost . Altenburg .
Frohwitter . Geissler & Partner
Galileiplatz 1
81679 München (DE)

(56) References cited:
- **Fusion Technology, vol. 16, no. 2, September 1989, (La Grange Park, IL, US), Y. Oka et al.: "D2O-Fueled Fusion Power Reactor using Electrochemically Induced D-Dn, D-Dp, and Deuterium-Tritium Reactions-Preliminary Design of a Reactor System", pages 263-267**
- **Fusion Technology, vol. 16, no. 2, September 1989, (La Grange Park, IL, US), V. C. ROGERS: "Isotopic Hydrogen Fusion in Metals", pages 254-259**
- **Technical Bulletin, Engelhard Industries, vol. 7, no. 1-2, 1966, Baker Platinum Division, (Sutton, Surrey, GB) H. BRODOWSKY et al.: "Solubility and Diffusion of Hydrogen and Deuterium in Palladium and Palladium Alloys", pages 41-50**
- **Paneth and Peters, Berichte der Deutschen Chemischen Gesellschaft, vol. 59 (8), 1926, pp. 2039-2048.**
- **Var alkemist i Tomegränd - en bok av och om John Tandberg, CWK Gleerup Bokförlag, Lund, Sweden, 1970, pp. 33,34,42,43.**

Remarks:
The file contains technical information submitted after the application was filed and not included in this specification

EP 0 463 089 B1

Figure 1. European patent specification of Fleischmann and Pons.

(5) The apparatus according to claim 4, wherein said lattice material comprises at least one element selected from group VIII and group IVA metals and alloys thereof.
(6) The apparatus according to claim 4, wherein said lattice material is characterized by at least one element selected from palladium, iron, cobalt, nickel, ruthenium, rhodium, osmium, iridium, titanium, zirconium, hafnium and alloys 20 thereof.
(7) The apparatus according to claim 1, wherein said source of deuterium atoms is a fluid.
(8) The apparatus according to claim 7, wherein said fluid comprises an electrolyte.
(9) The apparatus according to claim 8, wherein said accumulating and compressing means comprises means (18, 20, 41, 44, 48, 49) for electrolytically decomposing said electrolyte into deuterium which is accumulated and com- pressed onto and into said lattice material.
(10) The apparatus according to claim 9, wherein said electrolyte decomposing means comprises anode means (18, 41, 48) and at least one charge generating source (20, 44).
(11) The apparatus according to claim 10, wherein said lattice material is electrically conductive and said accumulating and compressing means comprises means (20) for connecting the lattice material as a cathode associated with 35 said electrolyte decomposing means.
(12) The apparatus according to claim 8, wherein said electrolyte is an aqueous solution comprising at least one water- miscible deuterium solvent component.
(13) The apparatus according to claim 12, wherein said deuterium solvent component comprises a mixture of isotopic hydrogen solvents of which deuterated water is at least 99.5% of the solvent component by volume.
(14) The apparatus according to claim 8, wherein said electrolyte includes lithium in a dissolved form.
(15) The apparatus according to any of the preceding claims, further comprising a means for converting heat generated in said lattice to work.
(16) A heat-generation method comprising the steps of:

(a) providing a source (12, 34, 42) of deuterium atoms;
(b) providing a lattice material (16, 28, 30, 32, 40, 43, 54, 212) known to dissolve deuterium atoms and having a crystal structure that is capable of being a host to high concentrations of deuterium atoms compressed into the lattice material while maintaining integrity of the crystal structure;
(c) contacting the lattice material with deuterium atoms from said source;
(d) supplying energy so as to produce a flow of deuterium atoms from the source into the lattice material; and thereby
(e) compressing deuterium atoms into the lattice material, during which compressing step the lattice material is capable of maintaining its structural integrity, until a predetermined condition is achieved at which excess 5 heat is generated by interaction between deuterium atoms and the lattice material, said predetermined con- dition being characterized by a chemical potential of the lattice material that is above a threshold level and excess heat being defined as evolved heat which is greater than the joule-heat equivalent used for dissolving deuterium in the lattice material.

(17) The method according to claim 16, comprising the further step of preparing at least one surface of said lattice material for contact with deuterium such that said surface comprises surface properties favorable to charging with atomic deuterium.
(18) The method according to claim 17, wherein the surface preparing step is characterized by machining the surface is following casting or annealing.
(19) The method according to claim 16, wherein the lattice material providing step is characterized by removing at least a portion of ordinary hydrogen present at said surface of the material lattice prior to the contacting step.
(20) The method according to claim 16, wherein said source of deuterium is a fluid.

(21) The method according to claim 20, wherein said fluid comprises an electrolytic fluid.
(22) The method according to claim 20, wherein said fluid is an aqueous solution comprising at least one water-miscible 25 deuterium solvent component.
(23) The method according to claim 21, wherein said contacting, supplying, and compressing steps are characterized by charging said lattice material by electrolytic compression.
(24) The method according to claim 23, wherein said charging step is characterized by performing a stepwise electrolytic charging of said lattice material.
(25) The method according to claim 16, further comprising the step of converting heat generated in said material into work.
(26) The method according to claim 16, wherein said lattice material comprises a material selected from palladium, iron, cobalt, nickel, ruthenium, rhodium, zirconium, hafnium, and alloys thereof.
(27) The method according to claim 16, wherein said lattice material comprises an electrically conductive lattice material.
(28) The method according to claim 16, further comprising disposing the source and the lattice material in a container (14).
(29) The method according to claim 16, further comprising the step of poisoning the catalytic surface to prevent the reaction of deuterium atoms bound to the surface with deuterated water to form deuterium gas.
(30) The method according to claim 21, wherein the lattice material comprises palladium or an alloy thereof.
(31) The method according to claim 30, wherein the steps (d) and (e) are characterized by compressing deuterium into said material lattice until the chemical potential above the chemical potential of a like lattice material equilibrated with said source at standard temperature and pressure is at least 0.5 eV.